

Cite this: *Mater. Horiz.*, 2021,  
8, 3201

# Functional nanomaterials, synergisms, and biomimicry for environmentally benign marine antifouling technology

Avishek Kumar,<sup>a</sup> Ahmed AL-Jumaili,<sup>ab</sup> Olha Bazaka,<sup>c</sup> Elena P. Ivanova,<sup>id c</sup>  
Igor Levchenko,<sup>id d</sup> Kateryna Bazaka<sup>aef</sup> and Mohan V. Jacob<sup>id \*a</sup>

Marine biofouling remains one of the key challenges for maritime industries, both for seafaring and stationary structures. Currently used biocide-based approaches suffer from significant drawbacks, coming at a significant cost to the environment into which the biocides are released, whereas novel environmentally friendly approaches are often difficult to translate from lab bench to commercial scale. In this article, current biocide-based strategies and their adverse environmental effects are briefly outlined, showing significant gaps that could be addressed through advanced materials engineering. Current research towards the use of natural antifouling products and strategies based on physiochemical properties is then reviewed, focusing on the recent progress and promising novel developments in the field of environmentally benign marine antifouling technologies based on advanced nanocomposites, synergistic effects and biomimetic approaches are discussed and their benefits and potential drawbacks are compared to existing techniques.

Received 13th July 2021,  
Accepted 18th October 2021

DOI: 10.1039/d1mh01103k

rsc.li/materials-horizons

## 1. Introduction

Any surface immersed in an aquatic environment is subject to colonization by marine organisms. Such uncontrolled colonization by micro- and macro-organisms, *i.e.* biofouling, is seldom desired since it often adversely affects the ability of the surface to perform its intended function. Not surprisingly, biofouling represents a serious problem for marine industry and intense efforts are currently made to resolve this challenge. Nanomaterials-based approaches are currently considered among the most promising anti-fouling techniques. Nanomaterials and functional nano-composites<sup>1</sup> feature a large set of unique properties that warrant their efficient application across various fields and in challenging operating environments, ranging from energy harvesting and conversion,<sup>2-4</sup> energy storage,<sup>5-7</sup> sensing,<sup>8-10</sup> bio-protection,<sup>11-13</sup> soil fertilization<sup>14</sup> and even space technology.<sup>15-17</sup>

Importantly, some nanocomposites exhibit self-healing and self-regenerative properties that make them very suitable for application under chemically testing conditions, from tropical saltwater to other planets<sup>18</sup> and outer space.<sup>19</sup> In the marine antifouling technology, the functional nanomaterials are currently under particular consideration.<sup>20-22</sup>

The examples of how biofouling leads to an overall deterioration of performance are numerous and significant, spanning shipping vessels, heat exchangers, oceanographic sensors and aquaculture systems.<sup>23</sup> For example, an increase in the roughness of the ship hull due to fouling can cause powering penalties of up to 86% at cruising speed.<sup>24</sup> Furthermore, ship fouling can result in bio-invasion, a process by which marine species are transported and unintentionally introduced into a non-native environment. Biofouling of autonomous environmental monitoring equipment, such as oceanographic sensors used to measure dissolved oxygen, turbidity, conductivity, pH and fluorescence of seawater, as well as energy conversion equipment is another challenge.<sup>25-28</sup>

Attachment of microorganisms to optical windows in cameras and optical sensors, and resultant degradation of the properties of the interface significantly limit their deployment time. Formation of the biofilm on the surface can also considerably disrupt the quality of the measurement and the useful operational lifetime of these sensors. For example, biofouling of proton selective glass membrane electrodes used for measuring pH inhibits the proper contact between liquid media and the electrodes.<sup>29</sup> In turbidity

<sup>a</sup> Electronics Materials Lab, College of Science and Engineering, James Cook University, Townsville, QLD 4811, Australia. E-mail: mohan.jacob@jcu.edu.au

<sup>b</sup> Medical Physics Department, College of Medical Sciences Techniques, The University of Mashreq, Baghdad, Iraq

<sup>c</sup> School of Science, RMIT University, PO Box 2476, Melbourne, VIC 3001, Australia

<sup>d</sup> Plasma Sources and Application Centre, NIE, Nanyang Technological University, 637616, Singapore

<sup>e</sup> Faculty of Engineering, Queensland University of Technology, Brisbane, QLD 4000, Australia

<sup>f</sup> School of Engineering, The Australian National University, Canberra, ACT 2601, Australia



**Fig. 1** Current trends in the development of antifouling coatings. These antifouling strategies can be mechanical, physical or chemical in their nature or rely on a combination of these mechanisms. From a simple lead cladding used hundreds years ago, the technology of antifouling has evolved to include nanostructures-based surfaces built on biomimetic and synergistic principles.

and chlorophyll sensors, the antifouling coating should be transparent to light so as not to interfere with the clarity of the optical window.<sup>30</sup> Hence, there is a significant impetus to develop antifouling techniques that prevent organism settlement without impeding sensor performance.

A wide range of antifouling (AF) techniques has been devised to combat the problem of micro- and macro-organism attachment and biofilm formation. Fig. 1 shows the antifouling strategies used in the past and at present. In terms of their action mechanism, these antifouling strategies can be mechanical, physical or chemical in their nature, or rely on a combination of these mechanisms. Chemical methods involve the use of a biocidal agent (or agents) that inhibit or limit the settlement of foulants using chemically active compounds. Although very effective against many macro-organisms, these chemicals are often non-species specific and can, therefore, influence non-target organisms.<sup>31–33</sup> One of the most well-known examples of this is the use of TBT (tributyltin), a broad spectrum biocide that has been used extensively since the 1960s to control marine biofouling. However, after its high toxicity to non-target marine species became apparent in the 1980s, the use of TBT was completely banned in 2008.<sup>34</sup> Influence of other antifouling agents on marine flora and fauna is also a potential problem.<sup>35</sup> The self-polishing copolymer (SPC) paints loaded with booster biocides, *e.g.* copper and zinc pyrithione are currently in use. However, Cu and Zn may pose an ecological risk due to their leaching from SPC into the ambient environment, which may over time lead to their built up to concentrations that are toxic to marine life. These and other ecological concerns have led to the use of biocide-based coatings being subject to stringent legislation, with calls for non-toxic physical methods to eventually replace biocide-based strategies entirely.<sup>36,37</sup>

Physical methods rely on the use of a protective antifouling coating that can either deter the organism from settling on the surface or enhance the release of the settled organism from the surface (*i.e.* fouling release coating). Although more environmentally-friendly than the biocide-based coatings, the stability and durability of such coatings in water and their potential effects on the ambient marine environment remain a matter of concern. Pure mechanical devices such as wipers and scrapers can be used to remove the foulants, however, they may not always be well suited for small-scale devices and can also damage the surface of such sensitive devices as sensors.<sup>38</sup> The wipers and scrapers may need to be adapted to ensure efficient yet minimally-damaging removal of foulants from these devices.

In this review, we first outline the importance and the current state of development of the antifouling technology; then, we briefly discuss main classical antifouling approaches that have been explored over the years; and show that even mature traditional approaches based on chemical agents still fail to provide efficient protection against fouling for hundreds of thousand marine vessels; finally, we explore the most promising, from the authors' point of view, strategies based on (i) a wide use of functional nanostructured materials; (ii) application of synergistic effects; and (iii) utilization of Nature-inspired biomimetic systems and surfaces.

Comprehensive investigation of the progress in marine antifouling technology developed thus far concludes that there is no single innovation available that is completely antifouling or fouling release.<sup>39–43</sup> Fouling in the marine context is a complex phenomenon which requires solutions that target concurrently its various processes and components. Thus, the quest for a single, simple technology that can combat the complicated process of marine fouling continues.

## 2. Biofouling: a serious threat to marine industry

At least 4000 fouling organisms have been identified and are classified on the basis of their size. These organisms can range from unicellular (*e.g.* bacteria) to multicellular (*e.g.* seaweed and barnacles). Bacteria, algae spores, larvae of invertebrates and diatoms are considered to be primary fouling micro-organisms, while barnacles, algae and mussels are common fouling macro-organisms. Marine biofouling is commonly defined as an undesirable colonization of any submerged surface by marine organisms. Typically, over the 5 years after the protective paint is applied to the surface of the vessels, the AF properties of these coatings deteriorate significantly, with the level of paint loss varying significantly across the surface of the vessel. In addition to AF protection loss for the painted surfaces, the AF paint particles may accumulate in the sediment, with high levels of pollution expected near ports and large ship lines.<sup>44</sup> For example, the highest level of particle accumulation detected in the samples acquired near Port of Colón, Panama reached  $81.6 \pm 41.8 \text{ ng g}^{-1}$ .<sup>45</sup>

Upon paint loss, the remaining unprotected surfaces of vessels exposed to sea water can be fouled by a great variety of organisms, including species of barnacles, tubeworms, seaweeds, mussels, sponges, mussels and diatoms.<sup>46</sup> These species vary significantly across geographies, and can change over time as the environmental conditions change or new fouling species are introduced. For maritime industry, biofouling and biofouling management (*i.e.* cost of time and cost of *e.g.* dry docking, foulant removal and re-application of paints) is associated with significant economic losses. An increase in surface roughness that takes place as a result of micro- and macro-fouling positively contribute to frictional drag, resulting in longer voyage times and greater fuel consumption. For example, a 30% increase in the coefficient of friction would result in the decrease in the speed of the vessel from 14 to 12 knots at the same value of the engine power, and a concomitant increase in voyage duration of  $\sim 17\%$ .<sup>47</sup> Furthermore, increasing the engine power to compensate for the speed loss would result in a  $\sim 63\%$  increase in the fuel consumption. It should be noted that cleaning methods used to remove the foulants, *e.g.* abrasive blasting, may also contribute to the increased roughness of the surface. For example, a study by Hakim *et al.* has shown that after ten months of operation, the fuel consumption of a ship the hull of which was painted with commercial antifouling paint experienced an increase in fuel consumption by  $\sim 20\%$ . Subsequent shot blasting and repainting was unable to return the fuel consumption to its initial value, with consumption penalty of 5% still remaining. Over the next 11 months of operation, the ship, now painted with a higher quality paint, only suffered a fuel consumption increase by 5%, highlighting the economic importance of appropriate biofouling prevention strategy for the industry. Notably, the costs of biofouling management, *i.e.* the costs associated with the application, removal, and re-application of hull paints and coatings, cleaning and resurfacing of hulls, and the cost of time when the

vessel is out of service is still much lower than that associated with excess fuel consumption. Still, over the life of the vessel, the cost of management can be considerable. A 2010 study of the costs of biofouling management on a mid-sized US naval surface ship Arleigh Burke-class destroyer has shown that cost to be \$56m per year for the entire DDG-51 class, which equates to  $\sim \$1\text{b}$  over 15 years.<sup>48</sup> These comparative estimates may be different for other types of vessels, and depend on the specifics of their operation, *e.g.* speed, power, speed of the propeller, displacement, the type of cargo they are carrying, fouling and weather conditions.<sup>49</sup>

In addition to direct economic costs to the vessel operator, an increase in CO<sub>2</sub> emissions associated with greater fuel usage increases the environmental footprint of these industries, and thus contributes to climate change. The latter, and in particular warming ocean temperatures, has a positive flow on effect on biofouling, putting positive pressure on fuel consumption. From the socio-economic perspective, greater fuel consumption and the need for biofouling management puts significant pressure on the cost of business operation. In parallel, the transfer of invasive species threatens the economic well-being of communities and industries that live off the sea due to the damage to the local environment. These costs are difficult to estimate with any degree of accuracy, yet they are likely to exceed billions of dollars, considering the critical role that marine industry plays in the global economy by supporting major parts of the international and inter-continental cargo traffic, harvesting of wild fish, farming fishery and aquaculture, petroleum and gas extraction from stationary and floating platforms, and many others that are based on the tremendous number of floatation and stationary shelf devices.

For high-traffic areas, biofouling parameters such as species make-up, thickness and weight are currently monitored with the help of large biofouling databases. In addition to direct sampling across European test-beds under the OCEANIC project across 20 countries and areas, the database also integrates data from a large collection of peer-reviewed literature and industry reports, providing further insights into the make-up of biofouling communities that grow on relevant substrata typically used in artificial structures, from ships transitioning through European waters to marine renewable energy structures operating up to 195 km offshore.<sup>50</sup> Along with the European Database project, global efforts to map the distribution of antifouling agent pollutants in shelf zones and port areas of many countries including but not limited to Brazil, Japan, Denmark, Korea, Panama are also in progress.<sup>51–54</sup> Across the world, the sampling sites for monitoring antifouling agents account for many thousands, thus causing severe economic damage to the national economies due to the need to serve the equipment, collect and process samples, *etc.* However, continuous monitoring is still needed since even after many years of ban, many antifouling agents can still be detected in the amounts that present a danger to marine flora and fauna. With potentially dangerous amounts of residual antifouling agents still present in the aquatic system and bottom sediments, further studies on the effect of forbidden antifouling agents on the marine ecosystem are also in progress.<sup>55–57</sup>

## ANTIFOULING AGENT CONTAMINATION - IS THIS A SERIOUS THREAT?

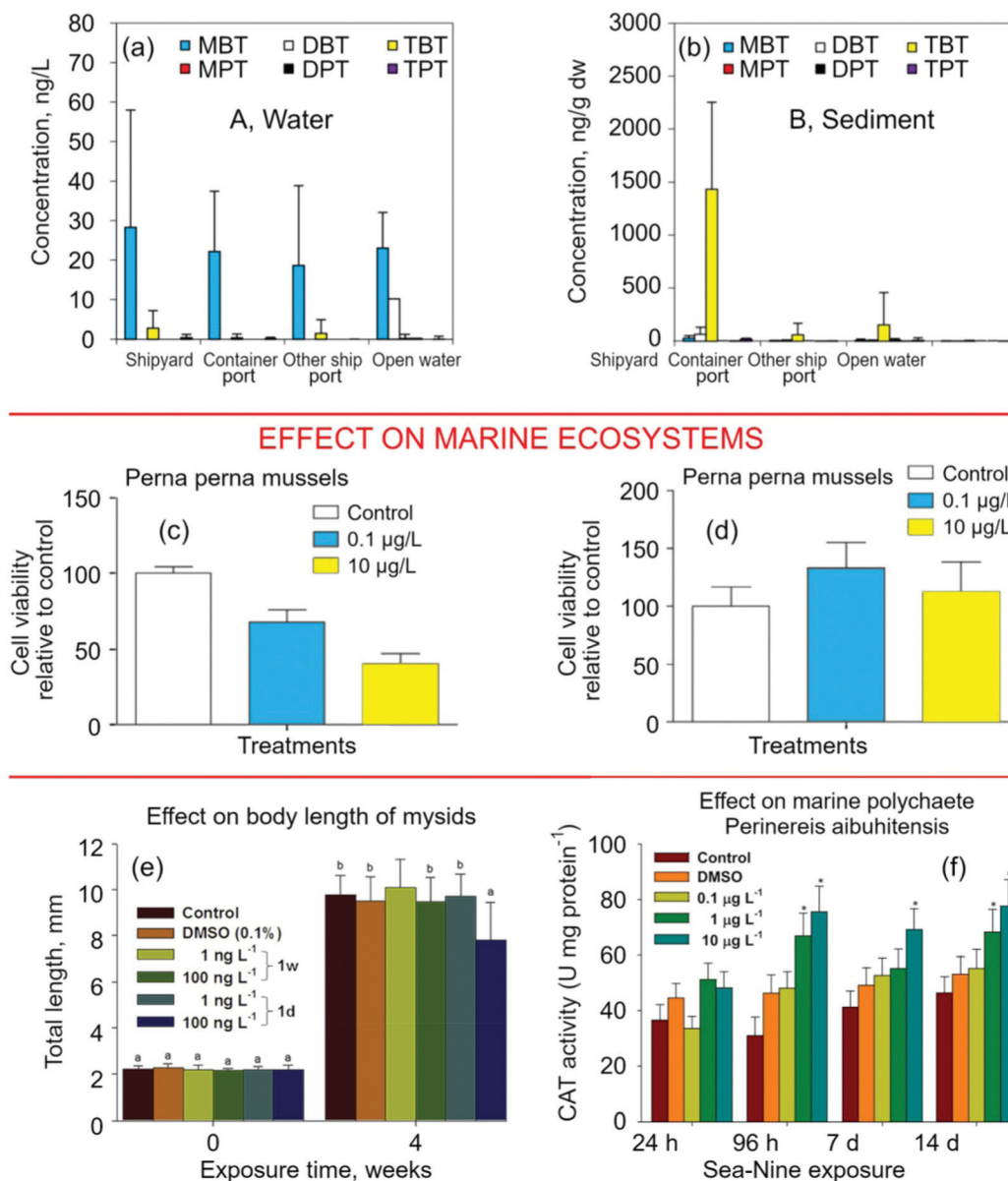


**Fig. 2** Antifouling agent contamination – is this a serious threat? (a and b) Mean concentration of organotins and new antifouling biocides in water and sediments from the three Korean Special Management Sea-Areas. Contents of some agents e.g. BMT in water and TBT in sediments are considerable. Reprinted with permission from Lam *et al.*, 2017.<sup>52</sup> (c and d) Immunological parameters of mussels *Perna perna* after exposure to chlorothalonil. Values are expressed as the mean  $\pm$  SE. Reprinted with permission from Guerreiro *et al.*, 2017.<sup>61</sup> (e) Effects of different concentrations of Sea-Nine on the total body length of mysids at intermittent (1 week) and constant (1 day) exposures for 4 weeks. Reprinted with permission from Do *et al.*, 2018.<sup>62</sup> (f) Effects of different concentrations of Sea-Nine 211 on the enzymatic activities of catalase (CAT) in *Perinereis aibuhitensis* at 24 h, 96 h, 7 days, and 14 days. Reprinted with permission from Eom *et al.*, 2019.<sup>58</sup>

Fig. 2 shows some examples of the recent investigation on the contents of antifouling agents and their effect on marine ecosystem. Organotin compounds (OTs), also known as stannanes, and tributyltin compounds in particular, were once extensively used as antifouling agents in marine applications to limit attachment of sessile organisms to surfaces exposed to sea water to maintain the efficiency of vessels and stationary structural surfaces submerged in water. Used for over 40 years

since the sixties and until their total ban in 2008, considerable levels of tributyltin (TBT) are still being measured in sediment along areas of high vessel activity, including commercial, tourist and fishing ports, harbors, shipyards, and marinas. In part, this is because of considerable half-life of this contaminant of over 30 years,<sup>59,60</sup> where the degradation dynamics depends on the chemistry of the water and the composition of the benthic deposits.

Fig. 2a and b shows the average concentration of OT pollutants as well as other types of antifouling biocides in seawater and sediment obtained from several Korean Special Management Sea-Areas. As one can see, the levels of some agents *e.g.* BMT in water and TBT in sediment remain relatively high, at concentrations that would be damaging to marine flora and fauna.

Fig. 2c and d illustrates the effect of the biocide chlorothalonil on the immune system of *Perna perna* mussels. Immunological parameters of mussels *P. perna* were evaluated after 96 h of exposure to chlorothalonil. Cell viability evaluated through MTT and neutral red assays, respectively; data are representative for 5–6 mussels in each treatment group.<sup>61</sup>

Fig. 2e depicts the changes in the total body length (mm) of mysids, the filter-feeding small, shrimp-like crustaceans upon exposure to 4,5-dichloro-2-*n*-octyl-4-isothiazolin-3-one, commonly known as Sea-Nine, at different concentrations of zero (used as control), 0.1% DMSO (employed as solvent control), 1 and 100 ng L<sup>-1</sup> at intermittent (1 week) and constant (1 day) exposure over the four week period.

Sea-Nine, also known as DCOIT, is a highly effective anti-foulant with a wide spectrum of biocidal activity and significant efficacy against major fouling marine species. Since the ban of TBT, the use of Sea-Nine and similar booster biocides, such as dichlofluanid or tolylfluanid, in marine antifouling paints has become more widespread. As a result, their environmental stability and toxicity to non-target organisms has become a subject of increased scrutiny and concern from environmental agencies, general public and regulatory bodies.<sup>62</sup> The results of the study shown in Fig. 2e confirm that these concerns may not be misplaced. While at 1 and 100 ng L<sup>-1</sup>, the concentrations of Sea-Nine used in this study are not sufficiently high to be lethal to mysids, examination of the data shows that exposure to higher levels of Sea-Nine leads to reduced length of the animals.

Similar studies on *Perinereis aibuhitensis*, a marine polychaete of significant economic value that occupy intertidal zones, showed that exposure to Sea-Nine 211 for 24 h, 96 h, 7 d, and 14 d had an effect on the enzymatic activities of catalase (CAT), as depicted in Fig. 2f. When considered jointly, these studies suggest that even at sub-lethal levels, this anti-fouling agent has a negative effect on these marine species, likely *via* a combination of lipid peroxidation, oxidative stress, and modulation of the acetylcholine-mediated transduction of action potentials. Hence, it is essential that the release, accumulation and biological effects of these biocides continue to be monitored, with the measurements of polychaete cellular defenses being one the means of such monitoring.

- Thus, common antifouling agents are often persistent and potentially dangerous contaminants, as evidenced by the most recent (2020–2021) studies all around the world; hence, new paradigms should be explored to satisfy the need for an environmentally friendly yet effective solution to this economically significant challenge, since the marine industry plays a critical role in the world's economy and food supply.

In order to design an effective strategy to mitigate fouling, it is important to understand the sequence of events that takes

place when surfaces are exposed to seawater, illustrated in Fig. 3. First, the formation of a conditioning film by physical adsorption of bio-secreted organic molecules (also known as slime) takes place within a few seconds after immersion. The conditioning film composed of glycoproteins, polysaccharides and proteins changes the surface properties of the immersed surface and sets the scene for primary colonization to occur. Within hours, bacteria begin to colonize this conditioning film, initiating the creation of a biofilm matrix. Subsequent biofilm formation occurs in several stages that can occur sequentially or simultaneously.

An initial step in biofilm formation is the transport of microscopic organism to the surface through the action of gravity, electrostatic interactions, Brownian motion and cell motility.<sup>63</sup> The second step is the reversible physical attachment of bacterial cells to the conditioning film *via* weak forces such as van der Waals forces, electrostatic and hydrophobic interactions.<sup>64</sup> Irreversible adhesion of bacteria follows, with the reversible attachment facilitated by the secretion of extracellular polymeric substances (EPS) that creates a biofilm matrix capable of attracting more organisms and particles.<sup>65</sup> The fourth stage comprises maturation and dispersion of biofilms, which expands the bacterial community. The development and expansion of biofilms take place *via* co-adhesion, binary division and mobility across the surface. In later stages of biofilm maturation, factors such as the impact of shear stress, reduction in nutrients supply and anaerobic growth conditions leads to the dissemination of singular cells or parts of biofilms from the heterogeneous mass.<sup>66</sup>

The microbial film provides sufficient nutrition for the colonization of multicellular species, increasing the degree of microfouling. The colonization by unicellular eukaryotes, such as diatoms, microalgae, and protozoa occurs within days to weeks after substrate immersion. Microalgae show adhesion behavior that is distinct from that of bacteria. Diatoms have been found to hold to surface through gravity, electrostatic interaction and van der Waals forces. After coming in contact with the surface, the cells attach *via* secretion of EPS. This attachment is reversible in nature and is known as primary adhesion.<sup>67,68</sup> During secondary stages of adhesion, motile diatoms use EPS for gliding over the surface for position adjustment while sessile diatoms remain fixed to a single site for extended periods of time, forming a stable matrix by excessive secretion of EPS.

The microfouling prompts the settlement of macroorganisms such as macroalgae, barnacles, bryozoans, molluscs, tunicates, polychaete and sponges in the process referred to as macrofouling. Biofilm cueing and physio-chemical cueing are important denominators for macrofouling settlement. Dominant species in the biofilm dictate the larval and spore settlement of macrofouling. Biofilms that show selective attraction towards certain larvae have been found in macro fouling species of bryozan,<sup>69</sup> barnacles,<sup>70</sup> and polychaete,<sup>71</sup> to name but a few. Invertebrate larvae have been found to explore the surface prior to final settlement. Barnacle cyprids use antennules for surface exploration, sensory functions and attachment *via* proteinaceous glue secretion. A combination of surface topography,

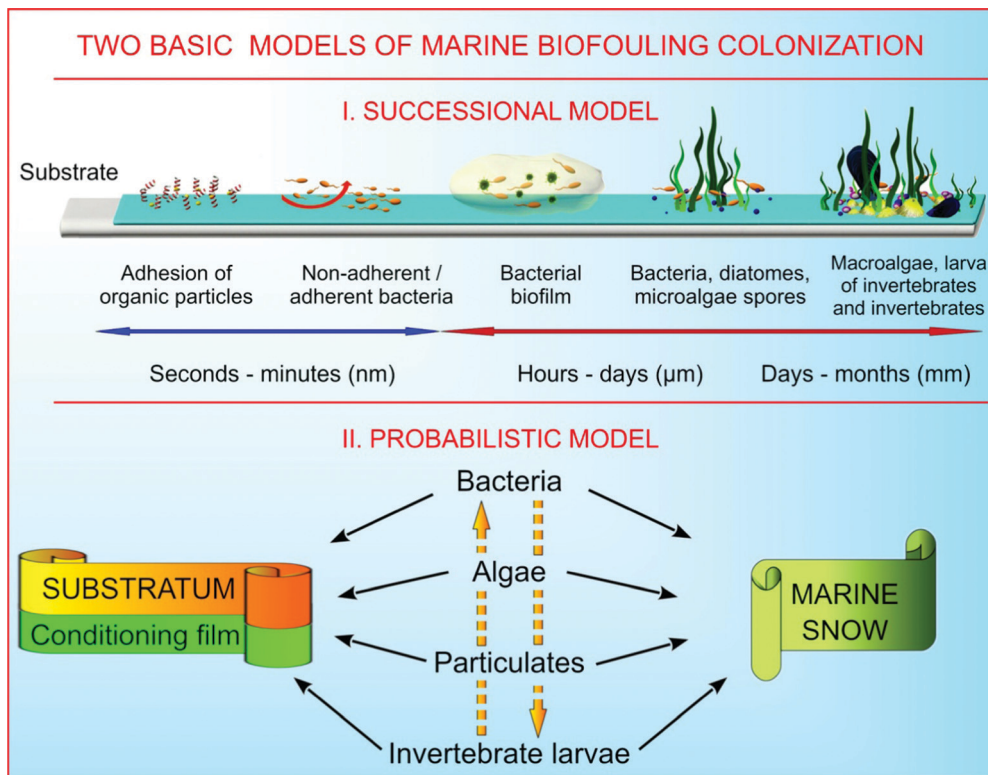


Fig. 3 Top panel: Schematic representation of fouling formation as a sequence of four processes – primary film formation, biofilm formation, diatom and protozoan colonization, and settlement of invertebrate larvae and algal spores. Reprinted with permission from Han *et al.*, 2021.<sup>87</sup> Bottom panel: Probabilistic model of marine biofouling colonization. It is now accepted that surface colonization proceeds *via* a more dynamic, so-called probabilistic model in which the absence of a stage does not impede the occurrence. After Clare *et al.*<sup>88</sup>

light intensity, primary fouling, and water flow influences cyprids preferred site of settlement.<sup>72</sup> However, this specific sequence of fouling events holds true for only a limited number of organisms. Biofilm development is antecedent to consequent fouling by macrofoulers, however is not a necessary condition. Marine micro- and macroorganism settlement and biofilm formation may occur simultaneously. Clare *et al.* showed that the zoospores of algae *Ulva linza* could settle on a pristine surface without the presence of a conditioning biofilm.<sup>73</sup> Besides, biofouling is a highly dynamic process, and the fouling community depends on the nature of the substrate, geographical location, season and organism-related factors such as cross-species competition and predation.

Ecological conditions such as water salinity, temperature, solar radiation and nutrient levels can vary considerably between different locations, directly affecting biofilm growth and development. Low salinity region affects the growth rate of most of the fouling organisms.<sup>74</sup> Few species of algae, slime, and bryozoa prefer low salinity regions. The water temperatures play a crucial part in the development of fouling on artificial structures, determining the breeding season and growth rate of marine organisms. Fouling on artificial structures in tropical region is much more severe than in cold waters, with reduced fouling in winter due to the reduction in water temperature and solar radiation intensity.<sup>75</sup>

The properties of the substrate also play an important role. It is generally believed that hydrophobic fouling organism

prefer to colonize hydrophobic surface and hydrophilic ones prefer to adhere to hydrophilic surfaces. Barnacles have been found to prefer hydrophilic surfaces whereas bryozoans adhere strongly to hydrophobic surfaces.<sup>76</sup> Furthermore, spores of green algae *Ulva linza* have been found to preferentially settle on the surface with low surface energy, yet their adherence to high energy surfaces was shown to be weak.<sup>77</sup> Besides surface energy, roughness and porosity of the surface also affect the initial settlement of fouling organisms. Highly irregular surfaces have an increased surface area which increases the number of adhesion points and region of colonization.<sup>78</sup>

### 3. Progress in antifouling technology in the last decades

Here we briefly outline the major directions and strategies currently used to address marine fouling with the aim to demonstrate that new approaches are required to increase the antifouling efficiency of these and other strategies.

#### 3.1. Biocide-based strategy

The biocide-based strategies were known as far back as the 7th century BC, when lead and copper sheets were used to control fouling by ancient Mediterranean civilizations, including Phoenicians and Ancient Greeks (1500–300 BC). Antifouling strategies

employing the use of copper, arsenic, and mercury oxide became prevalent in the late 18th and early 19th century, yet suffered from a short life span, high cost and inefficient performance.<sup>79</sup> A broad spectrum biocide, tributyltin (TBT) was introduced into commercial AF paints in the late 1950s, and was used extensively in the mid-1960s to effectively mitigate marine fouling for up to 5 years when applied onto ship hulls. In the early 1980s, it became apparent that compounds released from TBT-based self-polishing copolymer paints disrupt various enzymatic and metabolic functions in organisms, in some instances leading to their death. Following the phase-out of TBT in 2008, Cu-based biocides have once again gained prominence, and their minimal toxicity towards macroalgae was overcome through the use of booster biocides effective against micro- and macroalgae,<sup>80–82</sup> with common examples including photosynthetic organism-targeting Diuron, Irgarol 1051,<sup>83</sup> zinc and copper pyridinone,<sup>84</sup> and dichloro-octylisothiazolin (DCOIT, Sea Nine 211).<sup>85</sup> However, their use in AF paints has an uncertain future as they may also pose an environmental problem.<sup>86</sup> Organotin compounds, e.g. TBT derivative dibutyl tin, are also used in fouling release coatings.

Currently, the estimated overall application cost for a biocidal coating is about \$ 15 per m<sup>2</sup> per year.<sup>89</sup> There are three main categories of the biocide-based coatings that rely on impregnation and subsequent leaching out of the active biocide:<sup>90</sup> contact leaching coatings (insoluble matrix paints), soluble matrix paints and control depletion polymers (CDP), and self-polishing copolymers (SPC).<sup>91,92</sup> Contact leaching coatings have a water-insoluble matrix, which is made of high molecular weight binders such as vinyl, epoxy and acrylics with sufficient mechanical strength to incorporate high amounts of biocides. Active molecules are gradually released from the matrix upon contact with the micro-organism. A major limitation of these coatings is that the biocide release decreases with the immersion time and so does the antifouling effect. The soluble matrix paints and control depletion polymers (CDP) were developed to increase a lifespan of an existing antifouling coating. These coatings have binders based on rosins and their derivatives. The method is based on two processes that occur simultaneously – once submerged, a binder is dissolved, and a biocide is released into seawater. The CDP coating is effective for a period of up to 3 years.<sup>89</sup> Self-polishing copolymer coatings are based on biocide blended acrylic or methacrylic copolymers that are easily soluble in seawater, with attached foulants being removed together with the copolymer matrix. The biocides are bonded to the polymer backbone by, e.g. ester groups in the case of TBT, and their leaching rate is regulated through controlling the rate of dissolution of the copolymer matrix.<sup>93</sup> Upon immersion, seawater diffuses into a coating leading to the dissolution of the biocidal particle. The thickness of a leached layer reaches a steady value of 10–20 μm for the lifetime of the coating.<sup>66</sup> SPC coatings have a polishing rate of 5–20 μm per year which has extended the dry docking intervals for vessels for up to 5 years.<sup>94</sup>

### 3.2. Environmentally friendly antifouling coatings

In enzyme-based coatings<sup>96,98</sup> enzymes degrade adhesives used by organisms during settlement or generate other biocidal compounds.

Fig. 4a shows four principal mechanisms of enzymatic AF coatings. Essential requirements for the enzyme-based coating systems are: (1) retention of enzymatic activity when mixed with other coating components; (2) broad-spectrum AF activity; (3) long-term stability in dry (docking) and wet (submerged in seawater) conditions; and (4) minimal deterioration in coating performance.<sup>96</sup> Enzymes that can decompose adhesives, such as readily available, biodegradable and nontoxic serine proteases and glycosylases are widely used in direct enzymatic AF techniques, with demonstrated reduction of adhesion strength of green algae *Ulva linza*, diatom *Navicula perminuta* and barnacle cyprids. Trypsin, α-chymotrypsin and dextranase have also been found to be effective in reducing adhesion strength of organisms to the surface. Because in micro-fouling, polysaccharide-based bioadhesives are as dominant as the protein ones, a combination of proteolytic and polysaccharide-degrading enzymes can broaden the spectrum of direct enzyme-based techniques.<sup>95,96</sup> Sol-gel and covalent immobilization techniques are the most common methods of incorporating enzymes in an AF coating.<sup>97</sup>

Fouling release coatings are non-toxic coatings based on a dual mode of action: nonstick properties and a fouling release (FR) behavior. A FR coating provides an ultra-smooth topology, which minimizes adhesion strength between a surface and a fouling organism allowing for the fouling to be removed due to shear hydrodynamic stress during navigation. Silicone and fluoropolymers are two main hydrophobic polymers used in the fabrication of the FR coatings,<sup>101</sup> due to their hydrophobic nature and low surface energy.<sup>89</sup> Surface energy, elastic modulus and coating thickness are parameters that determine the degree of fouling and the ease of foulant removal.<sup>102–104</sup> Fluoropolymer FR coatings feature non-polar chemical moieties, thus the surface energy of these coatings fall in 10–20 mN m<sup>-1</sup> range and are lower than that of silicones. These polymers form smooth and non-porous surfaces with good anti-adhesion qualities, and can be applied as hard, glassy thin layers.<sup>105</sup> However, they could not withstand damage caused by sharp edges of barnacle shells.<sup>106</sup> Subsequently developed perfluoroalkyl polymers undergo surface reconstruction while immersed in water, and showed limited antifouling efficacy,<sup>22</sup> the latter in part addressed by the addition of crystalline polymers. A semifluorinated ether coating on a block copolymer of poly(styrene) and poly(isoprene) showed best foul release properties and was found to resist surface rearrangement.<sup>107</sup> However, fluoropolymers have high elastic modulus which hinders the easy release of accumulated foulants from the surface. Silicon-based FR coatings have the structural resemblance to ketones (R<sub>2</sub>CO), and require cross-linking in order to form a stable coating. These coatings are characterized by the low elastic modulus and low surface energy.<sup>108,109</sup> Inorganic nanofillers such as SiO<sub>2</sub>, TiO<sub>2</sub>, ZrO<sub>2</sub>, Fe<sub>3</sub>O<sub>4</sub> and Al<sub>2</sub>O<sub>3</sub> nanoparticles could be added to polydimethylsiloxane (PDMS) coatings to enhance their physical, chemical and mechanical properties.<sup>110,111</sup> An increase in hydrophilicity (contact angle of 10°) after UV radiation enhanced the self-cleaning properties of the nanocomposite.

Non-fouling (NF) coatings represent a separate group of environmentally friendly antifouling coatings. Fouling starts

## PROGRESS IN ANTIFOULING TECHNOLOGY IN THE LAST DECADES: EXAMPLES

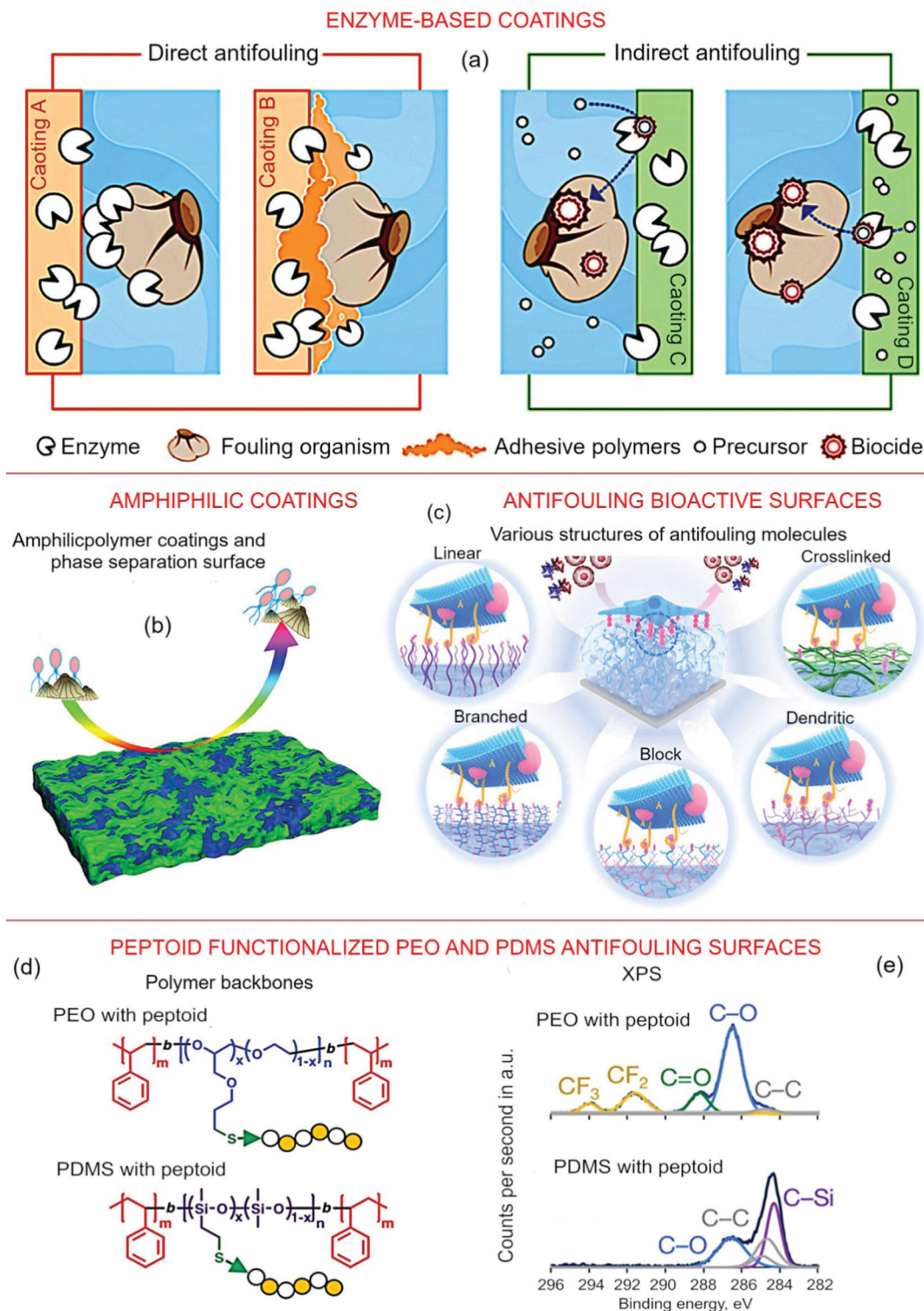


Fig. 4 (a) Schematic showing antifouling mechanisms of enzyme-based coatings. Reprinted with permission from Olsen *et al.*<sup>98</sup> (b) Schematic representation of an amphiphilic polymer coating and phase separation surface (a green hydrophilic polyethylene glycol segment and a blue lipophilic fluoropolymer segment). Reprinted with permission from Han *et al.*, 2021.<sup>92</sup> (c) Various structures of antifouling molecules (linear, branched, block, dendritic, and crosslinked) can be used to resist nonspecific protein adsorption and cell adhesion, and provide a 'spacer' for tethered bioactive molecules in displaying their genuine functions for cell interaction. Reprinted with permission from Chen *et al.*, 2021.<sup>99</sup> (d and e) Peptoid functionalized PEO and PDMS surfaces. Reproduced with permission from Patterson *et al.*, 2017.<sup>100</sup>



with the formation of conditioning films, a process of protein adhesion and adsorption on a surface. Hydrophilic surfaces based on PEG, zwitterionic, hydrogel and self-assembled monolayers have been designed to target this initial stage of fouling in both biomedical and marine fields.<sup>112,113</sup> The poly(ethylene glycol) (PEG) has been the most commonly used material due to its ability to prevent non-specific protein adhesion to a surface in a biomedical field because of low thrombogenicity.<sup>114,115</sup> PEG brush coatings are effective in resisting protein adsorption, but their excessive swelling compromises their mechanical strength and shortens their lifespan. To overcome this, attempts were made to fabricate copolymer brushes *via* surface-initiated atom-transfer radical polymerization, which showed most effective AF behavior in the thickness range of 20–40 nm against fouling of all types.<sup>116</sup> PEG surface modification can be a feasible AF strategy for biomedical devices or water membranes, but coating on large marine structures would certainly pose a difficult challenge. The zwitterionic polymers possessing both negative and positive charges have also been investigated. The principle of action is the same as that of hydrophilic PEG based polymers but the hydration is much stronger because of the ionic salvation. Zwitterionic polymers have shown resistance to protein and cell adsorption, demonstrating low spore settlement and a lower degree of adhesion of marine algae *Ulva*.<sup>117</sup>

Amphiphilic coatings are composed of contrasting hydrophobic and hydrophilic domains at submicron or nano scales, amphiphilic polymer surfaces combine the hydrophobic components that reduce polar interactions of secreted bioadhesives with the surface and protein repellency properties of hydrophilic components, where the superficial chemical heterogeneity confuses the approaching fouling organism into evading settlement. Kinetically and thermodynamically driven phase segregation of immiscible polymer blends creates the compositional heterogeneity at nanoscale, creating surface features/nanodomains comparable to dimensions of secreted bioadhesive that present energetically unfavourable hydrophobic/hydrophilic interaction (Fig. 4b).<sup>92</sup> Numerous attempts to functionalize the non-toxic coatings are known, to enhance the efficiency against the settlement of marine bacteria and other organisms.<sup>118–120</sup> Underwater surface reconstruction of amphiphilic polymers is another important factor that affects the AF property of the coating. Krishnan *et al.* fabricated amphiphilic block copolymer with fluorinated side chains and tested it against *Ulva* and *Navicula* algal species.<sup>121</sup> The amphiphilic surface showed a high level of removal of both species. Amphiphilic polymer derived from hydrophobic trifluoroethylamine (TFEA) modification of alginic acid (AA) and hyaluronic acid (HA) showed reduced adhesion of bacteria, diatoms, and barnacle cypris larvae.<sup>122</sup> Zoelen *et al.* studied the effects of the position and number of fluorinated moieties in an amphiphilic coating on AF performance against algal species *Ulva*. It was found that the position of fluorinated moieties altered the surface chemistry thus affecting AF behaviour while their number affected the fouling release properties.<sup>123</sup> Seetho *et al.* fabricated coatings having both amphiphilic and zwitterionic

properties, which displayed excellent antifouling performance against zoospores of *Ulva* in comparison to commercialized PDMS based coating (Sylgard 184).<sup>124</sup> Several examples of various structures of functionalized AF molecules are shown in Fig. 4c.

Hydrogels are environmentally benign materials that can retain a significant amount of water without dissolving. Jiang *et al.* fabricated poly(*N*-isopropyl acrylamide-*co*-2,3-bis((2,3-bis(ethylthio)-propyl)thio)propyl methacrylate) hydrogels loaded with Ag nanoparticles<sup>125</sup> that showed antimicrobial resistance against *Escherichia coli* and anti-algae performance. Zhang *et al.* fabricated anionic poly(acrylic acid/sulfopropyl methacrylate) and zwitterionic poly(acrylic acid/sulfobetaine methacrylate) tethered fibrillar hydrogel coatings.<sup>126</sup> The coatings exhibited about 90–95% decrease in the attachment of algae *Dunaliella tertiolecta* and *Navicula* sp. The fabricated coatings were all oleophobic, with oil contact angle greater than 150°. Peptoid and peptide-based coatings are the peptoid-based protein-resistant surfaces. Peptoids are synthetic peptidomimetic molecules with a peptide-like backbone and side chains appended to nitrogen atoms instead of alpha carbon as in amino acids. Lack of hydrogen bond donors, strong proton-accepting ability and water solubility are prerequisite for AF peptoid-based coatings. Patterson *et al.* functionalized a PDMS and a polyethylene oxide (PEO) surface with peptides and peptoids, respectively. The peptoid-functionalized surface showed the improved removal of *U. linza* and lower settlement of *N. incerta* than the peptide-based surfaces (Fig. 4d and e), likely due to the lack of hydrogen bond donors in the former coatings.<sup>100</sup>

Anti-fouling micro-topographical surfaces use a special topography that has a pronounced effect on roughness and wettability of the surface and has been shown to influence bioadhesion.<sup>127</sup> The attachment point theory and topography-induced wettability changes are used to explain the effect of topography on the antifouling behavior. The attachment point theory was introduced by Scardinio *et al.*, where the strength of adhesion of an organism to a surface is related to the number of available attachment points. Following this argument, surfaces with micro-topographical features that are smaller than the dimensions of the marine organism or its parts used to probe the surface during settling lead to weaker organism-surface interactions and an antifouling effect.<sup>128,129</sup> For example, Zhang *et al.* fabricated the textured patterns inspired by taro leaf, rose petal and shark skin on PDMS and evaluated their antifouling activity against algae *Nitzschia closterium*, *Phaeodactylum tricornutum* and *Chlorella*.<sup>130</sup> Sullivan *et al.* studied the effect of five different microtextured PDMS surface on diatom attachment in static field trials,<sup>131</sup> showing that microtexture features were ineffective against the settlement of diatoms, due to a combination of different settlement strategies showed by diatoms and colonization by agglomerates of planktonic and bacterial cells that rapidly mask the topography.<sup>132</sup> The topographical features also change the surface wettability, where increased surface roughness of hydrophobic/hydrophilic surfaces makes these surfaces superhydrophobic/superhydrophilic.<sup>133–135</sup>

### 3.3. Comparison of ecotoxicity of various biocides

Antifouling technology is transcending from biocide to non-biocide-based strategies, however, biocidal antifouling coatings still dominate the current market. Biocides-based methods are more effective in combatting biofouling than non-biocide methods.<sup>136</sup> The ecotoxicity of 14 commonly used biocides against common fouling species is shown in Fig. 5. Because of the adverse effects of biocides, regions like Europe, Oceania and some Asian countries have introduced strict rules and regulations on the use of biocides as antifoulants, but regions like South America have no regulations regarding the use of antifouling biocides.

Concerns associated with the impact of the biocide-containing coatings on the environment is driving current research towards environmentally benign antifouling solutions. Fouling release and non-fouling coatings based on wettability, contrasting surface chemistry, and topography have shown significant antifouling performance but their low stability, high cost and difficulty in large-scale productions are current challenges faced by these environmentally benign coatings. Nanoparticle reinforcement of fouling release coatings has led to improved stability but leaching of nanoparticles from such coatings presents other environmental challenges as toxicity of nanoparticles in aquatic systems is a major issue.

Textured coating inspired by natural self-cleaning surfaces such as sharkskin, lotus leaf can be promising future candidates. However, these coatings have been found ineffective once the surface features get buried under the fouling assemblage. Besides, the fouling community is diverse in their size, shape and mode of survival. The multifunctional coating can be a better alternative compared to the coatings with a single mode of action. The multifunctional coating can be designed by an optimal blend of surface topography, surface chemistry (hydrophobic, hydrophilic, amphiphilic, and zwitterionic) and natural antifouling products. Chen *et al.* fabricated antifouling

coatings using nanotopography combined with capsaicin, a natural biocide derived from pepper, showing promising results.<sup>137,138</sup>

## 4. Nanocomposite-based antifouling technology

The above outlined techniques were under intensive exploration for several decades, but the efficiency and natural benevolence of the present-days antifouling agents and methods is still under question. A huge resources are still spent to protect the aquatic systems and monitor the contamination levels, especially in the near-coastal areas (see Fig. 1 and 2).<sup>139</sup> Not surprisingly, innovative techniques are now under consideration to develop novel, green, and highly efficient methods to prevent marine fouling.<sup>140</sup> In this section, we will briefly demonstrate the potential of novel techniques for marine anti-fouling technologies, with the main emphasis on (i) the application of nanomaterials and nanocomposites for anti-fouling, (ii) biomimetic-based approaches for designing marine anti-fouling materials, and (iii) synergistic approaches and techniques. Also, several novel approaches that may evolve into useful relevant technologies in the near future will be explored, including the application of lasers and ultrasound. The main aim of this section is to outline the most promising trends in the development of marine antifouling materials and systems, with some examples highlighted in Fig. 6–16 below.

### 4.1. Novel antifouling nanocomposite-based materials

It is not surprising that the nanocomposites are under exploration as marine anti-fouling protection platforms. Attempts have also been made to *e.g.* incorporate biocide agents into nanostructures to ensure their controlled release and higher efficiency of anti-fouling coatings, but they still remain toxic for the aquatic systems.<sup>141,142</sup>

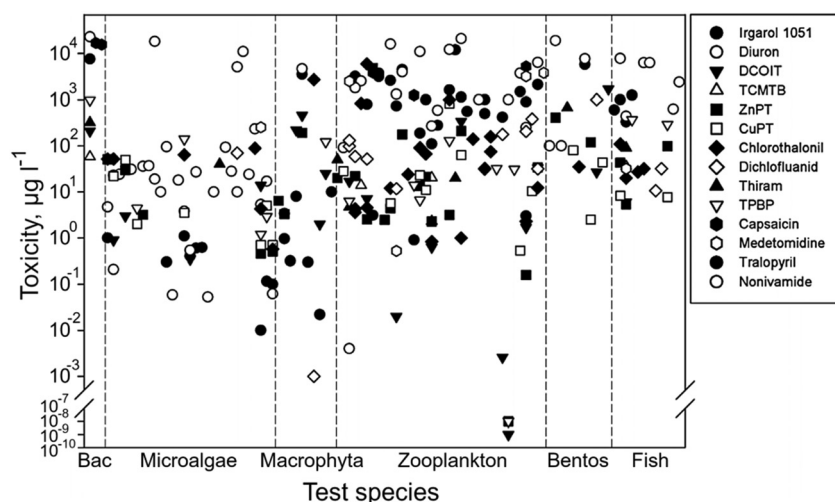


Fig. 5 A comparative chart illustrating the ecotoxicity of various biocides on marine fouling species. Reprinted from Martins *et al.*, 2018.<sup>33</sup>

Another approach is based on complex hierarchical structures<sup>1</sup> which use nanoparticles as antifouling agents.<sup>143,144</sup> Copper cladding was used as an antifouling material from the ancient times, so the antifouling membranes with copper oxide nanoparticles were successfully tested.<sup>145,146</sup> Complex

membranes<sup>147,148</sup> and membranes modified with copper nanoparticles were also tested.<sup>149</sup>

Fig. 6a illustrates the mechanism of enzymatic antifouling of a magnetically separable enzyme precipitate nanofiber-based coating (Mag-EPC). Acylase (AC) was used as an active agent of

## NANOCOMPOSITE-BASED ANTIFOULING TECHNOLOGY

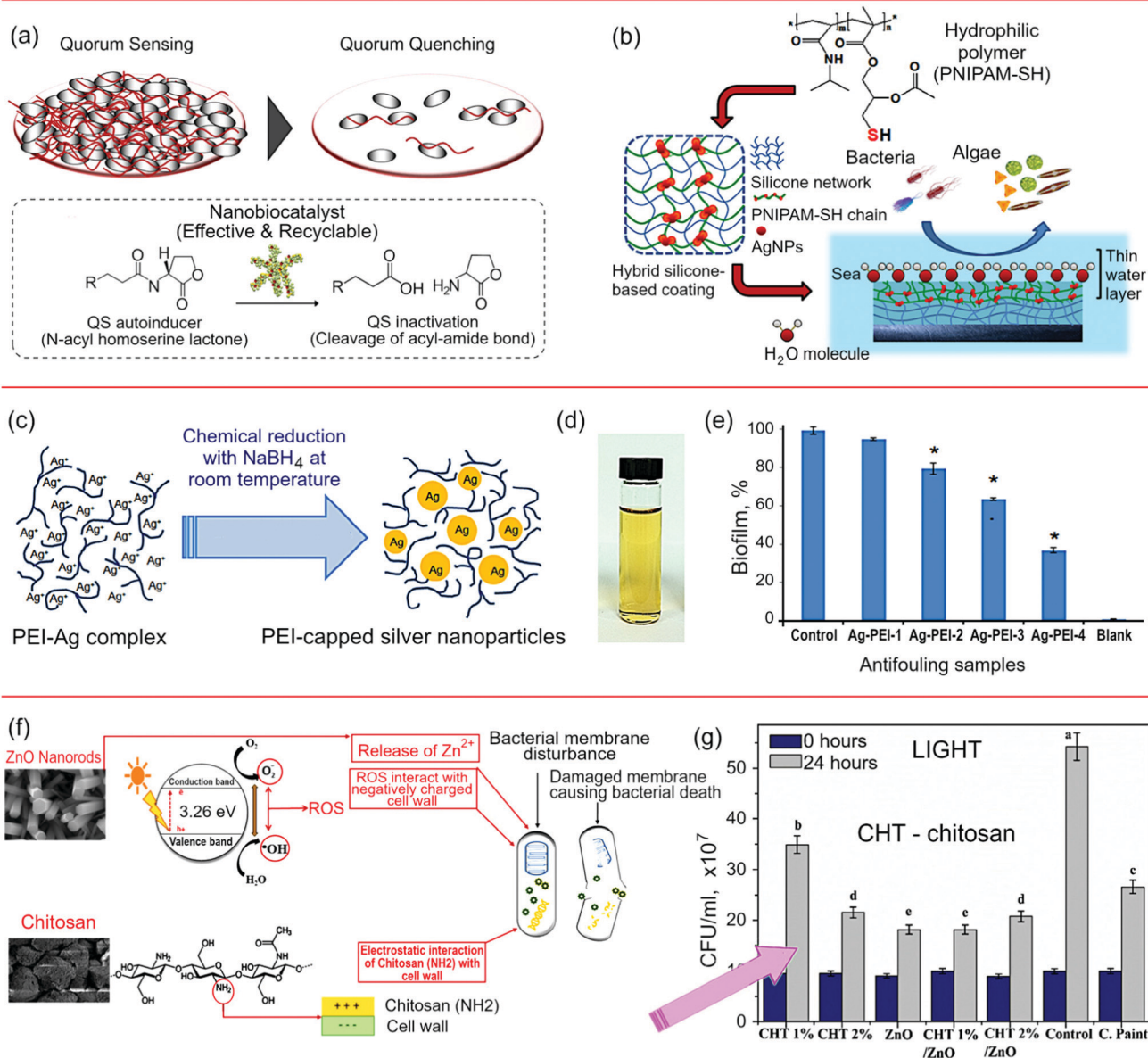


**Fig. 6** Nanocomposite-based alternatives to potentially toxic antifouling paints. (a) Antifouling strategy based on enzymatic activity of a magnetically separable enzyme precipitate coating (Mag-EPC). Acylase (AC) serves as the active agent, and carboxylated polyaniline nanofibers (cPANFs) act as the support onto which the enzyme molecules are attached and stabilized. Reprinted with permission from Lee *et al.*, 2017.<sup>150</sup> (b) Silver/silicone/hydrogel-based nanocomposites with a long-lasting antifouling activity demonstrated during field trials in South China Sea. Reprinted with permission from Tian *et al.*, 2019.<sup>151</sup> (c) Polyethyleneimine (PEI)-capped silver nanoparticles obtained *via* chemical reduction; (d) a colloid of Ag-PEI in water is a clear yellow liquid is effective in inhibiting the growth of *H. pacifica* bacterial biofilm at 10% v/v (e). Bars represent mean  $\pm$  SD, experiments were performed in triplicate. Reprinted with permission from Yee *et al.*, 2019.<sup>152</sup> (f) Chitosan/ZnO nanorod composite films were more effective in preventing *B. subtilis* and *E. coli* fouling onto fiberglass panels under light conditions (30–35 klux) than coatings made of pure chitosan, pure ZnO nanorods, and Zn-based antifouling paints. (g) A comparison of bioactivity between ZnO and chitosan/ZnO composite films against *B. subtilis* expressed as CFU ml<sup>-1</sup>  $\pm$  standard deviation after 0 and 24 h of incubation. Composites containing 2% chitosan showed the highest level of activity when compared to other composites. Reprinted with permission from Al-Belushi *et al.*, 2020.<sup>153</sup>

choice, and carboxylated polyaniline nanofibers (cPANFs) were selected as a platform onto which these active enzyme molecules were attached and stabilized in order to control the level of active agent loaded into the composite and to provide film stability. The attachment and growth of *Pseudomonas aeruginosa* on the surfaces of Mag-EPC films was significantly reduced under both static- and continuous-flow experimental conditions, with films with high level of enzyme loading showing a 5-time reduction in biofilm formation when compared to control. As such, Mag-EPC coatings containing acylase and similar enzymes may provide an attractive alternative to conventional paints by hindering early stages of marine biofilm formation through enzymatic quorum quenching of autoinducers.<sup>150</sup>

Fig. 6b illustrates the application of the hybrid nanocomposite films incorporating active silver nanoparticles and silicone hydrogels. The hydrophilic polymer was employed to enable the self-assembly of smooth spherical structures with a radius of 2–7  $\mu\text{m}$ . As the fraction of silver nanoparticles was increased, the spherical structures became increasingly coated with a thin layer of silicone, resulting in particles that were securely embedded within these films. The resulting films displayed excellent fouling-retarding properties against a variety of organisms, including algae, effectively reducing attachment of *Phaeodactylum tricornutum*, *Navicula torquatum* and *Chlorella* by ~37%, 37% and 52%, respectively, when compared to control surfaces. Tests in the South China Sea confirmed the efficacy of thus-fabricated hybrid coatings under field conditions, confirming their potential in marine antifouling applications.<sup>151</sup>

Fig. 6c–e illustrates the application of silver nanoparticles terminated with polyethyleneimine as fouling-retarding coatings via photocatalytic activity. The average size of the nanoparticles was estimated to be around  $2.6 \pm 1.1$  nm. When used as a colloidal suspension, this nanomaterial was effective in eliminating fouling agents from water (Fig. 6c), retarding biofilm assembly by *Halomonas pacifica*, a marine bacterial foulant frequently used as a model organism in similar studies, by >60% under static flow conditions (Fig. 6e).<sup>152</sup>

Fig. 6f shows the schematics of the proposed pathway of antifouling activity for composite films containing chitosan<sup>154</sup> and ZnO nanorods. When deposited onto the surfaces of fiberglass panels, these coatings demonstrated stronger efficacy in preventing biofilm formation than pristine chitosan, pristine films of ZnO nanorods, and even commercially available paint with Zn as an active agent. These experiments were conducted using *B. subtilis* as the model organism under controlled light conditions of 30–35 klux. The activity was maximised when chitosan was mixed with ZnO at the concentration of 2%. Fig. 6g shows the bacterial retarding ability of chitosan/ZnO composite when compared to pure ZnO against *B. subtilis*, expressed in terms of CFU  $\text{ml}^{-1}$  at 0 and 24 h of incubation. The results strongly suggest that chitosan/ZnO composite materials may serve as a suitable alternative to conventional fouling-retarding paints.<sup>153,155</sup>

Earlier in the article, we have mentioned strategies that rely on the use of enzymes to prevent organism attachment, growth

and biofilm formation. A related method relies on the use of materials that can mimic the activity of natural enzymes as an effective yet more affordable and flexible means to combat biofilm formation of surfaces. For example, Wang *et al.* have developed nano-core-shell structures composed of  $\text{CeO}_2@\text{C}$ , with the material showing activity similar to haloperoxidase enzyme. This nanomaterial is produced *via* coprecipitation by employing carbon spheres as templates. When applied on the surface of Ti plates as a thin coating,  $\text{CeO}_2@\text{C}$  films were able to retard attachment by model Gram-negative and Gram-positive bacteria, including marine *P. aeruginosa*, in bacterial suspension (Fig. 7a). In addition to strong antibacterial activity,  $\text{CeO}_2@\text{C}$  showed a desirable combination of stability, low toxicity for the environment and low cost.<sup>156</sup>

In addition to chemical and enzymatic means, antibacterial and antifouling effects can be attained by employing surfaces with specific topographies, such as protrusions with defined size, aspect ratio, shape and distribution. These can be fabricated using a wide range of methods, from “top-down” laser ablation and plasma etching to “bottom-up” self-assembly or chemical vapour deposition. Many of these methods would be difficult to realise for marine antifouling applications, whereas there are a number of methods that would be suited to scaling up. For example, Lee *et al.* was able to manufacture ZnO nanopillar arrays on a flexible substrate using a very fast ultrasound-assisted approach (Fig. 7b). These arrays were able to directly damage to cells *via* physical interactions with pillars as well as retard attachment *via* electrostatic interaction between cells and the nanopillar-decorated surfaces.<sup>157</sup> The availability of nanoscale surface features substantially increased the surface area available for the interactions between cells and ZnO active surfaces, with films able to achieve antibacterial efficacy of over 80%.<sup>158</sup>

Another method that takes inspiration from antifouling strategies that occur in nature is based on the generation of biochemically-active reactive oxygen species (ROS). These molecules play an important role in cellular signalling and antimicrobial defence, and have been used extensively to break down biofilms and kill biofilm-residing microorganisms. In marine environments, certain species of seaweed are able to retard fouling using ROS. Sathe *et al.* have been able to reproduce this ROS-based antifouling effect by employing ZnO films capable of producing ROS during photocatalysis (Fig. 7c and d). The antifouling properties of surfaces of fishing nets were significantly enhanced through their decoration with ZnO films when compared to both unmodified control and, more importantly, surfaces painted using conventional Cu-based antifouling paints. Field tests for 30 days under tropical conditions demonstrated a 3-fold reduction in the biofouling on the ZnO-decorated surfaces when compared to control. Importantly, genetic studies of the biofilm-forming communities in the ambient water in the proximity of these active surfaces showed that these materials were introducing selective pressure to artificially increase the presence of specific foulants or pathogenic organisms. As such, the development of this and similar materials show an important step in the direction of

## NANOCOMPOSITE-BASED ANTIFOULING TECHNOLOGY

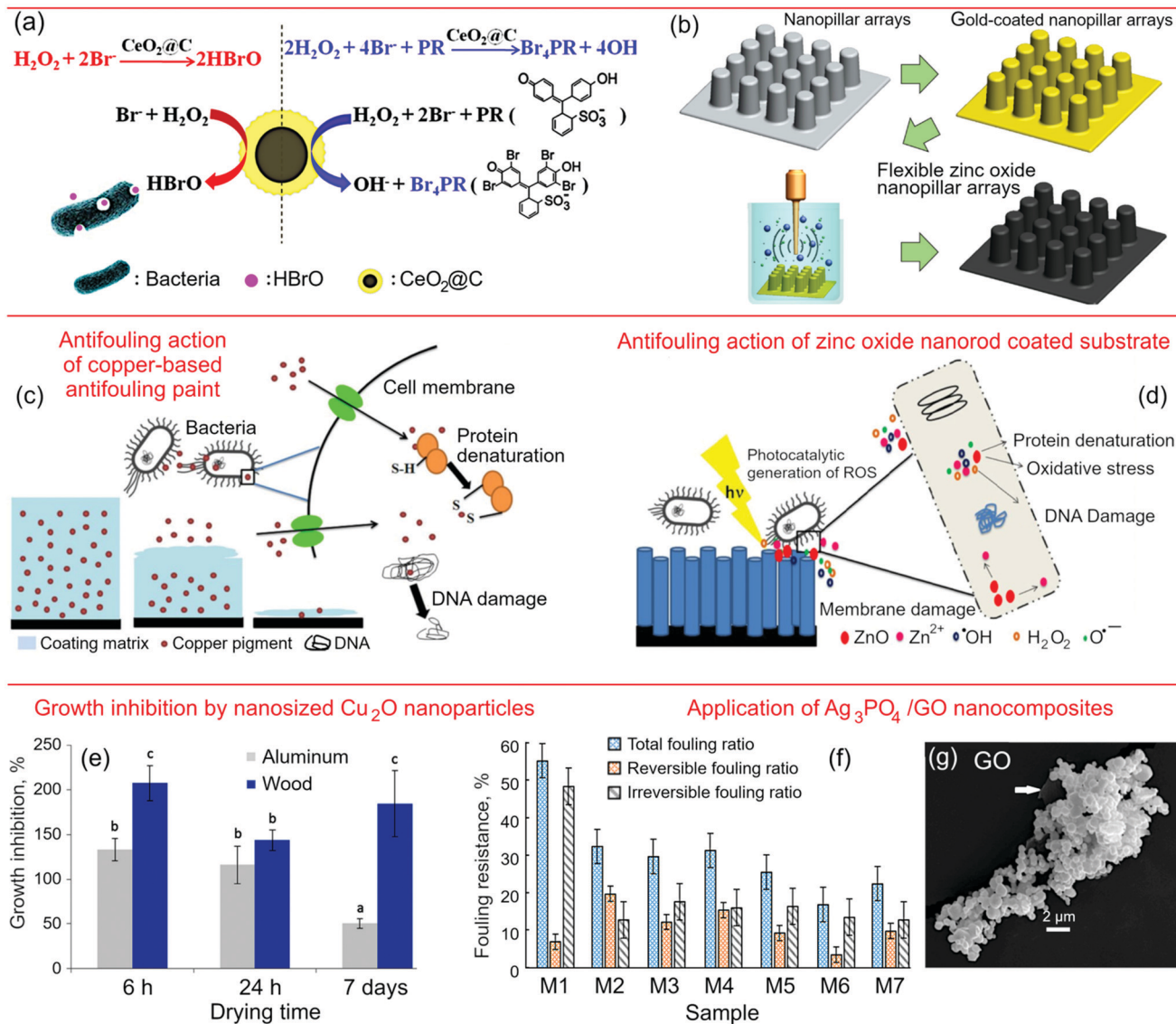


**Fig. 7** (a) Fabrication of stable, environmentally friendly core-shell CeO<sub>2</sub>@C nanostructures with substantial antibacterial efficacy against biofilm forming marine *Pseudomonas aeruginosa*. Reprinted with permission from Wang *et al.*, 2021.<sup>156</sup> (b) Scheme for the fabrication of antifouling nanopillar arrays, gold coated nanopillar arrays, and flexible zinc oxide nanopillar arrays using sonochemical process. Reprinted with permission from Lee *et al.*, 2018.<sup>158</sup> (c) Fouling-retarding mechanism for Cu-based paints and (d) for coatings composed of ZnO nanorods. Field tests under tropical conditions confirmed a 3-fold reduction in biofilm formation for ZnO coatings when compared to control. Reprinted with permission from Sathe *et al.*, 2017.<sup>159</sup> (e) Retardation of proliferation of *Isochrysis galbana* subsequent to the exposure of the organism to paint leachates for 5 days. Leachates were obtained by exposing painted bars to natural seawater for 180 days. Reprinted with permission from Adeleye *et al.*<sup>160</sup> (f and g) Fouling resistance parameters against BSA solution filtration of the Ag<sub>3</sub>PO<sub>4</sub>/GO nanocomposites. Reprinted with permission from Barzegar *et al.*, 2020.<sup>161</sup>

more environmentally benign antifouling technologies for aquatic applications.<sup>159</sup>

It should be noted that the efficacy of a specific strategy and the potentially negative environmental effects will depend, among other factors, on the environmental conditions. For example, Adeleye *et al.* have studied the temporal degradation of antifouling paints containing Cu as the primary biologically-active ingredient. The type and quantity of species released from the paint was influenced by water characteristics, *e.g.* its salinity, as well as the nature of the base surface

and how the paint was applied, in particularly the time available for paint drying. In addition to Cu ions, nanoscale particles of Cu<sub>2</sub>O were detected in the leachate. Fig. 7e shows that the leachate was able to retard the growth of *Isochrysis galbana* after the latter was exposed to it for 5 days. In this study, the paint leachates were generated by exposing painted bars to seawater for 180 days. The amount of leachate and subsequently its toxicity was found to depend on the time the paints was allowed to dry prior to the bar being immersed into the seawater.<sup>160</sup>

One more example of successful application of nanoparticles ( $\text{Ag}_3\text{PO}_4/\text{GO}$  nanocomposite) for anti-fouling application is illustrated in Fig. 7f. In this study, the antifouling nanomaterial was applied over polyethersulfone (PES) mixed matrix membranes, since fouling can significantly reduce the permeability and hence efficacy of these membranes. The use of  $\text{Ag}_3\text{PO}_4/\text{GO}$  notably reduced the irreversible fouling ratio by decreasing BSA adsorption on the surfaces and within the pores of the membranes. Fig. 7g shows the SEM image of  $\text{Ag}_3\text{PO}_4/\text{GO}$  nanocomposites.<sup>161</sup>

Thus, the nanomaterial-based antifouling systems provide quite an efficient and relatively ecological means of protection, with the excellent prospects for scaling up to industrial applications. Among other nanomaterial-based techniques, we should also discuss approaches that use some combinations of nanomaterials and biocides, such as inorganic nanomaterials loaded with booster biocides,<sup>162</sup> beta-cyclodextrin stabilized silver nanocomposites,<sup>163</sup> and capsaicin-induced nanopillar films. Note that capsaicin has a very long history in anti-fouling applications, but it is not sufficiently efficient when used on its own, yet it is a relatively ecologically benign agent. When loaded into nano-structures, capsaicin can show significantly improved anti-fouling performance.<sup>164</sup> Other techniques for enhancing the nanomaterial-based anti-fouling systems are also under investigation, such as pre-ozonation on nanofiltration membranes<sup>165</sup> and encapsulation of environmentally-friendly biocides within nanosystems.<sup>166</sup> For example, polymers fabricated from essential oils and essential oil derivatives, alone or in combination with antimicrobial nanoparticles of ZnO, have been shown to effectively prevent settlement of a wide range of organisms, including under aquatic test conditions.<sup>167,168</sup> When deposited using plasma-based methods, these coatings show good stability and optical transparency, which makes them suitable for application over optical windows for marine sensing applications.<sup>169,170</sup>

- Nano-composites and nanomaterial-based anti-fouling protection systems for marine applications are the important step towards future highly efficient and environmentally friendly anti-fouling agents; however, nanomaterial-based systems are still not sufficiently efficient and at higher doses, may often represent specific danger to the ecosystem. Despite the progress in the area of nanomaterials, better solutions are still needed, and they may be based on the biomimetic and synergistic systems.

#### 4.2. Novel nanocomposite-based superhydrophobic antifouling and fouling-release materials

Surface architectures and composites with a combination of roughness at micro- and nano-scales and favourable chemistry may display superhydrophobicity.<sup>171,172</sup> Fouling resistant or fouling release coatings based on superhydrophobic coatings with tailored surface topographies<sup>173</sup> are currently a subject of intense investigation,<sup>174,175</sup> including for marine antifouling applications. Superhydrophobic properties could potentially block the adsorption of living organisms and hence, prevent or slow down the formation of fouling on the treated surfaces.

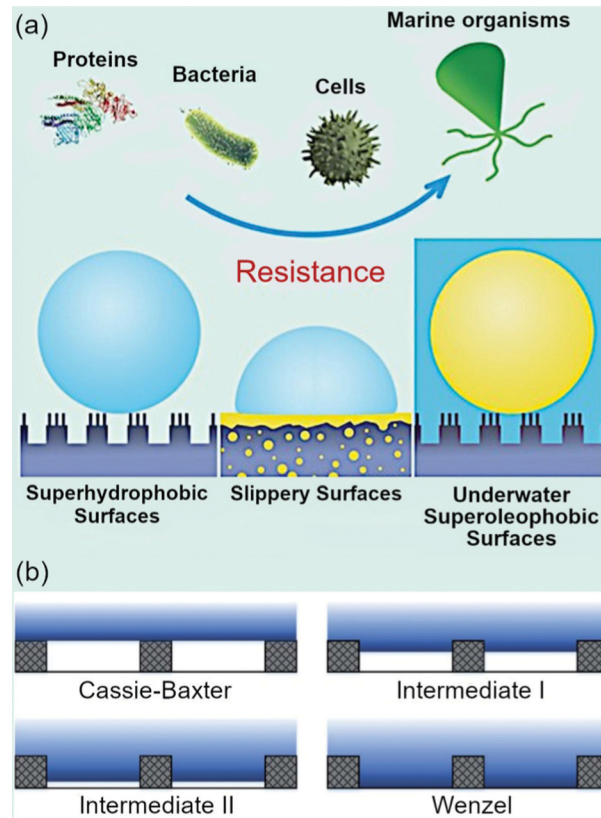


Fig. 8 Cassie–Baxter and Wenzel states. (a) Direct influence of the hydrophobic properties on the resistance to marine fouling. Reproduced with permission from Zhang *et al.*, 2016.<sup>185</sup> (b) Side view of contact between the water drop and pillars at four different wetting states, including Cassie–Baxter and Wenzel states, and transition states, in a bulk liquid. In the case of Cassie–Baxter state, the liquid does not contact the entire surface and is supported by the air trapped within topographic irregularities on the surface. In the case of Wenzel state, the liquid contacts the surface of irregularities. Reproduced with permission from Cho *et al.*, 2020.<sup>180</sup>

Superhydrophobic properties could potentially block the adsorption of living organisms and hence, prevent or slow down the formation of fouling on the treated surfaces (Fig. 8a). Superhydrophobicity is characterized by the contact angle (CA) exceeding  $150^\circ$  and sliding angle less than  $10^\circ$ . On a flat surface, CA of only about  $120^\circ$  could be produced by lowering the surface energy *via* chemical means. To reach above the  $120^\circ$  threshold, a sophisticated engineered surface morphology is required to minimize the interface between liquid and solid body.<sup>176</sup> The models that describe the influence of surface topography on the liquid–solid interface are continuing to evolve. In practice, however, the Cassie–Baxter (CB) and Wenzel (W) models are among most commonly used.<sup>177–179</sup> Superhydrophobicity is usually described by the Cassie–Baxter state, where the liquid cannot penetrate into the space that exists between protruding features of the textured surface (*i.e.*, between hillocks on the surface) due to air being trapped in that space, and as a result, a complex interface of solid–liquid–vapour is formed where the contact area between the liquid and

the solid phases are minimised. However, it is possible for the surface to transition from Cassie–Baxter to Wenzel states. This may happen *e.g.* when the water is driven into the surface with some force, displacing the air bubbles. The transition is illustrated in (Fig. 8b). Naturally, the static contact angles are different for these states and are also different from the angles intrinsic for Cassie–Baxter and Wenzel states.<sup>180</sup> In Wenzel state, the liquid penetrates completely into the hollows between surface irregularities, maximising the contact area between the liquid and the surface.<sup>181</sup> Unlike the slippery Cassie–Baxter surface from which droplets of water are easily displaced, the high liquid–solid contact area makes it difficult for the droplet to roll off the surface. Evidently, the Cassie–Baxter state is preferred for self-cleaning surfaces, where rolling droplets would physically displace particles and attached organisms. Self-cleaning surfaces can also be realised using surfaces in the Wenzel state, by introducing a water-repelling liquid that would effectively penetrate the surface protrusions and create a slippery layer from water would slide off with ease. In both instances, it would be difficult for the biomolecules (*e.g.* conditioning molecules released by cells in the proximity of the surface) and for the cells to attach to such surfaces. Importantly, the states could be efficiently controlled by the density, heights, shape and other geometrical parameters of the surface topography.<sup>182–184</sup> This opens the way for application of nano-textured surfaces in antifouling technology.

Superhydrophobic coatings do not contain chemically dangerous substances and thus could be considered an environmentally friendly technology. However, their fabrication at scale has always been a challenge.<sup>186</sup> Several promising materials that use nano-fillers in various base materials have recently been explored. Selim *et al.* have demonstrated two types of superhydrophobic antifouling materials with excellent fouling-release properties (Fig. 9a and b). These materials incorporated nanofillers made of either graphene oxide or graphene oxide/boehmite nanorods (GO- $\gamma$ -AlOOH) into polydimethylsiloxane (PDMS) matrix, with the inherent properties, quantity and distribution of the filler defining the self-cleaning and antifouling properties of the resulting composite. The fillers were prepared using thermochemical techniques that are relatively simple and amenable to scale up, with hydrothermal and chemical depositions used to synthesize reduced graphene oxide and GO- $\gamma$ -AlOOH, respectively.<sup>187</sup> The quality of thus-fabricated filler materials was high, with  $\gamma$ -AlOOH nanorods showing single crystallinity, an average diameter of 10–20 nm, and typical length of the rod of less than 200 nm. When the fouling-release efficacy of the composite coatings (at 3 wt% of filler) was compared to that of pristine PDMS under natural marine water field conditions for 45 days, the latter was found to be more heavily settled by organisms. In contrast, the PDMS/reduced graphene oxide composite showed a significantly lower fouling load, whereas PDMS/GO- $\gamma$ -AlOOH surfaces remained entirely unaffected by fouling. The homogeneity of dispersion was found to be critical to the impressive superhydrophobic and antifouling performance of PDMS/GO- $\gamma$ -AlOOH composite,

with uniform reduction in the surface free energy across the surface of the coating.

Superhydrophobic nanocomposite-based antifouling coatings could be synthesized without the use of relatively expensive graphene and graphene oxides, by using *e.g.* core–shell nanofillers as an alternative. For example, nanorod-like TiO<sub>2</sub>–SiO<sub>2</sub> core–shell particles were used to impregnate silicone matrices to produce superhydrophobic composites capable of fouling release under marine conditions.<sup>188</sup> Here, single crystal {101} TiO<sub>2</sub> nanorods ( $d = 20$  nm) were first hydrothermally synthesized, then sol–gel coated with silica shells with a thickness of 2–5 nm, and then dispersed in a silicone matrix at different filler concentrations (Fig. 9c). Fig. 9d illustrates the antifouling efficiency of the superhydrophobic composites with core–shell nanofillers. For this test, barnacles were used as the model organism that often dominates macrofouling in marine water. Over 7 days of exposure, cyprids were allowed to settle on the composite-coated surfaces. The study found the composite coatings to be more effective in retarding cyprid attachment (at 5–55% *vs.* 70% for the pristine silicone coatings), with similar levels of viability (at  $\sim 75\%$ ) across all sample groups. The attachment retarding ability of the silicone/TiO<sub>2</sub>–SiO<sub>2</sub> composite coating was closely related to the uniformity of dispersion of the filler material, with filler levels of 0.5 wt% showing the highest level of attachment prevention due to improved photocatalytic self-cleaning and fouling release behavior in the coating.

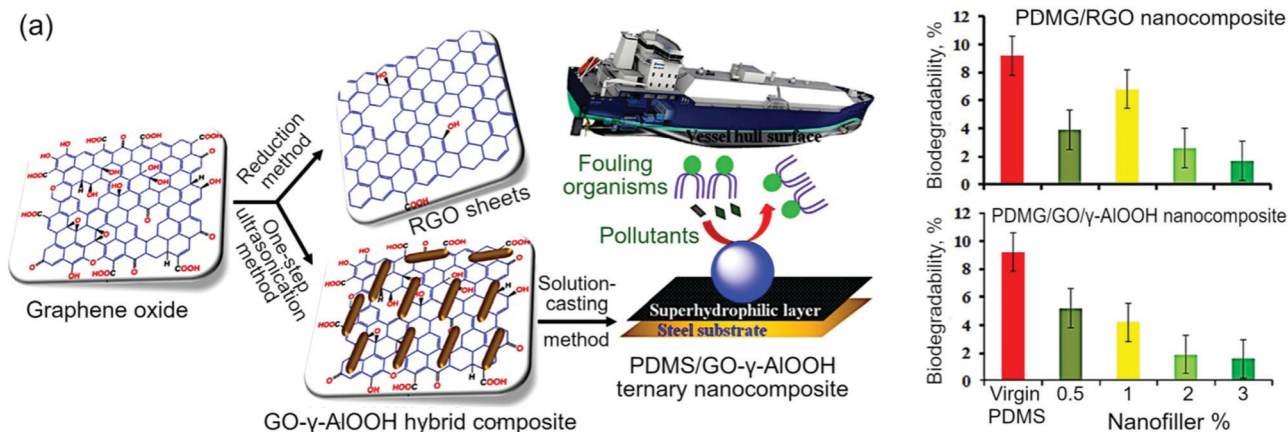
Silicone/ZnO nanorod composites also were recently proposed and tested as superhydrophobic antifouling coatings. ZnO nanorods ( $d = 30$ – $40$  nm,  $l = 0.5$ – $1$   $\mu\text{m}$ ) with a single-crystal (0001) wurtzite structure were incorporated into polydimethylsiloxane at a concentration of 0.5 wt%, producing a superhydrophobic material with increased surface roughness and reduced surface free energy that were stable over time. The stability is an important factor that determines the lifetime and hence feasibility and financial viability of proposed coatings for marine applications.<sup>189</sup> Fig. 9e illustrates the mechanism of superhydrophobicity realised in this coating, where the high density of packing of ZnO nanorods within the top of PDMS surface layer produces a rough surface that can trap pockets of air, reducing water–surface contact area following the Cassie–Baxter model. Optimization of filler concentration and distribution allows for the surface to remain in the “droplet sliding” Cassie–Baxter mode and prevent its transition to “droplet sticking” Wenzel mode. Optimization of surface topography also defines the convexity of the liquid/air interface, keeping it low and maintaining water contact angle values below the advancing value.<sup>190</sup> Fig. 9e shows the differences in the free energy of the coating surface prior to and subsequent to prolonged immersion in aqueous media. A significant increase in the water contact angle could be noticed for the nanofiller percentage 0.5.

Fig. 10a illustrates the preparation route for the superhydrophobic antifouling coating based on PDMS/exfoliated graphene oxide–Al<sub>2</sub>O<sub>3</sub> nanorod hybrid sheets composites. This technology involves first anchoring together graphene oxide

# NANOCOMPOSITE-BASED SUPERHYDROPHOBIC ANTIFOULING MATERIALS

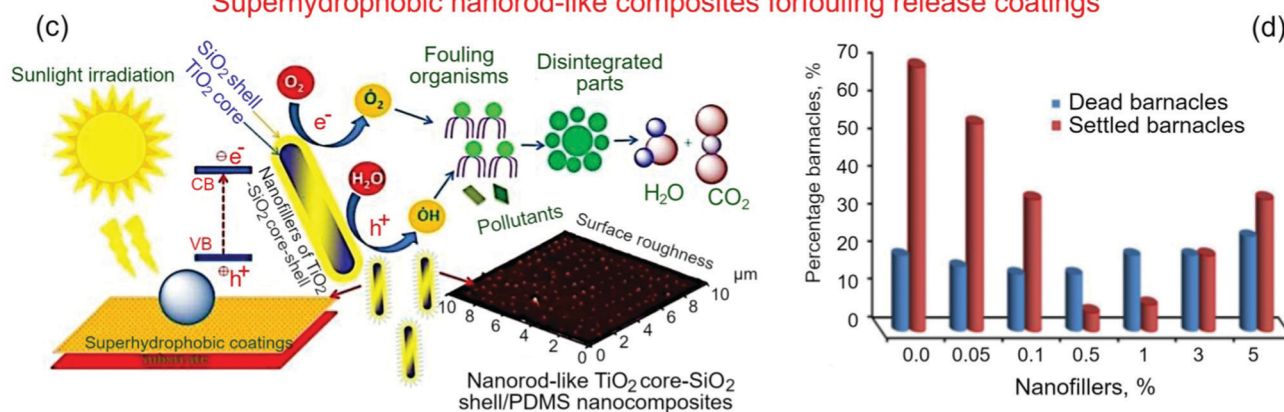
## Superhydrophobic and fouling-release coatings based on RGO and GO- $\gamma$ -AlOOH

(b)



## Superhydrophobic nanorod-like composites for fouling release coatings

(d)



## Superhydrophobic and foul-release mechanism of PDMS/ZnO nanorod composites

(f)

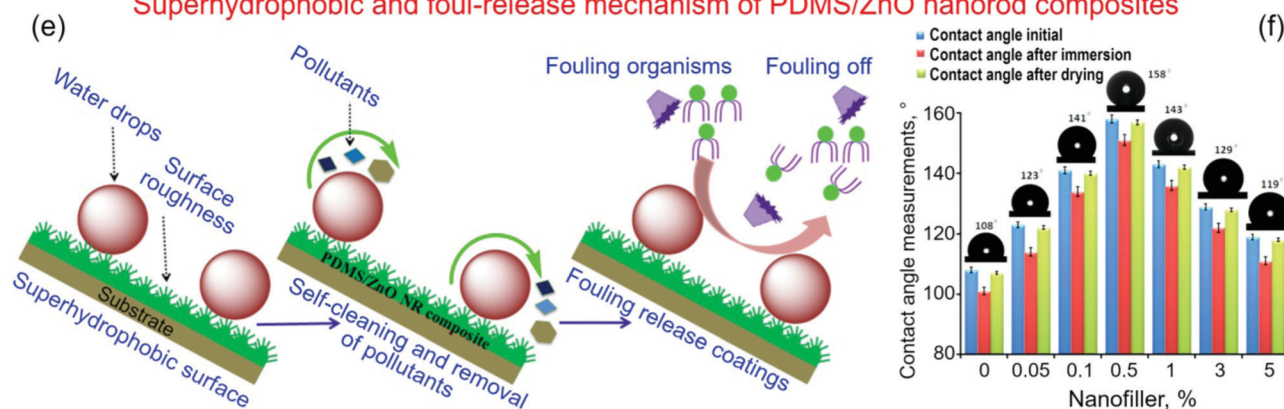


**Fig. 9** Nanocomposite-based superhydrophobic antifouling and fouling-release materials. (a) Graphene oxide is chemically reduced, and then ultrasonicated with  $\gamma$ -AlOOH to produce GO- $\gamma$ -AlOOH composite. (b) Degradation and microorganism attachment behavior of PDMG/RGO and PDMG/GO- $\gamma$ -AlOOH nanocomposites over 30 days of incubation in microorganism-rich medium. Reprinted with permission from Selim *et al.*, 2022.<sup>187</sup> (c) PDMS/nanorod-like TiO<sub>2</sub>-SiO<sub>2</sub> core-shell composites retard microorganism attachment through a combination of superhydrophobicity and photocatalytic performance, the latter attributed to the {101} crystal plane on the TiO<sub>2</sub> rod. (d) Attachment and mortality of barnacle cyprids on pristine and filler-enriched silicone matrix after 7 days of incubation. Reprinted with permission from Selim *et al.*, 2019.<sup>188</sup> (e) Antifouling efficacy of PDMS/ZnO (0.5 wt%) nanorod composites. (f) Water contact angle values of the silicone/ZnO nanorod composite antifouling coatings prior and subsequent to immersion tests (7 days) and for the dried coating. A significant increase in the water contact angle is evident for the nanofiller percentage of 0.5. Reprinted with permission from Selim *et al.*, 2019.<sup>189</sup>



## NANOCOMPOSITE-BASED SUPERHYDROPHOBIC ANTIFOULING MATERIALS

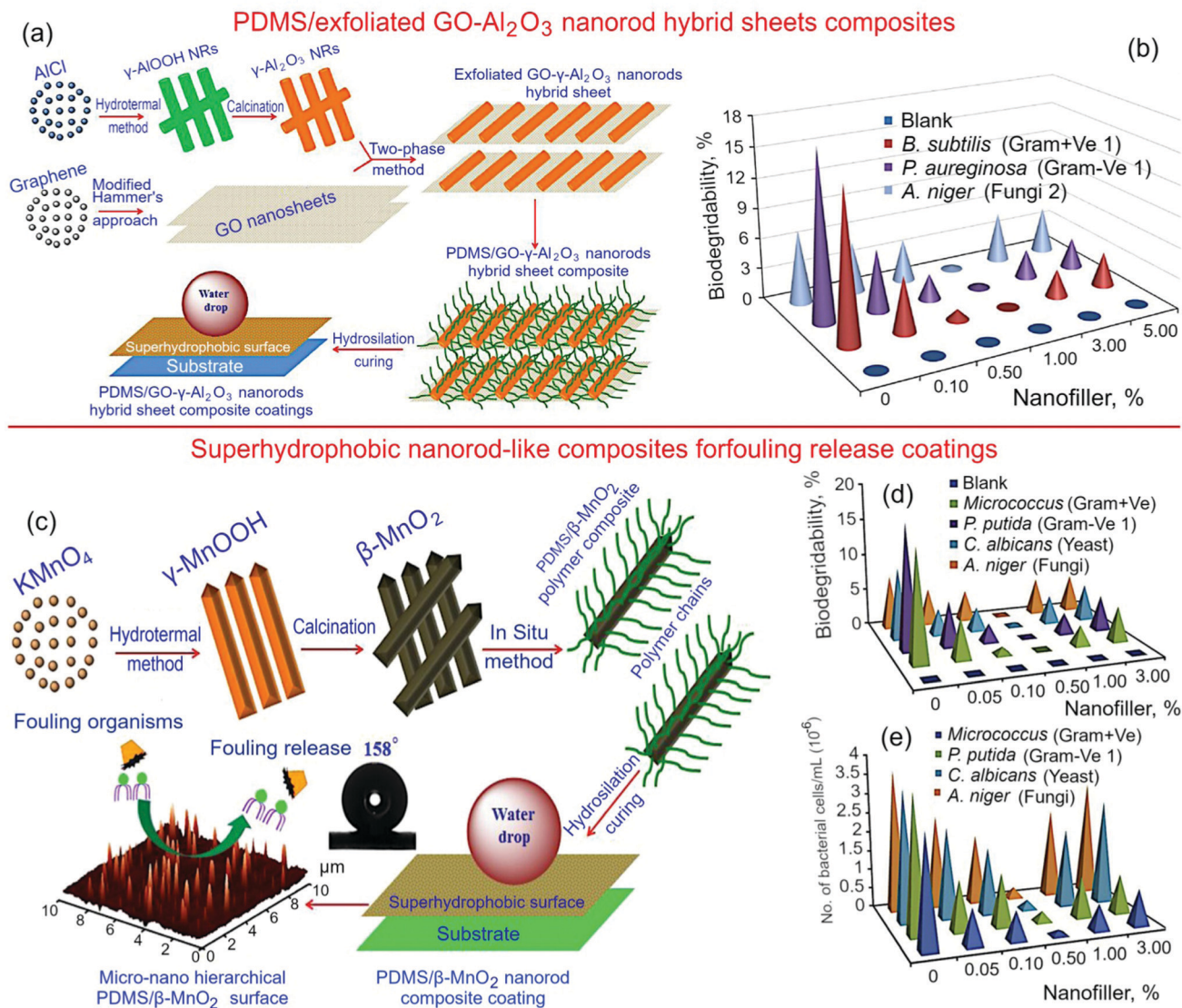


**Fig. 10** Nanocomposite-based superhydrophobic antifouling and fouling-release materials. (a) Introduction of exfoliated GO-Al<sub>2</sub>O<sub>3</sub> nanorod hybrid sheets into PDMS matrix followed by hydrosilation curing. (b) Biodegradability and microorganism attachment to pristine and GO-Al<sub>2</sub>O<sub>3</sub>-enriched PDMS matrices during 28 days of incubation in bacteria- and fungi-rich culture media. Reprinted with permission from Selim *et al.*, 2018.<sup>191</sup> (c) Hydrothermal synthesis and subsequent calcination of β-MnO<sub>2</sub> nanorods, followed by *in situ* synthesis of PDMS/β-MnO<sub>2</sub> nanorod composite films with high levels of surface roughness. (d) Biodegradability and (e) bacterial load (cells per ml) in biofilms developed on pristine and β-MnO<sub>2</sub> nanorod-enriched PDMS matrices over one month of incubation in culture media containing representative strains of microorganisms. Reprinted with permission from Selim *et al.*, 2019.<sup>192</sup>

sheets and alumina nanorods (γ-Al<sub>2</sub>O<sub>3</sub>,  $d = 20$  nm,  $l = 150$  nm), and then uniformly coating the resulting nanostructure with silicone, and subjecting the composite to hydrosilation curing. Optimization studies confirmed filler concentrations showed a decrease in the biodegradation and improved antifouling properties as the filler percentage increased up to 1 wt%, associated with the decrease in the surface free energy and increased micro- and nano-scale roughness.<sup>191</sup> Fig. 10b shows the results of the biodegradability tests over one month of exposure, confirming a desirable combination of cohesion, self-cleaning, and fouling release. As with previously discussed examples, the

quality of dispersion was shown to be critical to durability and performance of the composites.

In addition to ZnO and TiO<sub>2</sub> nanoparticles, structure and fouling release properties of a novel superhydrophobic composite for fouling release application based on silicone/β-MnO<sub>2</sub> nanorod combination was investigated, with results illustrated in Fig. 10(c–e). The structure and properties of β-MnO<sub>2</sub> nanorods were influenced by the preparation method, and in turn influenced the self-cleaning and antifouling properties of the matrix, the latter being also dependent on the concentration and quality of dispersion of the particles in silicone.

This is because the size (in this study  $d = 20\text{--}30\text{ nm}$ ,  $l = 0.5\text{--}1\text{ }\mu\text{m}$ ), and crystallinity (in this study, a [100] single crystal wurtzite structure) determine surface stability, antimicrobial and catalytic efficacy, and surface free energy of the material. Once dispersed in the matrix, the addition of fillers resulted in the concentration-dependent increase in the surface roughness, hydrophobicity and fouling release properties,<sup>192</sup> with well-dispersed composites showing the most promising levels of improvement in these characteristics. A 90 day-long field test using natural seawater confirmed sustained fouling release behaviour of the composite materials, with the greatest level of fouling prevention reported for the well-dispersed material sample groups.

### 4.3. Novel graphene oxide-based antifouling nanomaterials

Materials in the graphene family have been attracting an unprecedented level of interest from the material science community, with the interest stemming from an unusual combination of chemical and physical properties commonly displayed by these materials. These include, but are not limited to, biocompatibility, electro-catalytic activity, and thermal, physical and chemical stability.<sup>193</sup> Within the family, reduced graphene oxide is one of the best studied materials for the production of superhydrophobic materials,<sup>194</sup> based on such factors as inherent hydrophobicity, outstanding specific surface area, abrasion and wear resistance, and superior electrical and thermal conductivity.<sup>195</sup> In the area of antifouling coatings, nanostructures based on graphene oxide decorated with other one-dimensional particles have been demonstrated to be an effective filler material for self-cleaning fouling release silicone composites.<sup>196</sup>

The application of graphene oxide allows for the fabrication of very attractive nanocomposites with adjustable elastic modulus values, capable of efficient antifouling performance. The diatom attachment results described in a recent work by Jin *et al.*<sup>197</sup> follow the “harmonic motion effect” theory, where lighter colors and low Young’s moduli lead to reduced organism attachment to surfaces under hydrodynamic conditions. Composite membranes containing 0.36 wt% of graphene oxide displayed superior ability to retard fouling. The study also found graphene oxide to be an equally effective additive to graphene when it comes to improving antifouling performance of PDMS, yet graphene is often more affordable to produce. Fig. 10a–e show the importance of dispersion in the production of high-quality composite materials, with molding and curing also needed to give the final shape to the product.

Fig. 11f illustrates the results of diatom attachment onto composite membrane surfaces under static conditions after 8 days of incubation, and Fig. 10g provides comparative results of similar tests conducted under hydrodynamic conditions over 10 days. As it can be seen from the comparison of these two images, a sharp drop in the optical density ( $\text{OD}_{440}$ ) for the graphene oxide content of about 0.36 wt% is observed for the measurements performed under the hydrodynamic conditions.

Zhang *et al.* have recently demonstrated that nanocomposites containing the graphene oxide/silver nanoparticles could

provide an effective means of protection of such polymers as polypropylene from marine fouling. As with previous nanocomposite examples, there was a clear correlation between the quality of dispersion and the resulting antifouling behavior of graphene oxide/silver composites.<sup>198</sup> The antimicrobial activity of the graphene oxide/Ag complex is attributed to the synergistic effect of contact killing and chemical stress from the reactive oxidative species generated by the composite.<sup>200</sup> Fig. 11h illustrates the preparation of graphene oxide/silver nanoparticles nanocomposites, including two major steps: (1) ultrasonic bath for 30 min to ensure efficient deagglomeration of Ag particles, and (2) ice bath for 30 min and stirring at room temperature for 12 h. For the antifouling protection tests, the composite coating was dropped cast onto the surface of materials typically used to house marine sensors. These coated materials were subsequently immersed into media containing *H. pacifica* as well as a mixture of algae species. The coating showed effective reduction in the biofilm formation of 83% in the case of *H. pacifica* and of 56% against of the mixed species algae culture.

Fig. 11i illustrates one more example of the elastic graphene/silicone rubber composite membrane for antifouling applications.<sup>199</sup> Many of the natural marine surfaces capable of preventing fouling are unstable under hydrodynamic conditions, and that micron-scale deformations that form on the surfaces of elastic materials under these conditions may provide a mechanical mechanism for removing fouling agents from the surface more effectively. To confirm this mechanism was at play, the study compared the attachment of microorganisms on the surfaces of rigid polystyrene and of flexible graphene-silicone rubber composite membranes. Where under quasi-static conditions, the fouling repelling properties were similar between these two groups of materials, the elastic surfaces displayed superior performance under hydrodynamic conditions. This is because under turbulent flow, the elastic surfaces behaves as a spring and damper-backed system, that is it produces microflaws due to surface transverse shrinkage in response to sufficiently high stresses concentrated at the interface during microorganism settlement under these flow conditions. These stress-induced flaws is in addition to flaws that naturally occur on surfaces of both elastic and rigid materials, and contribute to the detachment of organisms under stronger turbulent flows. This mechanism can be exploited to design elastic composite coatings that would facilitate efficient microorganism detachment under low flow forces. Fig. 11j illustrates the number of colony forming units attached to the surfaces of pristine and graphene-enriched silicone composites, with the former showing a much greater bacterial load.

In this section we have outlined the most recent, within the last two years, progress and ideas for the nanocomposite-based antifouling strategies. It should be noted that the marine antifouling protection systems and platforms based on nanocomposites and functional nanomaterials could be considered as one of the most promising steps towards future highly efficient and environmentally friendly solutions to marine antifouling. The literature is rich with examples of different

## GRAPHENE OXIDE-BASED ANTIFOULING NANOMATERIALS



**Fig. 11** Graphene oxide- and graphene-based antifouling materials. (a–e) Multi-step synthesis of silicone membranes containing graphene or graphene oxide particles: preparation of dispersion containing graphene oxide (a) and silicone (b), their mixing (c), molding in an acrylic mold (d) and curing (e). (f) Diatom attachment under static (f, OD<sub>440</sub> results after 8 days) and hydrodynamic (g, OD<sub>440</sub> results after 10 days) conditions. Reprinted from Jin *et al.*, 2019 under terms of CC BY license.<sup>197</sup> (h) Fabrication of graphene oxide/silver nanoparticles nanocomposites. Reprinted from Zhang *et al.*, 2021 under terms of CC license.<sup>198</sup> (i) Organism–surface interactions on the rigid and elastic silicone/graphene membranes in turbulent flow. The contact area between the microorganism and the elastic surface is sufficiently small to allow its removal from the surface at a low external force (denoted by F<sub>2</sub>). (j) Viability of organisms harvested from the surfaces of membranes and expressed in terms of colony forming units. Reprinted with permission from Jin *et al.*, 2019.<sup>199</sup>

types of nanomaterials and nanocomposites successfully tested for antifouling applications, including nanoparticles, nanofibers, nanorods, nanosheets, flakes and many others

entrapped within traditional and unusual matrices. The diversity of potentially applicable nanomaterials, shapes and composites opens a wide door for the future progress in

nanomaterial-based antifouling technology. At the same time, the currently developed and aforementioned examples are yet to reach the level of efficiency for commercial applications. Furthermore, their potential to affect the environment when used at industrial scale is yet to be fully explored. Despite the progress in the area of nanomaterials, better solutions are still needed, and they may be based on the biomimetic and synergistic systems described below in Sections 4 and 5. Importantly, the biomimetic and synergistic approaches also to a large extent will rely on the advances in nanomaterials and nanotechnology.

## 5. Synergistic approaches for novel antifouling techniques

While novel nanomaterial-based antifouling systems demonstrate much higher efficiency as compared to the traditional means, they still represent some risk of environmental pollution of aquatic systems.<sup>201</sup> In tropical aquatic systems, these adverse effects are usually even more pronounced.<sup>202,203</sup> Not surprisingly, novel approaches are being explored to develop even more efficient and ecologically benign solutions.<sup>204,205</sup>

Synergistic effects on a subject (*i.e.* surfaces, living cells, *etc.*) arise when two or more agents used together produce a combined effect that significantly exceeds a simple sum of effects of agents when they are used separately. This happens in the cases when interaction between agents or/and of agents with the subject (*i.e.*, a substrate surface) produces a new phenomenon or process that can be initiated and sustained only in a system when two or more agents are used together. Synergistic effects have been demonstrated in a large number of complex systems and processes including low-temperature plasmas,<sup>206</sup> various surface-based processes,<sup>207</sup> in catalysis,<sup>208,209</sup> at plasma-liquid interfaces,<sup>210</sup> at different scales during

nanofabrication,<sup>211,212</sup> in nanomedicine<sup>213,214</sup> and many other fields. Not surprisingly, attempts have been made to harness these valuable phenomena to find synergistically interacting antifouling agents for marine applications.

One of the successful results was recently presented by Dupraz *et al.*<sup>215</sup> In their work, the toxicity of the antifouling compounds diuron, irgarol, zinc pyrithione, copper pyrithione and copper was tested on the three marine microalgae *Tisochrysis lutea*, *Skeletonema marinoi* and *Tetraselmis suecica*. A mixture of ZnPT together with Cu induced a strong synergistic effect on *T. suecica* while a strong antagonistic effect was observed on the two other species. The synergy was due to the transchelation of ZnPT into CuPT in the presence of Cu, CuPT being 14-fold more toxic than ZnPT for this species. The results are illustrated in Fig. 12 in the form of isobolograms (more details about the isobologram analysis could be found in this comprehensive topical review<sup>216</sup>). Fig. 12a illustrates the typical isobologram with the relevant notifications, and Fig. 12b and c show the isobolograms for *T. suecica*, demonstrating a strong synergistic effect that cannot be achieved by a simple combination of the antifouling agents. Importantly, only *T. suecica* has demonstrated a response to this synergistic effect and hence, the processes that cause synergistic effects are very complex and depend not only on the chemical agents but also on the properties of the biological target.

Fig. 13 shows several specific examples of the application of synergistic effects that can be found in the nanomaterial-based antifouling systems. The desirable synergistic effects are particularly pronounced when the antifouling agents are combined with nanomaterials.<sup>217</sup> Deng *et al.* reported the results of recent studies on the synergistic antifouling effect of a hybrid coating embedded with nanocomposite silver/tannic acid/silica (Ag@TA-SiO<sub>2</sub>) particles. Schematic diagram for different nanoparticles is illustrated in Fig. 13a. The ability of the system to retard fouling was tested on microalgae *N. closterium* and *Dicrateria zhanjiangensis*. The properties

### ISOBOLOGRAMS OF BINARY MIXTURES WITH SIMILAR AND DISSIMILAR MODES OF ACTION

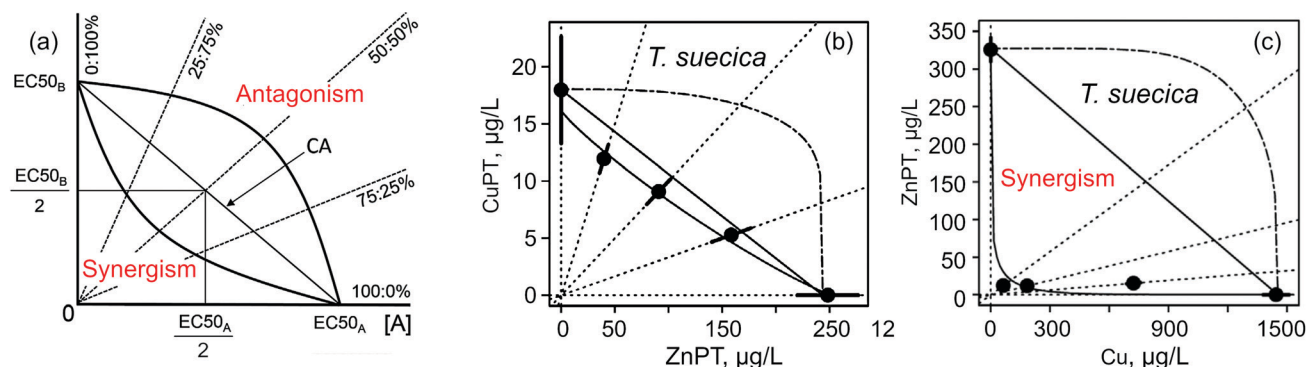
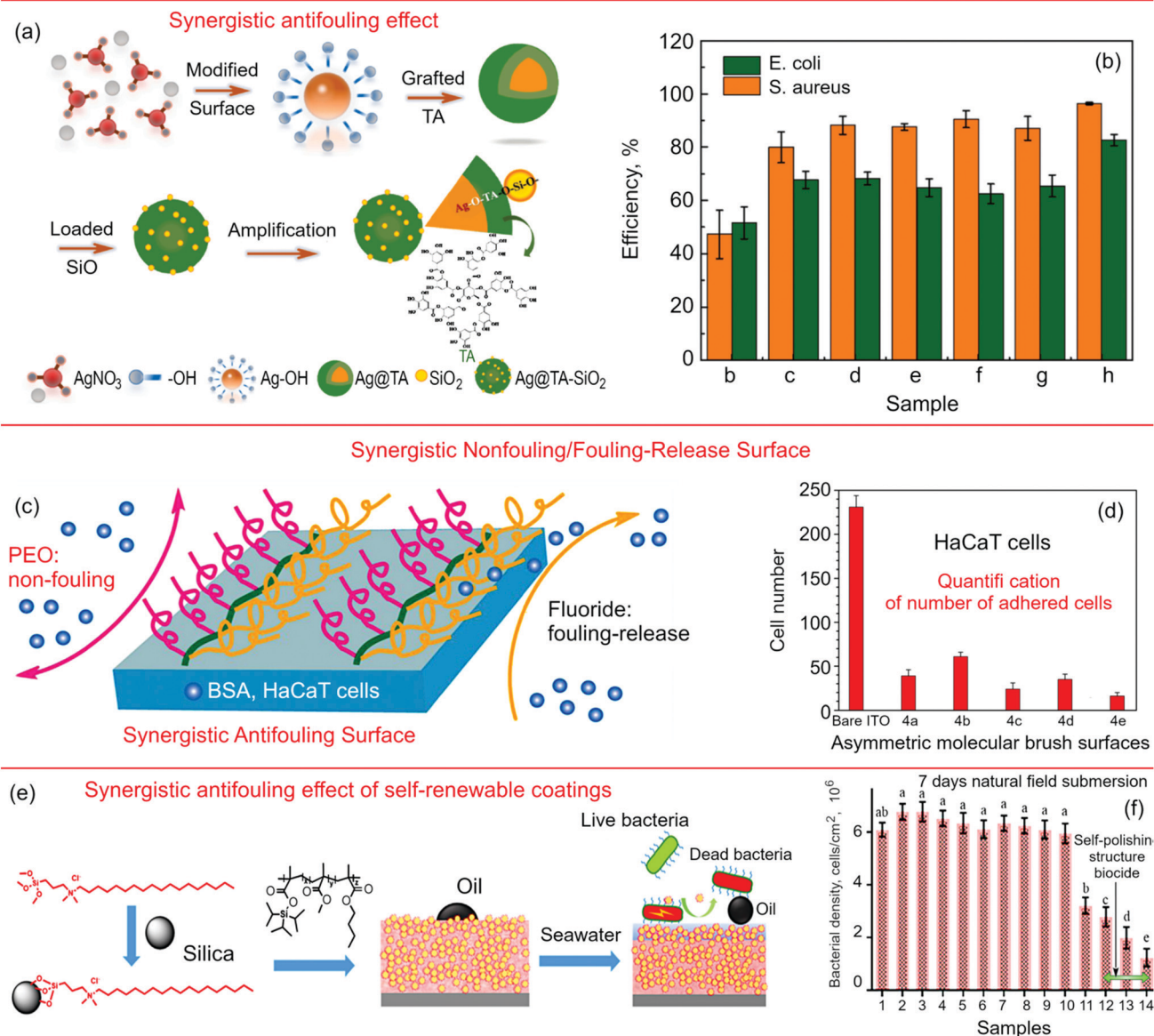


Fig. 12 (a) Illustration of an isobologram. Axes represent the concentration of the two pure substances in mixture A and B, also represented as mixture ratios 100 : 0% (A) and 0 : 100% (B). The dashed lines represent mixture ratios 75 : 25, 50 : 50 and 25 : 75% (A : B). The straight solid line identified as 'CA' is the CA isobole. The curved solid lines symbolize isoboles illustrating either antagonism (above CA) or synergism (below CA). (b and c) Example of isobolograms with similar (b) and dissimilar (c) modes of action: isobolograms for *T. suecica*, demonstrating a strong synergistic effect that cannot be achieved by a simple combination of the antifouling agents. Reprinted with permission from Dupraz *et al.*, 2018.<sup>215</sup>

## SYNERGISTIC APPROACHES



**Fig. 13** (a) Schematic diagram for different nanoparticles made of Ag, Ag@TA (silver/tannic acid), and Ag@TA-SiO<sub>2</sub> (silver/tannic acid/silica). The loading of SiO<sub>2</sub> microspheres can be selective towards specific sites on the surface of a core-shell Ag@TA template. The raspberry-like Ag@TA-SiO<sub>2</sub> nanoparticle structures are then formed. (b) The antibacterial efficiencies of the nano-structured surfaces towards *E. coli* and *S. aureus*, as compared with the bare glass control. Reprinted with permission from Deng *et al.*, 2021.<sup>219</sup> (c) Schematics of the synergistic surface and (d) quantification of cells appearing on asymmetric molecular brush surfaces. Reprinted with permission from Xu *et al.*, 2017.<sup>220</sup> (e) Fabrication of self-polishing film from SiO<sub>2</sub> nanoparticles decorated with biologically-active quaternary ammonium and fouling-retarding mechanism of this film in seawater. (f) The cell density of bacteria and diatoms on the surface of the film after being exposed to seawater under field test conditions for 7 days. Reprinted with permission from Wang *et al.*, 2020.<sup>221</sup>

of the polymeric matrix is so that it is able to effectively limit the attachment and settlement of the tested species by weakening the strength of cell adhesion to the polymer surfaces. In addition to this mechanism, temporal leaching of Ag@TA-SiO<sub>2</sub> nanoparticles from the polymer matrix hinders the ability of the attached cells to photosynthesize, thus decreasing their chlorophyll activity and reducing their ability to proliferate. These nanoparticles can also induce oxidative stress in these cells, with ROS damaging the cellular

membrane structure of these organisms.<sup>218</sup> Unlike *E. coli* and *S. aureus*, *N. closterium* and *Dicrateria zhanjiangensis* are planktonic rather than biofilm forming, and thus their interactions with the leached nanoparticles are expected to be different. The particles were more effective against *Dicrateria zhanjiangensis* when compared to *N. closterium*, attributed to the presence of the cellular wall in the latter organism.<sup>219</sup> The level of antimicrobial activity of these nano-structured surfaces when regarding the attachment of *E. coli* and

*S. aureus* were estimated at 46.5% and 52.0%, respectively, when compared to the attachment of these cells on the surfaces of unmodified glass.

Xu *et al.* have reported the preparation and testing of semifluorinated surfaces that feature synergistic nonfouling/fouling-release properties.<sup>220</sup> When compared to unmodified surfaces, surfaces coated with this chemically heterogeneous thin film composed of asymmetric molecular brushes showed substantially improved antifouling activity, characterized by reduced adsorption of proteins (a reduction of 45–75%) and lower attachment of cells (reduced by 70–90%) (Fig. 13c and d). The antifouling property of the surface was attributed to the presence of poly(ethyleneglycol) (PEO) side chains, and the fouling-release characteristic was derived from the low surface energy of poly(2,2,2-trifluoroethyl methacrylate) side chains. The molecular symmetry, degree of polymerization and length of side chains played a role in defining these properties, with asymmetry, a greater length and degree of polymerization in PEO associated with greater resistance to attachment of proteins (a 75% reduction compared to control) and cells (cell number reduced by 90%).

The synergistic antifouling effect of self-renewable coatings containing quaternary ammonium-functionalized SiO<sub>2</sub> nanoparticles has been described by Wang *et al.*<sup>221</sup> To fabricate these coatings, SiO<sub>2</sub> nanoparticles were first modified with biologically active quaternary ammonium, then the resulting QAS-SiO<sub>2</sub> particles were immobilized within a self-polishing polymer matrix. The resulting film offered a favorable combination of properties, including the ability to self-renew, a topography with features at nano and micro scales, as well as bactericidal function. This intricate topography was responsible for the superoleophobic property the surface gained upon exposure to artificial seawater. The presence of quaternary ammonium functionalities on the surface of SiO<sub>2</sub> particles was responsible for greater compatibility with the polymer matrix, with modified particles having less of an effect on the self-polishing rate of the polymer. A combination of self-renewal and self-renewal functions gave rise to a synergistic antifouling effect that was demonstrated both under laboratory (using *Shewanella loihicas* model organism) and field conditions. The quaternary ammonium-modified SiO<sub>2</sub> particles showed some efficacy in preventing the attachment of diatoms and plantigrades of the *Mytilus coruscus mussel*. Schematics of the coating is shown in Fig. 13e, and the bacterial and diatom density on the surfaces of coatings after field test for 7 days is shown in Fig. 13f.

• Synergistic effects can significantly boost the efficiency of nanomaterial-based anti-fouling protection systems for marine applications. In future, solid consolidated efforts need to be applied to deeper understand the processes that cause synergistic effects, and to explore a greater number of material systems to find strongly synergistic systems involving more than two materials, as these system can potentially demonstrate a powerful cumulative synergistic effects. Moreover, biomimetic systems considered below could also give rise to the synergistic properties.

## 6. Biomimetic approaches for novel antifouling techniques

Nature has served as an inspiration for humans in many fields of research and development, and has already suggested many a strategy for the design and development of highly efficient, broad-spectrum antifouling systems that are minimally harmful to the environment.<sup>222,223</sup> Currently, three main biomimetic strategies are considered: (i) application of natural antifoulants, (ii) designing surface microtopographies, and (iii) application of synthetic polymers. Fig. 14 shows several characteristic examples for these strategies, such as papain and capsaicin for the natural antifoulants, shark skin and lotus leaves surface structures for surface microtopographies, zwitterion and DOPA-based coatings for the synthetic polymer-based antifouling platforms.<sup>224</sup>

As evidence of the growing importance of this technology, there have been recent reports of significant research efforts to develop biomimetic anti-fouling surfaces with designed microtopographies and/or synthetic polymers.<sup>225</sup> Examples include mussel-inspired synthetic polymers,<sup>226,227</sup> zwitterionic coatings,<sup>228</sup> photopolymerized biomimetic self-adhesive surfaces,<sup>229</sup> antimicrobial peptides<sup>230</sup> and many others. Below we discuss several recent characteristic examples to outline the major direction in this family of technologies.

Zhao *et al.* have fabricated and tested stable biomimetic coatings on multivalent phosphorylcholine-containing poly(methacrylate) copolymers (PMGT) surfaces. These stable coatings are formed *via* post-crosslinking in an atmosphere enriched with moisture and triethylamine (TEA). Under these conditions,

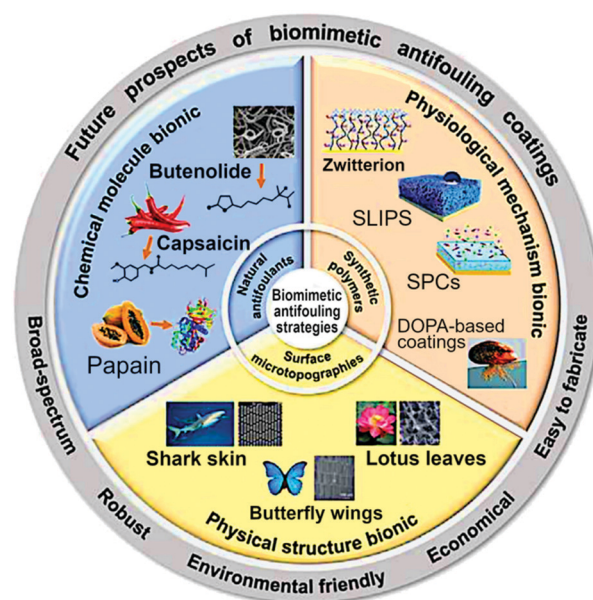
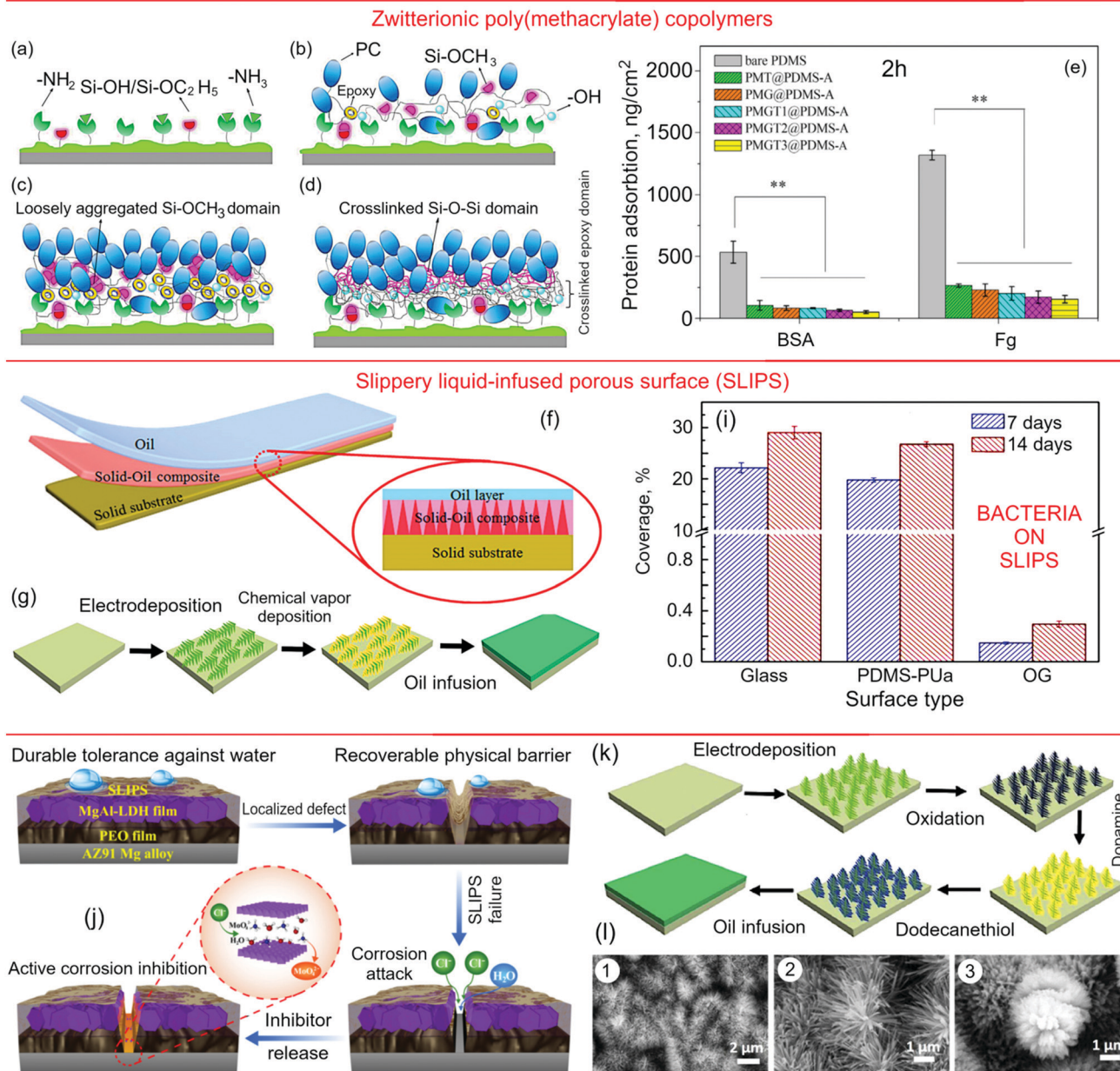


Fig. 14 Three main strategies to utilize the biomimetic approach: (i) application of natural antifoulants, (ii) designing surface microtopographies, and (iii) application of synthetic polymers. Reprinted with permission from Chen *et al.*, 2021.<sup>224</sup> Papain and capsaicin as natural antifoulants, shark skin and lotus leaves as sophisticated surface microtopographies, zwitterion and DOPA-based coatings as synthetic polymer-based antifouling platforms are the characteristic specific examples of the three strategies.

## BIOMIMETIC APPROACHES FOR NOVEL ANTIFOULING TECHNIQUES



**Fig. 15** Upper panel: (a–d) Possible mechanism for PMGT coating formation (incubation step, then PC moieties tended to orient towards the outer coating layer, and post-crosslinking) and (e) short-term protein adsorption onto different PDMS samples. Significant difference compared with bare PDMS is apparent. Reprinted with permission from Zhao *et al.*, 2019.<sup>231</sup> Mean panel: (f) The structure of slippery liquid-infused porous surfaces (SLIPS) inspired by the natural plant *Nepenthes pitcher*, also known as “monkey cups”, family *Nepenthaceae*, and (g) schematic illustration of the process combining electrodeposition, vapour deposition and oil infusion to realize superhydrophobic and oil-infused surface. Reprinted with permission from Quyang *et al.*, 2019.<sup>232</sup> (i) Statistical results of bacterial coverages on samples made of glass, poly(dimethylsiloxane) based polyurea (PDMS-PUa) and slippery organogel layer (OG) after immersion in a static culture solution inoculated with *Pseudoalteromonas* sp. for 7 and 14 days. Drastic drop of bacterial coverage could be noticed for the slippery organogel surface. Reprinted with permission from Zhang *et al.*, 2019.<sup>233</sup> Bottom panel: (j) Schematic protection mechanism for the smart anticorrosion system on Mg alloys. Reprinted with permission from Jiang *et al.*, 2019.<sup>234</sup> (k) Schematic steps of preparation of the liquid-infused surface based on vertical dendritic Co for achieving superhydrophobicity and lubricant infused surfaces. Reprinted with permission from Ouyang *et al.*, 2019.<sup>235</sup> (l) Slippery liquid-infused porous surfaces fabricated on CuZn: SEM images of the material in different preparation stages. (1, 2)  $\text{Cu(OH)}_2$  obtained by oxidizing Cu in a mixed solution containing 0.1 M  $(\text{NH}_4)_2\text{S}_2\text{O}_8$  and 2.5 M NaOH, and (3) further modification of  $\text{Cu(OH)}_2$  in dodecanethiol vapor. The ready materials serve as a barrier to abiotic seawater corrosion. Reprinted with permission from Qui *et al.*, 2019.<sup>236</sup>

zwitterionic phosphorylcholine functional groups are able to orient themselves in the direction of the outer surface. This

allows for the control of hydrophilicity, film stability and antifouling characteristics. Fig. 15(a–d) illustrates one of the

pathways for PMGT coating formation, and Fig. 15(e) shows the short-term protein adsorption onto different PDMS samples, with a significant difference evident when compared with bare PDMS.<sup>231</sup>

Ouyang *et al.* have demonstrated another nature-inspired approach to mitigate microorganism attachment onto surfaces of titanium. This approach was inspired by the naturally antifouling plant *Nepenthes pitcher*, also known as “monkey cups”, from the family *Nepenthaceae*. Titanium and titanium alloys are widely used in applications requiring prolonged exposure to highly corrosive seawater environment owing to their stability under these conditions. Yet, both titanium and its alloys are highly susceptible to fouling, which presents a significant challenge for the use of this family of metals. To mitigate this issue, dendritic Ag has been deposited onto the surface of Ti using electrodeposition technology. Then, dendritic Ag was modified with dodecanethiol vapors to obtain a superhydrophobic surface. The superhydrophobicity arises from a combination of hydrophobic moieties and the voids in the dendritic Ag matrix. At the same time, the surface is superoleophilic, which allows the oil to infuse into the matrix, driving out the air from it, thus producing a slippery liquid-infused porous surface (SLIPS). SLIPS-coated Ti was able to resist fouling by diatoms and green algae, with the number of attached organisms being 4 orders of magnitude lower when compared to uncoated Ti after 14 days of immersion. These results show that introducing SLIPS onto the surface of metals may provide a useful pathway for mitigating biofouling under seawater conditions.<sup>232</sup> The structure of SLIPS is illustrated in Fig. 15(f), and schematic illustration of the fabrication process combining electrodeposition, vapor deposition and oil infusion to realize superhydrophobic and oil-infused surface is shown in Fig. 15(g).

Zhang *et al.* have designed and tested another SLIPS platform that is promising for marine applications. One of the main advantages of this platform is its increased stability, which is needed to overcome the ease with which transitional SLIPS can be damaged under real-life conditions. These researchers designed a self-healing slippery organogel film, where silicone oil was infused into poly(dimethylsiloxane) based polyurea (PDMS-PUa) matrix. This matrix was fabricated from  $\alpha,\omega$ -aminopropyl terminated poly(dimethylsiloxane) (APT-PDMS) in combination with isophorone diisocyanate (IPDI). The chemical composition of this film allowed it to break and reform hydrogen bonds in urea groups between PDMS-PUa, resulting in material healing. The lubricant oil was also regenerated as the silicone oil was able to move across the PDMS-PUa matrix to the regeneration site. The organogel layer showed an excellent combination of a low water sliding angle of  $<10^\circ$  and biofilm-retarding properties under both static and dynamic environments (Fig. 15(i)).<sup>233</sup>

A bioinspired coating featuring a self-reparable slippery surface and an active corrosion inhibition for reliable protection of Mg alloy has been reported by Jiang *et al.*<sup>234</sup> Here, plasma electrolytic oxidation was used to modify a AZ91 Mg alloy, followed by the formation of a layered double hydroxide

film and an infusion of lubricant, producing a biomimetic surface with desirable nonwetting and self-healing characteristics. Importantly, thus-produced surfaces were more efficient in repelling water under immersion conditions when compared to traditional superhydrophobic surfaces, and as such would provide greater protection against corrosion. The layer of double hydroxide serves as a source of molybdate that is released from the film upon contact with  $\text{Cl}^-$  ions in the water.

Schematic steps of preparation of the biomimetic liquid-infused superhydrophobic surfaces based on vertical dendritic Co are shown in Fig. 15k. In this case, a liquid-infused surface was produced by introducing the silicone oils into the superhydrophobic Co dendrite matrix. Such liquid-infused matrices are able to effectively reduce the attachment of sulfate-reducing bacteria onto metals, the latter being a precondition step to the induction of microbiologically mediated corrosion. Fig. 15i shows several SEM images of the slippery liquid-infused porous surface fabricated on CuZn. Thus-fabricated materials also served as a barrier to abiotic seawater corrosion.<sup>236</sup>

The above-described nanostructured surfaces could be quite efficient in terms of bactericidal activity. However, because this effect is intimately linked to the interactions between the cells and the surface, any accumulation of dead cells or cellular debris may interfere with its potency against cell attachment and biofilm formation. This is well demonstrated using the example of lotus-leaf-inspired hierarchical structured surfaces with non-fouling or mechanical bactericidal performances. While the superhydrophobic and cell repelling nature of lotus leaf and lotus leaf-inspired surfaces is well documented, the ability of these surfaces to kill cells upon direct *via* inducing physical damage to the membrane is a more recent discovery. These findings have prompted researchers to develop surfaces that combine nano- and micro-scale feature with perfluorination for superior synergistic antibiofouling effect that have recently been reported by Jiang *et al.*<sup>237</sup> When tested against *E. coli*, these surfaces were able to repel attachment by more than 99%, with cells that managed to attach killed *via* the membrane rupturing effect. These results are superior to those that can be attained by surfaces that display solely superhydrophobicity or mechanical-type contact killing behaviour. Furthermore, these novel surfaces have the additional benefit of improved long-term efficacy with respect to antimicrobial activity, since it is founded entirely upon a physical mechanism of cell killing. Fig. 16 illustrates the fabrication of lotus leaf-like structures *via* a combination of plasma etching and a hydrothermal reaction, and SEM images of thus-produced structures.

• Biomimetic materials and material systems hold a great promise for the future antifouling technologies. Importantly, the attempts to combine several approaches into a single system could be the future trend in the marine antifouling protection systems. Bioinspired nanotechnology-based materials are currently under extensive investigation.<sup>238–242</sup> However, the approaches that are not based on the advanced materials but involving various physical mechanism are also under exploration, as exemplified below.



## LOTUS-LEAF-INSPIRED SURFACE WITH NON-FOULING PERFORMANCE



Fig. 16 Antifouling characteristics of surfaces inspired by lotus leaf surface topography. Upper panel: Plasma etching and hydrothermal etching are two strategies commonly used to produce lotus leaf-like topographies. Lower panel: SEM visualisation of silicon surfaces patterned with a single micro-scale ((a) and (b)), dual-scale ((c) and (d)), and single nanoscale ((e) and (f)) structures. Reprinted with permission from Jiang *et al.*, 2020.<sup>237</sup>

## 7. Physical approaches as medium technology between nanomaterials and bioinspired surfaces

As described above, nanomaterial-based techniques for marine antifouling are quite promising, and they could be made to be even more efficient when the synergistic and bio-mimetic effects and structures are involved. Along with these efforts, a search for the novel technologies exists with the aim to find approaches not based on some specific materials but utilizing some simple physical effects. Such technologies (collectively termed “physical antifouling”) promise to be ‘absolutely environmentally friendly’ since they do not assume emittance of any chemicals, even relatively benign to the environment. Below we outline just three examples. These examples are quite different with respect to their physical nature, involving distinct equipment and physical principles, to present a picture of a wide search for the environmentally friendly marine anti-fouling technologies: (i) ultrasonic-based antifouling control, (ii) nano-second pulsed laser cleaning of marine micro-biofoulings, and (iii) water jet-based antifouling technology optimised by genetic neural network.

Decontamination of surfaces using an ultrasound treatment is an effective means of keeping surfaces free from fouling under freshwater and seawater conditions,<sup>243</sup> with frequencies in the range of 20–50 kHz demonstrating the best results.

This is because sound waves within this frequency range can cause mortality in a range of species, including crustacean and bivalve larvae.<sup>244</sup> This is important because the agents affecting the microbiota can consequently impact on other species that interact with or depend on this microbiota. For example, recently, a dependence of growth performance and health status of European eel on the growth of relevant microbiota was investigated.<sup>245,246</sup> Knobloch *et al.* showed that an ultrasound treatment at the frequency range of 20–80 kHz produced by means of ultrasound transducers was capable of modulating the growth of microbiota of European sea bass (*Dicentrarchus labrax*), a species of fish of commercial significance for aquaculture over 71 days (see Fig. 17a for the experimental sequence). Inactive transducers placed in the same position in the middle of the tank were employed to act as controls. The primary aim of this study was to investigate the compatibility of ultrasound-based antifouling strategies for offshore platforms with objectives of fish farming that may take place within the same ecosystem (Fig. 17a and b).<sup>247</sup>

The results presented in Fig. 17b suggest that microbial communities present in the gut, on the skin surface and in the seawater show evident impact from the continuous exposure to ultrasound treatment, with the surface microbiota of farmed sea bass being most vulnerable to the treatment. While this study did not report any significant negative effects on the fish population itself, the impact that the treatment has on the

## NON-MATERIAL BASED APPROACHES FOR NOVEL ANTIFOULING TECHNIQUES

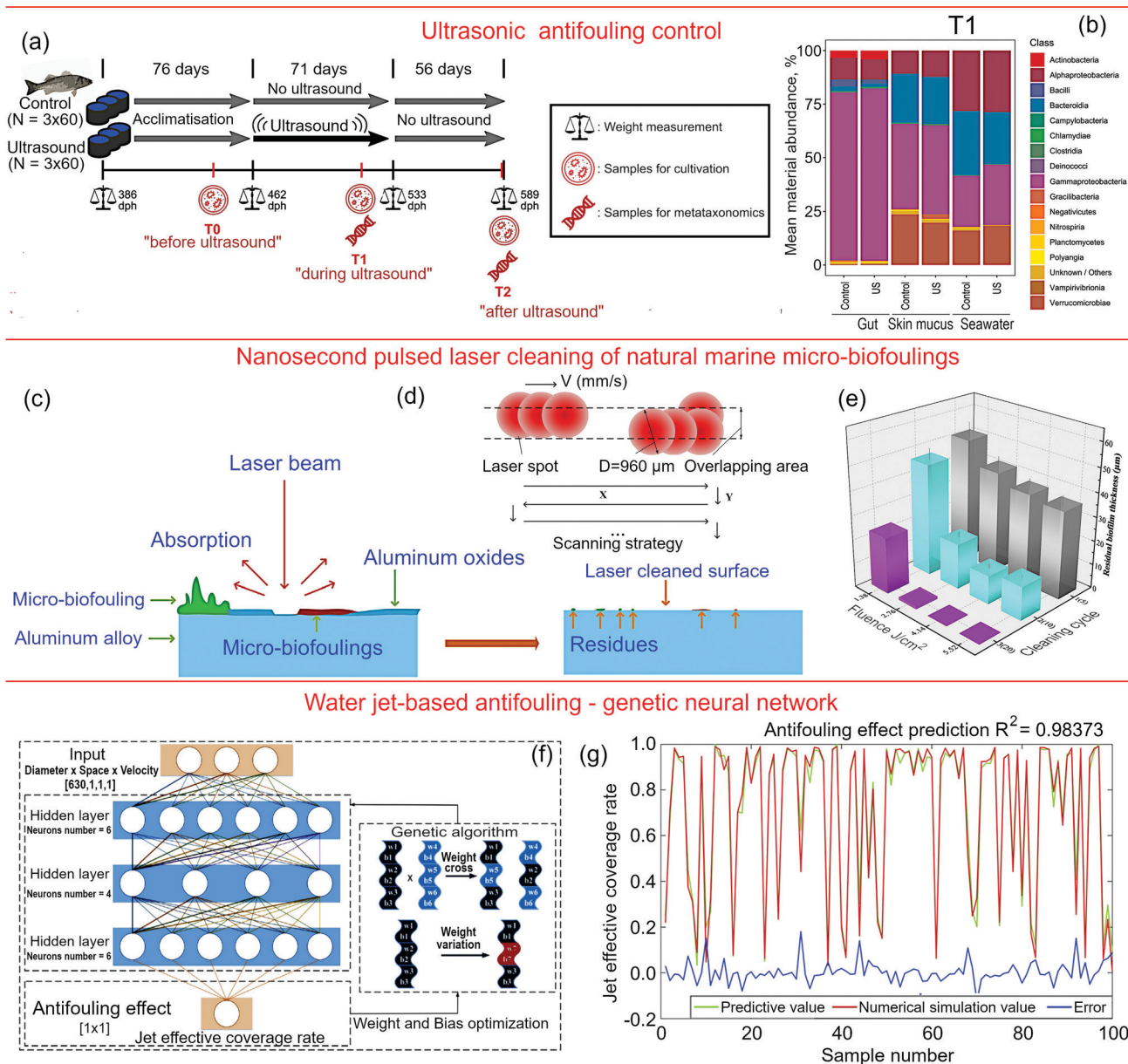


Fig. 17 (a) Experimental design to study the impact of ultrasonic antifouling on the health and growth of farmed European sea bass and its associated microbial communities, and (b) Gut, skin and ambient seawater microbiota with and without exposure to ultrasound treatment. Reprinted with permission from Knobloch *et al.*, 2021.<sup>247</sup> (c and d) Schematic representation of the laser cleaning scanning path and schematic of the laser cleaning of natural marine micro-biofouling from the surface of an Al alloy. (e) Thickness of biofilm that remained on the surface subsequent to cleaning with different cycle times and laser fluencies. Reprinted with permission from Tian *et al.*, 2020.<sup>248</sup> (f) Training of the genetic neural network to maximise the efflux of a water jet-based biomimetic antifouling strategy based on the combination of the jet parameters and (g) comparison of the predicted water jet distribution and antifouling values with the respective simulated values. Reprinted with permission from Liu *et al.*, 2020.<sup>249</sup>

biota of the skin of these animals may render the fish more susceptible to diseases and increase longer term mortality in the exposed populations.<sup>247</sup>

Tian *et al.* have demonstrated the application of nanosecond (30 ns) pulsed laser for the removal of natural marine biofouling with the thickness of about 60 µm from the surface of aluminum alloy. Schematic of the process is shown in Fig. 17c, and schematic of the laser cleaning scanning path is illustrated

in Fig. 17d.<sup>248</sup> The experiment was conducted using lasers of different fluence ranging from 1.38 to 5.52 J cm<sup>-2</sup> to investigate the effect of the latter on the removal of fouling organisms from the surfaces of aluminium. The removal was attained *via* laser-mediated vaporization and ablation of cells and biofilm molecules. Importantly, the surfaces did not sustain any significant damage as a result of the treatment, with the surface treated at a fluence of 5.52 J cm<sup>-2</sup> gaining an additional characteristic of

superhydrophobicity, which is desirable for the long-term prevention of fouling. Fig. 17e shows the dependence of thickness of the biofilm surface residue on the number of cleaning cycle and the laser fluences.

One more interesting example is the use of neural networks to simulate the water jet-based biomimetic antifouling approach for marine structures. Due to level of complexity typical of real-life biological systems, the traditional modelling could be problematic, so Liu *et al.* utilized the neural networks to optimize the design of a water jet-based biomimetic antifouling model. Fig. 17f shows the flow chart of the prediction of efflux effective coverage by the genetic neural network, and Fig. 17g shows the comparison of the predicted value with the simulated value.<sup>249</sup> This innovative method was first proposed by Liu *et al.*<sup>250</sup> where it was demonstrated that the efficacy of the attachment prevention of *Phaeodactylum tricornutum* could be effectively improved using this method. By hindering the early stages of marine biofilm formation, it is possible to effectively disrupt the entire fouling process. For practical applications, an outwardly oriented jets can be used to form a dynamic fouling-retarding later that is both effective and environmentally benign when compared to traditional chemical and physical methods of preventing fouling in aquatic systems. Introducing microbubbles containing plasma-generated highly reactive species into the water jet may significantly increase the efficacy of the cleaning treatment, as reactive species have been demonstrated to act both on the microorganisms as well as onto the molecules that make up the biofilm structure, leading to its more effective dispersal.<sup>251,252</sup>

- Physical approaches hold an intermediate position between the nanomaterial-based techniques and bioinspired surfaces and thus, benefit from their best advantages such as low toxicity due to the absence of chemical reagents, and high efficiency. It should be noted that the fabrication of surfaces that use physical approaches of antifouling may involve chemical reactions (*e.g.* during the laser or ultraviolet treatment) that can potentially release dangerous chemicals into the environment. It should also be mentioned that the processes that underpin the antifouling and killing mechanisms in the physical marine antifouling protection technologies are quite complex and currently not fully understood. Further progress in this area is required to maximise the benefit offered by this family of antifouling approaches, and importantly, combination of physical approaches with the sophisticatedly designed functional nanocomposites could be of a particular interest.

## 8. Future outlook and challenges

We started our review with a brief overview of the multi-century history of marine antifouling coatings, and this story still continues and still requires a strong, consolidated effort to find radical solution to this problem. In the next few years, the marine antifouling technology market is predicted to reach US \$15 billion, with strong emphasis on novel environmentally benign antifouling techniques to overcome drawbacks of

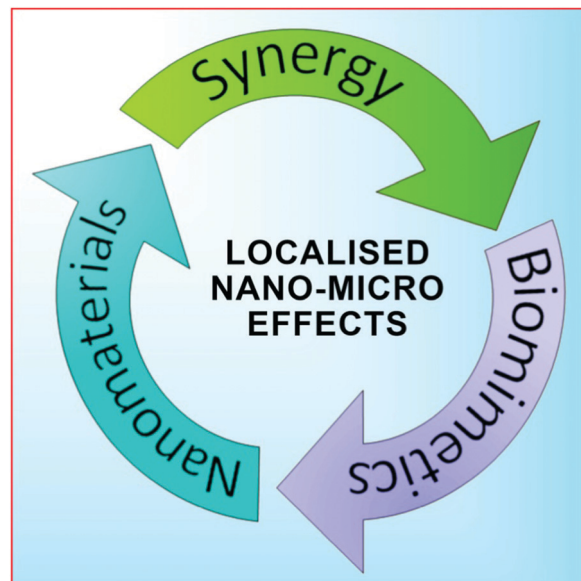


Fig. 18 Advanced functional nanomaterials, synergistic effects and biomimetic approaches could be keys to ensure non-toxic, environmentally friendly next generation antifouling technologies.

current engineered coatings. The general aim of this article was to show that (i) mature approaches based on various chemical agents still fail to ensure efficient solutions for hundreds of thousand marine vessels; (ii) the most promising, from the authors' point of view, future strategies should be based on (Fig. 18):

- Wide use of advanced, functional nanostructured materials;
- Application of synergistic effects and phenomena; and
- Utilization of nature-inspired biomimetic systems and surfaces.

Moreover, it is important to stress that while the traditional methods of preventing fouling are mainly based on the active chemistry, new strategies (based on nanoscale effects, synergies and biomimetics) are more physics-oriented in their nature and hence, they are fundamentally more environmentally friendly since they rely on strongly localized near-surface effects that do not release toxic elements into the environment but produce the anti-biofouling action using the nano- and micro-features of the surface, and enhance these effects through carefully designed synergies.

- Combined together, these three strategies promise to ensure a drastic boost in the efficiency, versatility and environmental innocuousness of future marine anti-biofouling material platforms, and realize nontoxic, durable, commercially viable, environmentally sustainable antifouling coatings that are urgently required.

## Author contributions

M. V. J., K. B.: conceptualization, funding acquisition, project administration, supervision, writing – review and editing.

A. K.: writing – original draft, writing – review and editing. I. L., A. A., E. I., O. B.: writing – review and editing.

## Conflicts of interest

There are no conflicts to declare.

## Acknowledgements

I. L. acknowledges the support from the Nanyang Technological University, Singapore. K. B. acknowledges the support from the National Australian University and Australian Research Council (DP180101254, DE130101550). O. B. acknowledges the support through an Australian Government Research Training Program Scholarship.

## References

- I. Levchenko, K. Bazaka, M. Keidar, S. Xu and J. Fang, Hierarchical multicomponent inorganic metamaterials: Intrinsically driven self-assembly at the nanoscale, *Adv. Mater.*, 2018, **30**, 1702226, DOI: 10.1002/adma.201702226.
- O. Baranov, I. Levchenko, J. M. Bell, J. W. M. Lim, S. Huang, L. Xu, B. Wang, D. U. B. Aussems, S. Xu and K. Bazaka, From nanometre to millimetre: a range of capabilities for plasma-enabled surface functionalization and nanostructuring, *Mater. Horiz.*, 2018, **5**, 765–798, DOI: 10.1039/C8MH00326B.
- J. Yang, L.-S. Tang, L. Bai, R.-Y. Bao, Z.-Y. Liu, B.-H. Xie, M.-B. Yang and W. Yang, High-performance composite phase change materials for energy conversion based on macroscopically three-dimensional structural materials, *Mater. Horiz.*, 2019, **6**, 250–273, DOI: 10.1039/C8MH01219A.
- Y. Wu, X. Huang, L. Huang and J. Chen, Strategies for rational design of high-power lithium-ion batteries, *Energy Environ. Mater.*, 2021, **4**, 19–45, DOI: 10.1002/eem2.12088.
- C. Wang, Y. V. Kaneti, Y. Bando, J. Lin, C. Liu, J. Li and Y. Yamauchi, Metal-organic framework-derived one-dimensional porous or hollow carbon-based nanofibers for energy storage and conversion, *Mater. Horiz.*, 2018, **5**, 394–407, DOI: 10.1039/C8MH00133B.
- S. M. Berger and T. B. Marder, Applications of triarylborane materials in cell imaging and sensing of bio-relevant molecules such as DNA, RNA, and proteins, *Mater. Horiz.*, 2021, DOI: 10.1039/D1MH00696G.
- R. Tamilselvi, G. S. Lekshmi, N. Padmanathan, V. Selvaraj, O. Bazaka, I. Levchenko, K. Bazaka and M. Mandhakini, NiFe<sub>2</sub>O<sub>4</sub>/rGO nanocomposites produced by soft bubble assembly for energy storage and environmental remediation, *Renewable Energy*, 2022, **181**, 1386–1401, DOI: 10.1016/j.renene.2021.07.088.
- J. F. Olorunyomi, S. T. Geh, R. A. Caruso and C. M. Doherty, Metal-organic frameworks for chemical sensing devices, *Mater. Horiz.*, 2021, **8**, 2387–2419, DOI: 10.1039/D1MH00609F.
- J. Broek, I. C. Weber, A. T. Güntner and S. E. Pratsinis, Highly selective gas sensing enabled by filters, *Mater. Horiz.*, 2021, **8**, 661–684, DOI: 10.1039/D0MH01453B.
- X. Wen, S. Sun and P. Wu, Dynamic wrinkling of a hydrogel-elastomer hybrid microtube enables blood vessel-like hydraulic pressure sensing and flow regulation, *Mater. Horiz.*, 2020, **7**, 2150–2157, DOI: 10.1039/D0MH00089B.
- X. Zhang, Y. Wang, J. Cai, K. Wilson and A. F. Lee, Bio/Hydrochar sorbents for environmental remediation, *Energy Environ. Mater.*, 2020, **3**, 453–468, DOI: 10.1002/eem2.12074.
- P. H. Wadekar, R. V. Khose, D. A. Pethsangave and S. Some, The effect of bio-inspired co-electrolytes for enhancement of electrochemical properties of supercapacitors, *Energy Environ. Mater.*, 2020, **3**, 429–435, DOI: 10.1002/eem2.12097.
- O. Bazaka, K. Bazaka, V. K. Truong, I. Levchenko, M. V. Jacob, Y. Estrin, R. Lapovok, B. Chichkov, E. Fadeeva, P. Kingshott, R. J. Crawford and E. P. Ivanova, Effect of titanium surface topography on plasma deposition of antibacterial polymer coatings, *Appl. Surf. Sci.*, 2020, **521**, 146375, DOI: 10.1016/j.apsusc.2020.146375.
- G. V. Sree, P. Rajasekaran, O. Bazaka, I. Levchenko, K. Bazaka and M. Mandhakini, Biowaste valorization by conversion to nanokeratin-urea composite fertilizers for sustainable and controllable release of carbon and nitrogen, *Carbon Trends*, 2021, **5**, 100083, DOI: 10.1016/j.cartre.2021.100083.
- I. Levchenko, M. Keidar, J. Cantrell, Y.-L. Wu, H. Kuninaka, K. Bazaka and S. Xu, Explore space using swarms of tiny satellites, *Nature*, 2018, **562**, 185–187, DOI: 10.1038/d41586-018-06957-2.
- I. Levchenko, K. Bazaka, T. Belmonte, M. Keidar and S. Xu, Advanced materials for next generation spacecraft, *Adv. Mater.*, 2018, **30**, 1802201, DOI: 10.1002/adma.201802201.
- I. Levchenko, S. Xu, S. Mazouffre, D. Lev, D. Pedrini, D. Goebel, L. Garrigues, F. Taccogna and K. Bazaka, Perspectives, frontiers, and new horizons for plasma-based space electric propulsion, *Phys. Plasmas*, 2020, **27**, 020601, DOI: 10.1063/1.5109141.
- I. Levchenko, S. Xu, S. Mazouffre, M. Keidar and K. Bazaka, Mars colonization: Beyond getting there, *Glob. Chall.*, 2018, **2**, 1800062, DOI: 10.1002/gch2.201800062.
- I. Levchenko, S. Xu, G. Teel, D. Mariotti, M. L. R. Walker and M. Keidar, Recent progress and perspectives of space electric propulsion systems based on smart nanomaterials, *Nat. Commun.*, 2018, **9**, 879, DOI: 10.1038/s41467-017-02269-7.
- A. M. C. Maan, A. H. Hofman, W. M. de Vos and M. Kamperman, Recent developments and practical feasibility of polymer-based antifouling coatings, *Adv. Funct. Mater.*, 2020, **30**, 2000936, DOI: 10.1002/adfm.202000936.
- R. Chen, Y. Zhang, Q. Xie, Z. Chen, C. Ma and G. Zhang, Transparent polymer-ceramic hybrid antifouling coating with superior mechanical properties, *Adv. Funct. Mater.*, 2021, **31**, 2011145, DOI: 10.1002/adfm.202011145.
- Z. Wang, L. Scheres, H. Xia and H. Zuillhof, Developments and challenges in self-healing antifouling materials, *Adv.*

- Funct. Mater.*, 2020, **30**, 1908098, DOI: 10.1002/adfm.201908098.
- 23 J. Bannister, M. Sievers, F. Bush and N. Bloecher, Biofouling in marine aquaculture: A review of recent research and developments, *Biofouling*, 2019, **35**, 631–648, DOI: 10.1080/08927014.2019.1640214.
- 24 M. P. Schultz, Effects of coating roughness and biofouling on ship resistance and powering, *Biofouling*, 2007, **23**, 331–341, DOI: 10.1080/08927010701461974.
- 25 H. Titah-Benbouzid and M. Benbouzid, Biofouling issue on marine renewable energy converters: A state of the art review on impacts and prevention, *Int. J. Energy Convers.*, 2017, **5**, 67–78, DOI: 10.15866/irecon.v5i3.12749.
- 26 F. Laranjeiro, P. Sánchez-Marín, I. B. Oliveira, S. Galante-Oliveira and C. Barroso, Fifteen years of imposex and tributyltin pollution monitoring along the Portuguese coast, *Environ. Pollut.*, 2018, **232**, 411–421, DOI: 10.1016/j.envpol.2017.09.056.
- 27 R. Ciriminna, F. V. Bright and M. Pagliaro, Ecofriendly antifouling marine coatings, *ACS Sustainable Chem. Eng.*, 2015, **3**(4), 559–565, DOI: 10.1021/sc500845n.
- 28 S. Pradhan, S. Kumar, S. Mohanty and S. K. Nayak, Environmentally benign fouling-resistant marine coatings: A review, *Polym.-Plast. Technol. Mater.*, 2019, **58**, 498–518, DOI: 10.1080/03602559.2018.1482922.
- 29 S. Lee, B. L. Ibey, G. L. Coté and M. V. Pishko, Measurement of pH and dissolved oxygen within cell culture media using a hydrogel microarray sensor, *Sens. Actuators, B*, 2008, **128**, 388–398, DOI: 10.1016/j.snb.2007.06.027.
- 30 K. Murphy, B. Heery, T. Sullivan, D. Zhang, L. Paludetti, K. T. Lau, D. Diamond, E. Costa, N. O'Connor and F. Regan, A low-cost autonomous optical sensor for water quality monitoring, *Talanta*, 2015, **132**, 520–527, DOI: 10.1016/j.talanta.2014.09.045.
- 31 B.-M. Kim, M. Saravanan, D.-H. Lee, J.-H. Kang, M. Kim, J.-H. Jung and J.-S. Rhee, Exposure to sublethal concentrations of tributyltin reduced survival, growth, and 20-hydroxyecdysone levels in a marine mysid, *Mar. Environ. Res.*, 2018, **140**, 96–103, DOI: 10.1016/j.marenvres.2018.06.006.
- 32 M. N. Haque, D.-H. Lee, B.-M. Kim, S.-E. Nam and J.-S. Rhee, Dose- and age-specific antioxidant responses of the mysid crustacean *Neomysis awatschensis* to metal exposure, *Aquat. Toxicol.*, 2018, **201**, 21–30, DOI: 10.1016/j.aquatox.2018.05.023.
- 33 S. E. Martins, G. Fillmann, A. Lillicrap and K. V. Thomas, Review: ecotoxicity of organic and organo-metallic antifouling co-biocides and implications for environmental hazard and risk assessments in aquatic ecosystems, *Biofouling*, 2018, **34**, 34–52, DOI: 10.1080/08927014.2017.1404036.
- 34 L. Gipperth, The legal design of the international and European Union ban on tributyltin antifouling paint: Direct and indirect effects, *J. Environ. Manag.*, 2009, **90**, S86–S95.
- 35 L. Chen and J. C. W. Lam, SeaNine 211 as antifouling biocide: a coastal pollutant of emerging concern, *J. Environ. Sci.*, 2017, **61**, 68–79, DOI: 10.1016/j.jes.2017.03.040.
- 36 M. Srinivasan and G. W. Swain, Managing the use of copper-based antifouling paints, *Environ. Manage.*, 2007, **39**, 423–441, DOI: 10.1007/s00267-005-0030-8.
- 37 E. M. McNeil, Antifouling: Regulation of biocides in the UK before and after Brexit, *Mar. Policy*, 2018, **92**, 58–60, DOI: 10.1016/j.marpol.2018.02.015.
- 38 D. Oliveira and L. Granhag, matching forces applied in underwater hull cleaning with adhesion strength of marine organisms, *J. Mar. Sci. Eng.*, 2016, **4**, 66, DOI: 10.3390/jmse4040066.
- 39 L. Chen and P. Y. Qian, Review on molecular mechanisms of antifouling compounds: an update since 2012, *Mar. Drugs*, 2017, **15**, 1–20, DOI: 10.3390/md15090264.
- 40 Y.-S. Moon, M. Kim, C. P. Hong, J.-H. Kang and J.-H. Jung, Overlapping and unique toxic effects of three alternative antifouling biocides (Diuron, Irgarol 1051, Sea-Nine 211) on non-target marine fish, *Ecotoxicol. Environ. Saf.*, 2019, **180**, 23–32, DOI: 10.1016/j.ecoenv.2019.04.070.
- 41 T. Gu, R. Jia, T. Unsal and D. Xu, Toward a better understanding of microbiologically influenced corrosion caused by sulfate reducing bacteria, *J. Mater. Sci. Technol.*, 2019, **35**, 631–636, DOI: 10.1016/j.jmst.2018.10.026.
- 42 D. M. Yebra, S. Kiil and K. Dam-Johansen, Antifouling technology - past, present and future steps towards efficient and environmentally friendly antifouling coatings, *Prog. Org. Coat.*, 2004, **50**, 75–104, DOI: 10.1016/j.porgcoat.2003.06.001.
- 43 M. R. Detty, R. Ciriminna, F. V. Bright and M. Pagliaro, Environmentally benign sol-gel antifouling and foul-releasing coatings, *Acc. Chem. Res.*, 2014, **47**(2), 678–687, DOI: 10.1021/ar400240n.
- 44 A. Mukherjee, M. Joshi, S. C. Misra and U. S. Ramesh, Antifouling paint schemes for green SHIPS, *Ocean Eng.*, 2019, **173**, 227–234, DOI: 10.1016/j.oceaneng.2018.12.057.
- 45 J. A. Batista-Andrade, S. S. Caldas, R. M. Batista, I. B. Castro, G. Fillmann and E. G. Primel, From TBT to booster biocides: Levels and impacts of antifouling along coastal areas of Panama, *Environ. Pollut.*, 2018, **234**, 243–252, DOI: 10.1016/j.envpol.2017.11.063.
- 46 L. Chen, Y. Duan, M. Cui, R. Huang, R. Su, W. Qi and Z. He, Biomimetic surface coatings for marine antifouling: Natural antifoulants, synthetic polymers and surface microtopography, *Sci. Total Environ.*, 2021, **766**, 144469, DOI: 10.1016/j.scitotenv.2020.144469.
- 47 M. L. Hakim, B. Nugroho, M. N. Nurrohman, I. K. Suastika and I. K. A. P. Utama, Investigation of fuel consumption on an operating ship due to biofouling growth and quality of anti-fouling coating, *IOP Conf. Ser.: Earth Environ. Sci.*, 2019, **339**, 012037, DOI: 10.1088/1755-1315/339/1/012037.
- 48 M. P. Schultz, J. A. Bendick, E. R. Holm and W. M. Hertel, Economic impact of biofouling on a naval surface ship, *Biofouling*, 2011, **27**, 87–98, DOI: 10.1080/08927014.2010.542809.
- 49 D. Thomas, S. Surendran and N. J. Vasa, A simplified approach for voyage analysis of fouled hull in a tropical marine environment, *Ships Offshore Struct.*, 2021, **16**, 762–772, DOI: 10.1080/17445302.2020.1781745.

- 50 P. A. Vinagre, T. Simas, E. Cruz, E. Pinori and J. Svenson, Marine biofouling: A European database for the marine renewable energy sector, *J. Mar. Sci. Eng.*, 2020, **8**, 495, DOI: 10.3390/jmse8070495.
- 51 V. O. Agostini, E. Muxagata, G. L. L. Pinho, I. S. Pessi and A. J. Macedo, Bacteria-invertebrate interactions as an asset in developing new antifouling coatings for man-made aquatic surfaces, *Environ. Pollut.*, 2021, **271**, 116284, DOI: 10.1016/j.envpol.2020.116284.
- 52 N. H. Lam, H. Jeong, S. Kang, D.-J. Kim, M.-J. Ju, T. Horiguchi and H.-S. Cho, Organotin and new antifouling biocides in water and sediments from three Korean special management sea areas following ten years of tributyltin regulation: Contamination profiles and risk assessment, *Mar. Pollut. Bull.*, 2017, **121**, 302–312, DOI: 10.1016/j.marpolbul.2017.06.026.
- 53 T. Onduka, K. Kono, M. Ito, N. Ohkubo, T. Hano, K. Ito and K. Mochida, Ecological risk assessment of an antifouling biocide triphenyl (octadecylamine) boron in the Seto Inland Sea, *Jpn. Mar. Pollut. Bull.*, 2020, **157**, 111320, DOI: 10.1016/j.marpolbul.2020.111320.
- 54 J. L. M. Viana, M. S. Diniz, S. R. V. Santos, R. T. Verbinnen, M. A. P. Almeida and T. C. R. S. Franco, Antifouling biocides as a continuous threat to the aquatic environment: Sources, temporal trends and ecological risk assessment in an impacted region of Brazil, *Sci. Total Environ.*, 2020, **730**, 139026, DOI: 10.1016/j.scitotenv.2020.139026.
- 55 J. A. Batista-Andrade, S. S. Caldas, R. M. Batista, I. B. Castro, G. Fillmann and E. G. Primel, From TBT to booster biocides: Levels and impacts of antifouling along coastal areas of Panama, *Environ. Pollut.*, 2018, **234**, 243–252, DOI: 10.1016/j.envpol.2017.11.063.
- 56 J. T. Koning, U. E. Bollmann and K. Bester, The occurrence of modern organic antifouling biocides in Danish marinas, *Mar. Pollut. Bull.*, 2020, **158**, 111402, DOI: 10.1016/j.marpolbul.2020.111402.
- 57 F. E. L. Abreu, R. M. Batista, I. B. Castro and G. Fillmann, Legacy and emerging antifouling biocide residues in a tropical estuarine system (Vitoria state, SE, Brazil), *Mar. Pollut. Bull.*, 2021, **166**, 112255, DOI: 10.1016/j.marpolbul.2021.112255.
- 58 H.-J. Eom, Md. N. Haque, S.-E. Nam, D.-H. Lee and J.-S. Rhe, Effects of sublethal concentrations of the antifouling biocide Sea-Nine on biochemical parameters of the marine polychaete *Perinereis aibuhitensis*, *Comp. Biochem. Physiol. Part C*, 2019, **222**, 125–134, DOI: 10.1016/j.cbpc.2019.05.001.
- 59 W. J. Langston, N. D. Pope, K. M. Langston, S. C. M. O'Hara, P. E. Gibbs and P. L. Pascoe, Recovery from TBT pollution in English Channel environments: A problem solved?, *Mar. Pollut. Bull.*, 2015, **95**, 551–564, DOI: 10.1016/j.marpolbul.2014.12.011.
- 60 N. H. Lam, H. Jeong, S. Kang, D.-J. Kim, M.-J. Ju, T. Horiguchi and H.-S. Cho, Organotin and new antifouling biocides in water and sediments from three Korean Special Management Sea Areas following ten years of tributyltin regulation: Contamination profiles and risk assessment, *Mar. Pollut. Bull.*, 2017, **121**, 302–312, DOI: 10.1016/j.marpolbul.2017.06.026.
- 61 A. S. Guerreiro, R. C. Rola, M. T. Rovani, S. R. Costa and J. Z. Sandrini, Antifouling biocides: Impairment of bivalve immune system by chlorothalonil, *Aquat. Toxicol.*, 2017, **189**, 194–199, DOI: 10.1016/j.aquatox.2017.06.012.
- 62 J. W. Do, Md. N. Haque, H.-J. Lim, B. H. Min, D.-H. Lee, J.-H. Kang, M. Kim, J.-H. Jung and J.-S. Rhee, Constant exposure to environmental concentrations of the antifouling biocide Sea-Nine retards growth and reduces acetylcholinesterase activity in a marine mysid, *Aquat. Toxicol.*, 2018, **205**, 165–173, DOI: 10.1016/j.aquatox.2018.10.019.
- 63 J. Palmer, S. Flint and J. Brooks, Bacterial cell attachment, the beginning of a biofilm, *J. Ind. Microbiol. Biotechnol.*, 2007, **34**, 577–588, DOI: 10.1007/s10295-007-0234-4.
- 64 W. M. Dunne, Bacterial adhesion: Seen any good biofilms lately?, *Clin. Microbiol. Rev.*, 2002, **15**, 155–166, DOI: 10.1128/CMR.15.2.155-166.2002.
- 65 H.-C. Flemming, T. Griebel and G. Schaule, Antifouling strategies in technical systems: Short review, *Water Sci. Technol.*, 1996, **34**, 517–524, DOI: 10.1007/978-3-642-19940-0\_5.
- 66 D. M. Yebra, S. Kiil, K. Dam-Johansen and C. Weinell, Reaction rate estimation of controlled-release antifouling paint binders: Rosin-based systems, *Prog. Org. Coat.*, 2005, **53**, 256–275, DOI: 10.1016/j.porgcoat.2005.03.008.
- 67 I. Amara, W. Mileda, R. B. Slama and N. Ladhari, Antifouling processes and toxicity effects of antifouling paints on marine environment. A review, *Environ. Toxicol. Pharmacol.*, 2018, **57**, 115–130, DOI: 10.1016/j.etap.2017.12.001.
- 68 F. T. Arce, R. Avci, I. B. Beech, K. E. Cooksey and B. Wigglesworth-Cooksey, A live bioprobe for studying diatom-surface interactions, *Biophys. J.*, 2004, **87**, 4284–4297, DOI: 10.1529/biophysj.104.043307.
- 69 K. A. Cameron and P. L. Harrison, Density of coral larvae can influence settlement, post-settlement colony abundance and coral cover in larval restoration, *Sci. Rep.*, 2020, **10**, 5488, DOI: 10.1038/s41598-020-62366-4.
- 70 E. R. Holm, M. McClary and D. Rittschof, Variation in attachment of the barnacle *Balanus amphitrite*: Sensation or something else?, *Mar. Ecol.: Prog. Ser.*, 2000, **153**, 162, DOI: 10.3354/meps202153.
- 71 T. Harder, C. Lam and P.-Y. Qian, Induction of larval settlement in the polychaete *Hydroides elegans* by marine biofilms: An investigation of monospecific diatom films as settlement cues, *Mar. Ecol.: Prog. Ser.*, 2002, **105**, 112, DOI: 10.3354/meps229105.
- 72 N. Lagersson, Settlement behavior and antennular biomechanics in cypris larvae of *Balanus amphitrite* (Crustacea: Thecostraca: Cirripedia), *Mar. Biol.*, 2002, **141**, 513–526, DOI: 10.1007/s00227-002-0854-1.
- 73 A. S. Clare and J. T. Høeg, *Balanus amphitrite* or *Amphibalanus amphitrite*? A note on barnacle nomenclature, *Biofouling*, 2008, **24**, 55–57, DOI: 10.1080/08927010701830194.

- 74 P. Almeida and J. W. P. Coolena, Modelling thickness variations of macrofouling communities on offshore platforms in the Dutch North Sea, *J. Sea Res.*, 2020, **156**, 101836, DOI: 10.1016/j.seares.2019.101836.
- 75 C. Hellio and D. Yebra, *Advances in marine antifouling coatings and technologies*, Elsevier, 1st edn, 2009, ISBN 978-1-84569-386-2.
- 76 N. Aldred and A. S. Clare, Mechanisms and principles underlying temporary adhesion, surface exploration and settlement site selection by barnacle cyprids: A short review, in *Functional Surfaces in Biology*, ed. S. N. Gorb, Springer, Dordrecht, 2009, DOI: 10.1007/978-1-4020-6695-5\_3.
- 77 M. E. Callow, J. A. Callow, L. K. Ista, S. E. Coleman, A. C. Nolasco and G. P. Lopez, Use of self-assembled monolayers of different wettabilities to study surface selection and primary adhesion processes of green algal (Enteromorpha) zoospores, *Appl. Environ. Microbiol.*, 2000, **66**, 3249–3254, DOI: 10.1128/AEM.66.8.3249-3254.2000.
- 78 D. Howell and B. Behrends, A review of surface roughness in antifouling coatings illustrating the importance of cut-off length, *Biofouling*, 2006, **22**, 401–410, DOI: 10.1080/08927010601035738.
- 79 K. A. Dafforn, J. A. Lewis and E. L. Johnston, Antifouling strategies: history and regulation, ecological impacts and mitigation, *Mar. Pollut. Bull.*, 2011, **62**, 453–465, DOI: 10.1016/j.marpolbul.2011.01.012.
- 80 B.-M. Kim, K. Kim, I.-Y. Choi and J.-S. Rhee, Transcriptome response of the Pacific oyster, *Crassostrea gigas* susceptible to thermal stress: A comparison with the re-sponse of tolerant oyster, *Mol. Cell. Toxicol.*, 2017, **13**, 105–113, DOI: 10.1007/s13273-017-0011-z.
- 81 L. Chen, C. Xia and P. Y. Qian, Optimization of antifouling coatings incorporating butenolide, a potent antifouling agent via field and laboratory tests, *Prog. Org. Coat.*, 2017, **109**, 22–29, DOI: 10.1016/j.porgcoat.2017.04.014.
- 82 D. J. Blackwood, C. S. Lim, S. L. Teo, X. Hu and J. Pang, Macrofouling induced localized corrosion of stainless steel in Singapore seawater, *Corros. Sci.*, 2017, **129**, 152–160, DOI: 10.1016/j.corsci.2017.10.008.
- 83 J. R. Kucklick and M. D. Ellisor, A review of organotin contamination in arctic and subarctic regions, *Emerg. Contam.*, 2019, **5**, 150–156, DOI: 10.1016/j.emcon.2019.04.003.
- 84 L. Shtykova, C. Fant, P. Handa, A. Larsson, K. Berntsson, H. Blanck, R. Simonsson, M. Nyd and H. I. Helinda, Adsorption of antifouling booster biocides on metal oxide nanoparticles: Effect of different metal oxides and solvents, *Prog. Org. Coat.*, 2009, **64**, 20–26, DOI: 10.1016/j.porgcoat.2008.07.005.
- 85 T. Onduka, D. Ojima, M. Ito, K. Ito, K. Mochida and K. Fujii, Toxicity of the antifouling biocide Sea-Nine 211 to marine algae, crustacea, and a polychaete, *Fisheries Sci.*, 2013, **79**, 999–1006, DOI: 10.1007/s12562-013-0678-6.
- 86 K. Thomas and S. Brooks, The environmental fate and effects of antifouling paint biocides, *Biofouling*, 2010, **26**, 73–88, DOI: 10.1080/08927010903216564.
- 87 X. Han, J. Wu, X. Zhang, J. Shi, J. Wei, Y. Yang, B. Wu and Y. Feng, Special issue on advanced corrosion-resistance materials and emerging applications. The progress on antifouling organic coating: From biocide to biomimetic surface, *J. Mater. Sci. Technol.*, 2021, **61**, 46–62, DOI: 10.1016/j.jmst.2020.07.002.
- 88 A. Clare, D. Rittschof, D. Gerhart and J. Maki, Molecular approaches to nontoxic antifouling, *Invertebr. Reprod. Dev.*, 1992, **22**, 67–76, DOI: 10.1080/07924259.1992.9672258.
- 89 S. Chambers, K. R. Stokes, F. C. Walsh and R. J. K. Wood, Modern approaches to marine antifouling coatings, *Surf. Coat. Technol.*, 2006, **201**, 3642–3652, DOI: 10.1016/j.surfcoat.2006.08.129.
- 90 I. B. Gomes, M. Sims and L. C. Sims, Copper surfaces in biofilm control, *Nanomaterials*, 2020, **10**, 2491, DOI: 10.3390/nano10122491.
- 91 M. S. Selim, M. Shenashen, S. A. El-Safty, S. Higazy, M. M. Selim, H. Isago and A. Elmarakbi, Recent progress in marine foul-release polymeric nanocomposite coatings, *Prog. Mater. Sci.*, 2017, **87**, 1–32, DOI: 10.1016/j.pmatsci.2017.02.001.
- 92 X. Han, J. Wu, X. Zhang, J. Shi, J. Wei, Y. Yang, B. Wu and Y. Feng, The progress on antifouling organic coating: From biocide to biomimetic surface, *J. Mater. Sci. Technol.*, 2021, **61**, 46–62, DOI: 10.1016/j.jmst.2020.07.002.
- 93 B. Antizar-Ladislao, Environmental levels, toxicity and human exposure to tributyltin (TBT)-contaminated marine environment – A review, *Environ. Int.*, 2008, **34**, 292–308, DOI: 10.1016/j.envint.2007.09.005.
- 94 E. Almeida, T. C. Diamantino and O. de Sousa, Marine paints: the particular case of antifouling paints, *Prog. Org. Coat.*, 2007, **59**, 2–20, DOI: 10.1016/j.porgcoat.2007.01.017.
- 95 I. Banerjee, R. C. Pangule and R. S. Kane, Antifouling coatings: Recent developments in the design of surfaces that prevent fouling by proteins, bacteria, and marine organisms, *Adv. Mater.*, 2011, **23**, 690–718, DOI: 10.1002/adma.201001215.
- 96 E. Aykin, B. Omuzbukun and A. Kacar, Microfouling bacteria and the use of enzymes in eco-friendly antifouling technology, *J. Coat. Technol. Res.*, 2019, **16**, 847–856, DOI: 10.1007/s11998-018-00161-7.
- 97 S. M. Olsen, L. T. Pedersen, M. H. Laursen, S. Kiil and K. Dam-Johansen, Enzyme-based antifouling coatings: A review, *Biofouling*, 2007, **23**, 369–383, DOI: 10.1080/08927010701566384.
- 98 S. M. Olsen, L. T. Pedersen, M. H. Hermann, S. Kiil and S. Dam-Johansen, Enzyme-based solutions for marine antifouling coatings, *Adv. Marine Antifouling Coat. Technol.*, 2009, 623–643, DOI: 10.1533/9781845696313.3.623.
- 99 Q. Chen, D. Zhang, J. Gu, H. Zhang, X. Wu, C. Cao, X. Zhang and R. Liu, The impact of antifouling layers in fabricating bioactive surfaces, *Acta Biomater.*, 2021, **126**, 45–62, DOI: 10.1016/j.actbio.2021.03.022.
- 100 A. L. Patterson, B. Wenning, G. Rizis, D. R. Calabrese, J. A. Finlay, S. C. Franco, R. N. Zuckermann, A. S. Clare, E. J. Kramer, C. K. Ober and R. A. Segalman, Role of

- backbone chemistry and monomer sequence in amphiphilic oligopeptide- and oligopeptoid-functionalized PDMS- and PEO-based block copolymers for marine antifouling and fouling release coatings, *Macromolecules*, 2017, **50**, 2656–2667, DOI: 10.1021/acs.macromol.6b02505.
- 101 A. M. Brzozowska, S. Maassen, R. G. Z. Rong, P. I. Benke, C.-S. Lim, E. M. Marzinelli, D. Jańczewski, S. L.-M. Teo and G. J. Vancso, Effect of variations in micropatterns and surface modulus on marine fouling of engineering polymers, *ACS Appl. Mater. Interfaces*, 2017, **9**, 17508–17516, DOI: 10.1021/acsami.6b14262.
- 102 J. Kim, B. J. Chisholm and J. Bahr, Adhesion study of silicone coatings: The interaction of thickness, modulus and shear rate on adhesion force, *Biofouling*, 2007, **23**, 113–120, DOI: 10.1080/08927010701189708.
- 103 H. Jin, W. Bing, L. Tian, P. Wang and J. Zhao, Combined effects of color and elastic modulus on antifouling performance: A study of graphene oxide/silicone rubber composite membranes, *Materials*, 2019, **12**, 2608, DOI: 10.3390/ma12162608.
- 104 A. K. Halvey, B. Macdonald, A. Dhyani and A. Tuteja, Design of surfaces for controlling hard and soft fouling, *Philos. Trans. A Math. Phys. Eng. Sci.*, 2019, **377**, 20180266, DOI: 10.1098/rsta.2018.0266.
- 105 J. R. Griffith and J. D. Bultman, Fluorinated naval coatings, *Ind. Eng. Chem. Prod. Res. Dev.*, 1978, **17**, 8–9, DOI: 10.1021/i360065a003.
- 106 Y. Gu, L. Yu, J. Mou, D. Wu, M. Xu, P. Zhou and Y. Ren, Research strategies to develop environmentally friendly marine antifouling coatings, *Mar. Drugs*, 2020, **18**, 371, DOI: 10.3390/MD18070371.
- 107 E. Martinelli, S. D. Hill, J. A. Finlay, M. E. Callow, J. A. Callow, A. Glisenti and G. Galli, Amphiphilic modified-styrene copolymer films: Antifouling/fouling release properties against the green alga *Ulva linza*, *Prog. Org. Coat.*, 2016, **90**, 235–242, DOI: 10.1016/j.porgcoat.2015.10.005.
- 108 P. Hu, Q. Xie, C. Ma and G. Zhang, Silicone-based fouling-release coatings for marine antifouling, *Langmuir*, 2020, **36**, 2170–2183, DOI: 10.1021/acs.langmuir.9b03926.
- 109 S. Holberg, R. Losada, F. H. Blaikie, H. H. W. B. Hansen, S. Soreau and R. C. A. Onderwater, Hydrophilic silicone coatings as fouling release: Simple synthesis, comparison to commercial, marine coatings and application on fresh water-cooled heat exchangers, *Mater. Today Commun.*, 2020, **22**, 100750, DOI: 10.1016/j.mtcomm.2019.100750.
- 110 A. Derbalah, S. A. El-Safty, M. A. Shenashen and N. A. A. Ghany, Mesoporous alumina nanoparticles as host tunnel-like pores for removal and recovery of insecticides from environmental samples, *ChemPlusChem*, 2015, **80**, 1119–1126, DOI: 10.1002/cplu.201500098.
- 111 M. S. Selim, S. A. El-Safty, M. A. El-Sockary, A. I. Hashem, O. M. A. Elenien, A. M. EL-Saeed and N. A. Fathallah, Smart photo-induced silicone/TiO<sub>2</sub> nanocomposites with dominant [110] exposed surfaces for self-cleaning foul-release coatings of ship hulls, *Mater. Design*, 2016, **101**, 218–225, DOI: 10.1016/j.matdes.2016.03.124.
- 112 M. C. Parrott and J. M. DeSimone, Relieving PEGylation, *Nat. Chem.*, 2012, **4**, 13–14, DOI: 10.1038/nchem.1230.
- 113 E. Wassel, M. Es-Sounia, A. Laghrissi, A. Roth, M. Dietze and M. Es-Souni, Scratch resistant non-fouling surfaces via grafting non-fouling polymers on the pore walls of supported porous oxide structures, *Mater. Des.*, 2019, **163**, 107542, DOI: 10.1016/j.matdes.2018.107542.
- 114 A. G. Nurioglu and A. C. C. Esteves, Non-toxic, non-biocide-release antifouling coatings based on molecular structure design for marine applications, *J. Mater. Chem. B*, 2015, **3**, 6547–6570, DOI: 10.1039/C5TB00232J.
- 115 W. Taylor and R. A. Jones, Protein adsorption on well-characterized polyethylene oxide brushes on gold: Dependence on molecular weight and grafting density, *Langmuir*, 2013, **29**, 6116–6122, DOI: 10.1021/la40054833.
- 116 W. Yandi, S. Mieszkina, P. Martin-Tanchereau, M. E. Callow, J. A. Callow, L. Tyson, B. Liedberg and T. Ederth, Hydration and chain entanglement determines the optimum thickness of poly (HEMA-co-PEG10MA) brushes for effective resistance to settlement and adhesion of marine fouling organisms, *ACS Appl. Mater. Interfaces*, 2014, **6**, 11448–11458, DOI: 10.1021/am502084x.
- 117 C. Ventura, A. J. Guerin, O. El-Zubir, A. J. Ruiz-Sanchez, L. I. Dixon, K. J. Reynolds, M. L. Dale, J. Ferguson, A. Houlton, B. R. Horrocks, A. S. Clare and D. A. Fulton, Marine antifouling performance of polymer coatings incorporating zwitterions, *Biofouling*, 2017, **33**, 892–903, DOI: 10.1080/08927014.2017.1383983.
- 118 N. Aldred, G. Li, Y. Gao, A. S. Clare and S. Jiang, Modulation of barnacle (*Balanus amphitrite* Darwin) cyprid settlement behavior by sulfobetaine and carboxybetaine methacrylate polymer coatings, *Biofouling*, 2010, **26**, 673–683, DOI: 10.1080/08927014.2010.506677.
- 119 R. Yang, H. Jang, R. Stocker and K. K. Gleason, Synergistic Prevention of biofouling in seawater desalination by zwitterionic surfaces and low-level chlorination, *Adv. Mater.*, 2014, **26**, 1711–1718, DOI: 10.1002/adma.201304386.
- 120 W. Yang, Contribution of charges in polyvinyl alcohol networks to marine antifouling, *ACS Appl. Mater. Interfaces*, 2017, **9**, 18295–18304, DOI: 10.1021/acsami.7b04079.
- 121 S. Krishnan, Anti-biofouling properties of comblike block copolymers with amphiphilic side chains, *Langmuir*, 2006, **22**, 5075–5086.
- 122 S. Bauer, M. Alles, M. P. Arpa-Sancet, E. Ralston, G. W. Swain, N. Aldred, A. S. Clare, J. A. Finlay, M. E. Callow, J. A. Callow and A. Rosenhahn, Resistance of amphiphilic polysaccharides against marine fouling organisms, *Biomacromolecules*, 2016, **17**, 897–904, DOI: 10.1021/acs.biomac.5b01590.
- 123 W. Zoelen, H. G. Buss, N. C. Ellebracht, N. A. Lynd, D. A. Fischer, J. Finlay, S. Hill, M. E. Callow, J. A. Callow, E. J. Kramer, R. N. Zuckermann and R. A. Segalman, Sequence of hydrophobic and hydrophilic residues in amphiphilic polymer coatings affects surface structure and marine antifouling/fouling release properties, *ACS Macro Lett.*, 2014, **3**, 364–368, DOI: 10.1021/mz500090n.



- 124 K. Seetho, S. Zhang, K. A. Pollack, J. Zou, J. E. Raymond, E. Martinez and K. L. Wooley, Facile synthesis of a phosphorylcholine-based zwitterionic amphiphilic copolymer for anti-biofouling coatings, *ACS Macro Lett.*, 2015, **4**, 505–510, DOI: 10.1021/mz500818c.
- 125 D. Jiang, Y. Zhang, F. Zhang, Z. Liu, J. Han and X. Wu, Antimicrobial and antifouling nanocomposite hydrogels containing polythioether dendron: High-loading silver nanoparticles and controlled particle release, *Colloid Polym. Sci.*, 2016, **294**, 2021–2028, DOI: 10.1007/s00396-016-3967-7s.
- 126 R. Zhang, L. Zhang, N. Tian, S. Ma, Y. Liu, B. Yu, X. Pei and F. Zhou, The Tethered fibrillar hydrogels brushes for underwater antifouling, *Adv. Mater.*, 2017, **4**, 1601039, DOI: 10.1002/admi.201601039.
- 127 S. Verma, S. Mohanty and S. Nayak, A review on protective polymeric coatings for marine applications, *J. Coat. Technol. Res.*, 2019, **16**, 307–338, DOI: 10.1007/s11998-018-00174-2.
- 128 J. Fu, H. Zhang, Z. Guo, D. Feng, V. Thiyagarajan and H. Yao, Combat biofouling with microscopic ridge-like surface morphology: A bioinspired study, *J. R. Soc., Interface*, 2018, **15**, 20170823, DOI: 10.1098/rsif.2017.0823.
- 129 L. Xiao, J. A. Finlay, M. Röhrig, S. Mieszkin, M. Worgull, H. Hölscher, J. A. Callow, M. E. Callow, M. Grunze and A. Rosenhahn, Topographic cues guide the attachment of diatom cells and algal zoospores, *Biofouling*, 2018, **34**, 86–97, DOI: 10.1080/08927014.2017.1408801.
- 130 Y. Zhang, W. Zhao, Z. Chen, Z. Liu, H. Cao, C. Zhou and P. Cui, Influence of biomimetic boundary structure on the antifouling performances of siloxane modified resin coatings, *Colloids Surf., A*, 2017, **528**, 57–64, DOI: 10.1016/j.colsurfa.2017.05.044.
- 131 T. Sullivan and F. Regan, Marine diatom settlement on microtextured materials in static field trials, *J. Mater. Sci.*, 2017, **52**, 5846–5856, DOI: 10.1007/s10853-017-0821-3.
- 132 K. Efimenko, J. Finlay, M. Callow, J. Callow and J. Genzer, Development and testing of hierarchically wrinkled coatings for marine antifouling, *ACS Appl. Mater. Interfaces*, 2009, **1**, 1031–1040, DOI: 10.1021/am9000562.
- 133 S. K. Kyei, G. Darko and O. Akaranta, Chemistry and application of emerging ecofriendly antifouling paints: A review, *J. Coat. Technol. Res.*, 2020, **17**, 315–332, DOI: 10.1007/s11998-019-00294-3.
- 134 M. Carve, A. Scardino and J. Shimeta, Effects of surface texture and interrelated properties on marine biofouling: A systematic review, *Biofouling*, 2019, **35**, 597–617, DOI: 10.1080/08927014.2019.1636036.
- 135 M. S. Selim, M. A. Shenashen, A. Elmarakbi, N. A. Fatthallah, S. Hasegawa and S. A. El-Safty, Synthesis of ultrahydrophobic and thermally stable inorganic–organic nanocomposites for self-cleaning foul release coatings, *Chem. Eng. J.*, 2017, **320**, 653–666, DOI: 10.1016/j.cej.2017.03.067.
- 136 M. Winfield, A. Downer, J. Longyear, M. Dale and G. Barker, Comparative study of biofilm formation on biocidal antifouling and fouling-release coatings using next-generation DNA sequencing, *Biofouling*, 2018, **34**, 464–477, DOI: 10.1080/08927014.2018.1464152.
- 137 Z. Lu, Z. Chen, Y. Guo, Y. Ju, Y. Liu, R. Feng, C. Xiong, C. K. Ober and L. Dong, Flexible hydrophobic antifouling coating with oriented nanotopography and nonleaking Capsaicin, *ACS Appl. Mater. Interfaces*, 2018, **10**, 9718–9726, DOI: 10.1021/acsami.7b19436.
- 138 X. Han, J. Wu, X. Zhang, J. Shi, J. Wei, Y. Yang, B. Wu and Y. Feng, Special Issue on advanced corrosion-resistance materials and emerging applications. The progress on antifouling organic coating: from biocide to biomimetic surface, *J. Mater. Sci. Technol.*, 2021, **61**, 46–62, DOI: 10.1016/j.jmst.2020.07.002.
- 139 H. R. Z. Tadros, E. M. Elkady and S. M. Saleh, Comparative study for marine antifouling agents based on natural sarcophine product and ZnO nanomaterials, *Egypt. J. Aquat. Res.*, 2021, **47**, 191–197, DOI: 10.1016/j.ejar.2020.12.002.
- 140 N. Schwartz, S. Dobretsov, S. Rohde and P. J. Schupp, Comparison of antifouling properties of native and invasive *Sargassum* (Fucales, Phaeophyceae) species, *Eur. J. Phycol.*, 2017, **52**, 116–131, DOI: 10.1080/09670262.2016.1231345.
- 141 F. Maia, A. P. Silva, S. Fernandes, A. Cunha, A. Almeida, J. Tedim, M. L. Zheludkevich and M. G. S. Ferreira, Incorporation of biocides in nanocapsules for protective coatings used in maritime applications, *Chem. Eng. J.*, 2015, **270**, 150–157, DOI: 10.1016/j.cej.2015.01.076.
- 142 F. Avelas, R. Martins, T. Oliveira, F. Maia, E. Malheiro, A. M. V. M. Soares, S. Loureiro and J. Tedim, Efficacy and ecotoxicity of novel anti-fouling nanomaterials in target and non-target marine species, *Mar. Biotechnol.*, 2017, **19**, 164–174, DOI: 10.1007/s10126-017-9740-1.
- 143 C. A. Bode-Aluko, O. Perea, H. H. Kyaw, L. Al-Naamani, M. Z. Al-Abri, M. T. Z. Myinte, A. Rossouw, O. Fatobaa, L. Petrika and S. Dobretsov, Photocatalytic and antifouling properties of electrospun TiO<sub>2</sub> polyacrylonitrile composite nanofibers under visible light, *Mater. Sci. Eng. B*, 2021, **264**, 1149132, DOI: 10.1016/j.mseb.2020.114913.
- 144 W. He, P. Liu, J. Zhang and X. Yao, Emerging applications of bioinspired slippery surfaces in biomedical fields, *Chem. – Eur. J.*, 2018, **24**, 14864–14877, DOI: 10.1002/chem.201801368.
- 145 M. S. A. Saraswathi, D. Rana, K. Divya, S. Gowrishankar, S. Sakthivel, S. Alwarappan and A. Nagendran, Highly permeable, antifouling and antibacterial poly(ether imide) membranes tailored with poly (hexamethylenebiguanide) coated copper oxide nanoparticles, *Mater. Chem. Phys.*, 2020, **240**, 122224, DOI: 10.1016/j.matchemphys.2019.122224.
- 146 M. S. S. A. Saraswathi, D. Rana, K. Divya, S. Gowrishankar and A. Nagendran, Versatility of hydrophilic and anti-fouling PVDF ultrafiltration membranes tailored with polyhexanide coated copper oxide nanoparticles, *Polym. Test.*, 2020, **84**, 106367, DOI: 10.1016/j.polymertesting.2020.106367.

- 147 K. Gao, Y. Su, L. Zhou, M. He, R. Zhang, Y. Liu and Z. Jiang, Creation of active-passive integrated mechanisms on membrane surfaces for superior antifouling and antibacterial properties, *J. Membr. Sci.*, 2018, **548**, 621–631, DOI: 10.1016/j.memsci.2017.10.042.
- 148 H. E. Yong, K. Krishnamoorthy, K. T. Hyun and S. J. Kim, Preparation of ZnO nanopaint for marine antifouling application, *J. Ind. Eng. Chem.*, 2015, **29**, 39–42, DOI: 10.1016/j.jiec.2015.04.020.
- 149 J. Zhang, Y. Xu, S. Chen, J. Li, W. Han, X. Sun, D. Wu, Z. Hu and L. Wang, Enhanced antifouling and antibacterial properties of poly(ether sulfone) membrane modified through blending with sulfonated poly(aryl ether sulfone) and copper nanoparticles, *Appl. Surf. Sci.*, 2018, **434**, 806–815, DOI: 10.1016/j.apsusc.2017.11.007.
- 150 J. Lee, I. Lee, J. Nam, D. S. Hwang, K. M. Yeon and J. Kim, Immobilization and stabilization of acylase on carboxylated polyaniline nanofibers for highly effective antifouling application via quorum quenching, *ACS Appl. Mater. Interfaces*, 2017, **9**, 15424–15432, DOI: 10.1021/acsami.7b01528.
- 151 S. Tian, D. Jiang, J. Pu, X. Sun, Z. Li, B. Wu, W. Zheng, W. Liu and Z. Liu, A new hybrid silicone-based antifouling coating with nanocomposite hydrogel for durable antifouling properties, *Chem. Eng. J.*, 2019, **370**, 1–9, DOI: 10.1016/j.cej.2019.03.185.
- 152 M. S.-L. Yee, P.-S. Khiew, W. S. Chiu, Y.-F. Tan and C.-O. Leong, Polyethyleneimine-capped silver nanoparticles as antifouling photocatalyst for wastewater treatment, *Mater. Today: Proc.*, 2019, **19**, 1497–1506, DOI: 10.1016/j.matpr.2019.11.174.
- 153 M. A. Al-Belushi, M. T. Z. Myint, H. H. Kyaw, L. Al-Naamani, R. Al-Mamari, M. Al-Abri and S. Dobretsov, ZnO nanorod-chitosan composite coatings with enhanced antifouling properties, *Int. J. Biol. Macromolecules*, 2020, **162**, 1743–1751, DOI: 10.1016/j.ijbiomac.2020.08.096.
- 154 J. Revuelta, I. Fraile, D. T. Monterrey, N. Pena, R. Benito-Arenas, A. Bastida, A. Fernandez-Mayoralas and E. Garcia-Junceda, Heparanized chitosans: Towards the third generation of chitinous biomaterials, *Mater. Horiz.*, 2021, **8**, 2596.
- 155 S. Dobretsov, P. Sathe, T. Bora, M. Barry, M. T. Z. Myint and M. A. Abri, Toxicity of different zinc oxide nanomaterials at 3 trophic levels: implications for development of low-toxicity antifouling agents, *Environ. Toxicol. Chem.*, 2020, **39**, 1343–1354, DOI: 10.1002/etc.4720.
- 156 N. Wang, W. Li, Y. Ren, J. Duan, X. Zhai, F. Guan, L. Wang and B. Hou, Investigating the properties of nano core-shell CeO<sub>2</sub>@C as haloperoxidase mimicry catalyst for antifouling applications, *Colloids Surf., A*, 2021, **608**, 125592, DOI: 10.1016/j.colsurfa.2020.125592.
- 157 T. Bus, M. L. Dale, K. J. Reynolds and C. W. M. Bastiaansen, Thermoplastic, rubber-like marine antifouling coatings with micro-structures via mechanical embossing, *Biofouling*, 2020, **36**, 138–145, DOI: 10.1080/08927014.2020.1734576.
- 158 K. Lee, C. Kim, S. Jeong, Y. Song, N. Bae, S. Lee and K. Lee, Ultrasonic fabrication of flexible antibacterial ZnO nanopillar array film, *Colloids Surf., B*, 2018, **170**, 172–178, DOI: 10.1016/j.colsurfb.2018.06.007.
- 159 P. Sathe, K. Laxman, M. T. Z. Myint, S. Dobretsov, J. Richter and J. Dutta, Bioinspired nanocoatings for biofouling prevention by photocatalytic redox reactions, *Sci. Rep.*, 2017, **7**, 3624, DOI: 10.1038/s41598-017-03636-6.
- 160 A. S. Adeleye, E. A. Oranu, M. Tao and A. A. Keller, Release and detection of nanosized copper from a commercial antifouling paint, *Water Res.*, 2016, **102**, 374–382, DOI: 10.1016/j.watres.2016.06.056.
- 161 H. Barzegar, M. A. Zahed and V. Vatanpour, Antibacterial and antifouling properties of Ag<sub>3</sub>PO<sub>4</sub>/GO nanocomposite blended polyethersulfone membrane applied in dye separation, *Water Proc. Eng.*, 2020, **38**, 101638, DOI: 10.1016/j.jwpe.2020.101638.
- 162 E. Gutner-Hoch, R. Martins, T. Oliveira, F. Maia, A. M. V. M. Soares, S. Loureiro, C. Pillar, I. Preiss, M. Weis, S. B. Larroze, T. Teixeira, J. Tedim and Y. Benayahu, Antimicrofouling efficacy of innovative inorganic nanomaterials loaded with booster biocides, *J. Mar. Sci. Eng.*, 2018, **6**, 1–12, DOI: 10.3390/jmse6010006.
- 163 N. Punitha, P. Saravanan, R. Mohan and P. S. Ramesh, Antifouling activities of beta-cyclodextrin stabilized peg based silver nanocomposites, *Appl. Surf. Sci.*, 2017, **392**, 126–134, DOI: 10.1016/j.apsusc.2016.07.114.
- 164 X. Zhai, P. Ju, F. Guan, Y. Ren, X. Liu, N. Wang, Y. Zhang, J. Duan, C. Wang and B. Hou, Electrodeposition of capsaicin-induced ZnO/Zn nanopillar films for marine antifouling and antimicrobial corrosion, *Surf. Coat. Technol.*, 2020, **397**, 125959, DOI: 10.1016/j.surfcoat.2020.125959.
- 165 H. Vatankeh, C. C. Murray, J. W. Brannum, J. Vanneste and C. Bellona, Effect of pre-ozonation on nanofiltration membrane fouling during water reuse applications, *Sep. Purif. Technol.*, 2018, **205**, 203–211, DOI: 10.1016/j.seppur.2018.03.052.
- 166 L. Ruggiero, F. Bartoli, M. R. Fidanza, F. Zurlo, E. Marconi, T. Gasperi, S. Tuti, L. Crociani, E. Di Bartolomeo, G. Caneva, M. A. Ricci and A. Sod, Encapsulation of environmentally-friendly biocides in silica nanosystems for multifunctional coatings, *Appl. Surf. Sci.*, 2020, **514**, 145908, DOI: 10.1016/j.apsusc.2020.145908.
- 167 A. Al-Jumaili, P. Mulvey, A. Kumar, K. Prasad, K. Bazaka, J. Warner and M. V. Jacob, Eco-friendly nanocomposites derived from geranium oil and zinc oxide in one step approach, *Sci. Rep.*, 2019, **9**, 5973, DOI: 10.1038/s41598-019-42211-z.
- 168 A. Kumar, S. Mills, K. Bazaka, N. Bajema, I. Atkinson and M. V. Jacob, Biodegradable optically transparent terpinen-4-ol thin films for marine antifouling applications, *Surf. Coat. Technol.*, 2018, **349**, 426–433, DOI: 10.1016/j.surfcoat.2018.05.074.
- 169 K. Bazaka, M. V. Jacob and B. F. Bowden, Optical and chemical properties of polyterpenol thin films deposited via plasma-enhanced chemical vapor deposition, *J. Mater. Res.*, 2011, **26**, 1018–1025, DOI: 10.1557/jmr.2011.23.
- 170 K. Bazaka, M. V. Jacob, V. K. Truong, F. Wang, W. A. A. Pushpamali, J. Y. Wang, A. V. Ellis, C. C. Berndt,

- R. J. Crawford and E. P. Ivanova, Plasma-enhanced synthesis of bioactive polymeric coatings from monoterpene alcohols: A combined experimental and theoretical study, *Biomacromolecules*, 2010, **11**(8), 2016–2026, DOI: 10.1021/bm100369n.
- 171 M. S. Selim, S. A. El-Safty, A. Abbas and M. A. Shenashen, Facile design of graphene oxide-ZnO nanorod-based ternary nanocomposite as a superhydrophobic and corrosion-barrier coating, *Colloids Surf., A*, 2021, **611**, 125793, DOI: 10.1016/j.colsurfa.2020.125793.
- 172 W. Dong, B. Li, J. Wei, N. Tian, W. Liang and J. Zhang, Environmentally friendly, durable and transparent anti-fouling coatings applicable onto various substrates, *J. Colloid Interface Sci.*, 2021, **591**, 429–439, DOI: 10.1016/j.jcis.2021.02.014.
- 173 C. Piferi, K. Bazaka, D. L. D'Aversa, R. Di Girolamo, C. De Rosa, H. E. Roman, C. Riccardi and I. Levchenko, Hydrophilicity and hydrophobicity control of plasma-treated surfaces via fractal parameters, *Adv. Mater. Interfaces*, 2021, **8**, 2100724, DOI: 10.1002/admi.202100724.
- 174 G. Wang, A. Li, K. Li, Y. Zhao, Y. Ma and Q. He, A fluorine-free superhydrophobic silicone rubber surface has excellent self-cleaning and bouncing properties, *J. Colloid Interface Sci.*, 2021, **588**, 175–183, DOI: 10.1016/j.jcis.2020.12.059.
- 175 M. S. Selim, S. A. El-Safty and M. A. Shenashen, in *Superhydrophobic Polymer Coatings*, Chapter 8 – Superhydrophobic foul resistant and self-cleaning polymer coating, ed. S. K. Samal, S. Mohanty and S. K. Nayak, Elsevier Scientific Publisher Company, New York, 2019, pp. 181–203, DOI: 10.1016/B978-0-12-816671-0.00009-6.
- 176 D. Kim and S. Ryu, How and when the cassie-baxter droplet starts to slide on textured surfaces, *Langmuir*, 2020, **36**, 14031–14038, DOI: 10.1021/acs.langmuir.0c02614.
- 177 A. B. D. Cassie and S. Baxter, Wettability of porous surfaces, *Trans. Faraday Soc.*, 1944, **40**, 546–551, DOI: 10.1039/TF9444000546.
- 178 Z. Chang and Y. Lu, Fabrication of superhydrophobic surfaces with Cassie–Baxter state, *J. Dispers. Sci. Technol.*, 2020, DOI: 10.1080/01932691.2020.1848571.
- 179 A. Azimi and P. He, Effect of gravity in the Cassie-to-Wenzel transition on a micropatterned surface, *MRS Commun.*, 2020, **10**, 129–134, DOI: 10.1557/mrc.2019.160.
- 180 Y. Cho and C. H. Park, Objective quantification of surface roughness parameters affecting superhydrophobicity, *RSC Adv.*, 2020, **10**, 31251, DOI: 10.1039/d0ra03137b.
- 181 R. N. Wenzel, Resistance of solid surfaces to wetting by water, *Ind. Eng. Chem.*, 1936, **28**, 988–994, DOI: 10.1021/ie50320a024.
- 182 T.-S. Wong, S. H. Kang, S. K. Y. Tang, E. J. Smythe, B. D. Hatton, A. Grinthal and J. Aizenberg, Bioinspired self-repairing slippery surfaces with pressure-stable omniphobicity, *Nature*, 2011, **477**, 443–447, DOI: 10.1038/nature10447.
- 183 M. Nosonovsky, Slippery when wetted, *Nature*, 2011, **477**, 412–413, DOI: 10.1038/477412a.
- 184 A. Giacomello, S. Meloni, M. Chinappi and C. M. Casciola, Cassie–Baxter and Wenzel states on a nanostructured surface: Phase diagram, metastabilities, and transition mechanism by atomistic free energy calculations, *Langmuir*, 2012, **28**, 10764–10772, DOI: 10.1021/la3018453.
- 185 P. Zhang, L. Lin, D. Zang, X. Guo and M. Liu, Designing bioinspired anti-biofouling surfaces based on a superwettability strategy, *Small*, 2016, **13**, 1503334, DOI: 10.1002/smll.201503334.
- 186 I. Levchenko, S. Xu, O. Baranov, O. Bazaka, E. P. Ivanova and K. Bazaka, Plasma and polymers: recent progress and trends, *Molecules*, 2021, **26**, 4091, DOI: 10.3390/molecules26134091.
- 187 M. S. Selim, N. A. Fatthallah, S. A. Higazy, Z. Hao and P. J. Mo, A comparative study between two novel silicone/graphene-based nanostructured surfaces for maritime antifouling, *J. Colloid Interface Sci.*, 2022, **606**, 367–383, DOI: 10.1016/j.jcis.2021.08.026.
- 188 M. S. Selim, S. A. El-Safty, A. M. Azzam, M. A. Shenashen, M. A. El-Sockary and O. M. A. Elenien, Silicone/TiO<sub>2</sub>–SiO<sub>2</sub> nanorod-like composites for marine fouling release coatings, *ChemistrySelect*, 2019, **4**, 3395–3407, DOI: 10.1002/slct.201803314.
- 189 M. S. Selim, H. Yang, F. Q. Wang, N. A. Fatthallah, Y. Huang and S. Kuga, Silicone/ZnO nanorod composite coating as a marine antifouling surface, *Appl. Surf. Sci.*, 2019, **466**, 40–50, DOI: 10.1016/j.apsusc.2018.10.004.
- 190 Y. Deng, D. Mager, Y. Bai, T. Zhou, Z. Liu, L. Wen, Y. Wu and J. G. Korvink, Inversely designed micro-textures for robust Cassie–Baxter mode of super-hydrophobicity, *Comput. Methods Appl. Mech. Eng.*, 2018, **341**, 113–132, DOI: 10.1016/j.cma.2018.06.034.
- 191 M. S. Selim, S. A. El-Safty, N. A. Fatthallah and M. A. Shenashen, Silicone/graphene oxide sheet-alumina nanorod ternary composite for superhydrophobic antifouling coating, *Prog. Org. Coat.*, 2018, **121**, 160–172, DOI: 10.1016/j.porgcoat.2018.04.021.
- 192 M. S. Selim, H. Yang, S. A. El-Safty, N. A. Fatthallah, M. A. Shenashen, F. Q. Wang and Y. Huang, Superhydrophobic coating of silicone/ $\beta$ -MnO<sub>2</sub> nanorod composite for marine antifouling, *Colloids Surf., A*, 2019, **570**, 518–530, DOI: 10.1016/j.colsurfa.2019.03.026.
- 193 B. Wu, X. Cui, H. Jiang, N. Wu, C. Peng, Z. Hu, X. Liang, Y. Yan, J. Huang and D. Li, A superhydrophobic coating harvesting mechanical robustness, passive anti-icing and active de-icing performances, *J. Colloid Interface Sci.*, 2021, **590**, 301–310.
- 194 B. Bai and B. Zhang, Fabrication of superhydrophobic reduced-graphene oxide/nickel coating with mechanical durability, self-cleaning and anticorrosion performance, *Nano Mater. Sci.*, 2020, **2**, 151–158.
- 195 P. K. Narayanam, P. Soni, V. D. Botcha, G. Singh and S. S. Major, Transparent and Hydrophobic “Reduced graphene oxide–titanium dioxide” nanocomposites for nonwetting device applications, *ACS Appl. Nano Mater.*, 2018, **1**, 5691–5701.

- 196 M. Zhang, Z. Wu, F. Meng and H. Lin, Facile preparation of grass-like hierarchical structured  $\gamma$ -ALOOH coated stainless steel mesh with superhydrophobic and superoleophilic for highly efficient oil-water separation, *Sep. Purif. Technol.*, 2019, **212**, 347–354.
- 197 H. Jin, W. Bing, L. Tian, P. Wang and J. Zhao, Combined effects of color and elastic modulus on antifouling performance: A study of graphene oxide/silicone rubber composite membranes, *Materials*, 2019, **12**, 2608, DOI: 10.3390/ma12162608.
- 198 X. Zhang and Ø. Mikkelsen, Graphene oxide/silver nanocom on sensor housing materials, *J. Cluster Sci.*, 2021, DOI: 10.1007/s10876-020-01953-x.
- 199 H. Jin, T. Zhang, W. Bing, S. Dong and L. Tian, Antifouling performance and mechanism of elastic graphene–silicone rubber composite membranes, *J. Mater. Chem. B*, 2019, **7**, 488, DOI: 10.1039/c8tb02648c.
- 200 K. Prasad, G. S. Lekshmi, K. Ostrikov, V. Lussini, J. Blinco, M. Mohandas, K. Vasilev, S. Bottle, K. Bazaka and K. Ostrikov, Synergic bactericidal effects of reduced graphene oxide and silver nanoparticles against Gram-positive and Gram-negative bacteria, *Sci. Rep.*, 2017, **7**, 1591, DOI: 10.1038/s41598-017-01669-5.
- 201 J. Figueiredo, S. Loureiro and R. Martins, Hazard of novel anti-fouling nanomaterials and the biocides DCOIT and silver to marine organisms, *Environ. Sci.: Nano*, 2020, **7**, 1670–1680, DOI: 10.1039/D0EN00023J.
- 202 E. P. S. de Jesus, L. P. de Figueiredo, F. Maia, R. Martins and J. Nilin, Acute and chronic effects of innovative antifouling nanostructured biocides on a tropical marine microcrustacean, *Mar. Pollut. Bull.*, 2021, **164**, 111970, DOI: 10.1016/j.marpolbul.2021.111970.
- 203 E. Gutner-Hoch, R. Martins, F. Maia, T. Oliveira, M. Shpigel, M. Weis, J. Tedim and Y. Benayahu, Toxicity of engineered micro- and nanomaterials with antifouling properties to the brine shrimp *Artemia salina* and embryonic stages of the sea urchin *Paracentrotus lividus*, *Environ. Pollut.*, 2019, **251**, 530–537, DOI: 10.1016/j.envpol.2019.05.031.
- 204 L. A. Nassif, S. Rioual, W. Farah, M. Fauchon, Y. Toueix, C. Hellio, M. Abboud and B. Lescop, Electrophoretic deposition of zinc alginate coatings on stainless steel for marine antifouling applications, *J. Environ. Chem. Eng.*, 2020, **8**, 104246, DOI: 10.1016/j.jece.2020.104246.
- 205 D. Q. Feng, J. He, S. Y. Chen, P. Su, C. H. Ke and W. Wang, The plant alkaloid camptothecin as a novel antifouling compound for marine paints: Laboratory bioassays and field trials, *Mar. Biotechnol.*, 2018, **20**, 623–638, DOI: 10.1007/s10126-018-9834-4.
- 206 I. Levchenko, S. Xu, O. Cherkun, O. Baranov and K. Bazaka, Plasma meets metamaterials: Three ways to advance space micropropulsion systems, *Adv. Phys.: X*, 2021, **6**, 1834452, DOI: 10.1080/23746149.2020.1834452.
- 207 I. Levchenko, K. Bazaka, O. Baranov, O. Cherkun, M. Keidar and S. Xu, Processes at plasma–matter interfaces: An overview and future trends, *AAPPS Bull.*, 2020, **30**, 37–48, DOI: 10.22661/AAPPSBL.2020.30.3.37.
- 208 S. P. Suresh, G. S. Lekshmi, S. D. Kirupha, M. Ariraman, O. Bazaka, I. Levchenko, K. Bazaka and M. Mandhakini, Superhydrophobic fluorine-modified cerium-doped mesoporous carbon as an efficient catalytic platform for photodegradation of organic pollutants, *Carbon*, 2019, **147**, 323–333, DOI: 10.1016/j.carbon.2019.02.074.
- 209 Q. Xiang, X. Ma, D. Zhang, H. Zhou, Y. Liao, H. Zhang, S. Xu, I. Levchenko and K. Bazaka, Interfacial modification of titanium dioxide to enhance photocatalytic efficiency towards H<sub>2</sub> production, *J. Colloid Interface Sci.*, 2019, **556**, 376–385, DOI: 10.1016/j.jcis.2019.08.033.
- 210 I. Levchenko, K. Bazaka, O. Baranov, R. M. Sankaran, A. Nomine, T. Belmonte and S. Xu, Lightning under water: Diverse reactive environments and evidence of synergistic effects for material treatment and activation, *Appl. Phys. Rev.*, 2018, **5**, 021103, DOI: 10.1063/1.5024865.
- 211 Z. J. Han, S. Yick, I. Levchenko, E. Tam, M. M. A. Yajadda, S. Kumar, P. J. Martin, S. Furman and K. Ostrikov, Controlled synthesis of a large fraction of metallic single-walled carbon nanotube and semiconducting carbon nanowire networks, *Nanoscale*, 2011, **3**, 3214–3220, DOI: 10.1039/C1NR10327J.
- 212 S. Alancherry, K. Bazaka, I. Levchenko, A. Al-Jumaili, B. Kandel, A. Alex, F. C. R. Hernandez, O. K. Varghese and M. V. Jacob, Fabrication of nano-onion-structured graphene films from citrus sinensis extract and their wetting and sensing characteristics, *ACS Appl. Mater. Interfaces*, 2020, DOI: 10.1021/acsami.0c04353.
- 213 Z. Chen, S. Zhang, I. Levchenko, I. I. Beilis and M. Keidar, In vitro demonstration of cancer inhibiting properties from stratified self-organized plasma-liquid interface, *Sci. Rep.*, 2017, **7**, 12163, DOI: 10.1038/s41598-017-12454-9.
- 214 G. S. Lekshmi, R. Tamilselvi, R. Geethalakshmi, S. D. Kirupha, O. Bazaka, I. Levchenko, K. Bazaka and M. Mandhakini, Multifunctional oil-produced reduced graphene oxide – silver oxide composites with photocatalytic, antioxidant, and antibacterial activities, *J. Colloid Interface Sci.*, 2022, **608**, 294–305, DOI: 10.1016/j.jcis.2021.08.048.
- 215 V. Dupraz, S. Stachowski-Haberkorn, D. Menard, G. Limon, F. Akcha, H. Budzinski and N. Cedergreen, Combined effects of antifouling biocides on the growth of three marine microalgal species, *Chemosphere*, 2018, **209**, 801–814, DOI: 10.1016/j.chemosphere.2018.06.139.
- 216 R.-Y. Huang, L. Pei, Q. Liu, S. Chen, H. Dou, G. Shu, Z. Yuan, J. Lin, G. Peng, W. Zhang and H. Fu, Isobologram analysis: A comprehensive review of methodology and current research, *Front. Pharmacol.*, 2019, **10**, 1222, DOI: 10.3389/fphar.2019.01222.
- 217 Z. Li, D. Rana, Z. Wang, T. Matsuura and C. Q. Lan, Synergic effects of hydrophilic and hydrophobic nanoparticles on performance of nanocomposite distillation membranes: An experimental and numerical study, *Sep. Purif. Technol.*, 2018, **202**, 45–58, DOI: 10.1016/j.seppur.2018.03.032.
- 218 A. M. Shumatbaeva, J. E. Morozova, Y. V. Shalaeva, A. F. Saifina, A. T. Gubaidullin, V. V. Syakaev, A. S. Sapunova,

- A. D. Voloshina, I. R. Nizameev, M. K. Kadirov, K. S. Bulygina, V. M. Babaev and I. S. Antipin, Synthesis of Ag–AgCl nanoparticles capped by calix resorcinarene–mPEG conjugate and their antimicrobial activity, *Colloids Surf., A*, 2020, **602**, 125124, DOI: 10.1016/j.colsurfa.2020.125124.
- 219 Y. Deng, G.-L. Song, D. Zheng and Y. Zhang, Fabrication and synergistic antibacterial and antifouling effect of an organic/inorganic hybrid coating embedded with nano-composite Ag@TA-SiO<sub>2</sub> particles, *Colloids Surf., A*, 2021, **613**, 126085, DOI: 10.1016/j.colsurfa.2020.126085.
- 220 B. Xu, Y. J. Liu, X. W. Sun, J. H. Hu, P. Shi and X. Y. Huang, Semifluorinated synergistic nonfouling/fouling-release surface, *ACS Appl. Mater. Interfaces*, 2017, **9**, 16517–16523, DOI: 10.1021/acsami.7b03258.
- 221 D. Wang, J. Xu, J. Yang and S. Zhou, Preparation and synergistic antifouling effect of self-renewable coatings containing quaternary ammonium-functionalized SiO<sub>2</sub> nanoparticles, *J. Colloid Interface Sci.*, 2020, **563**, 261–271, DOI: 10.1016/j.jcis.2019.12.086.
- 222 H. Yan, Q. Wu, C. Yu, T. Zhao and M. Liu, Recent progress of biomimetic antifouling surfaces in marine, *Adv. Mater. Interfaces*, 2020, **7**, 2000966, DOI: 10.1002/admi.202000966.
- 223 W. Zhang, R. Wang, Z. M. Sun, X. Zhu, Q. Zhao, T. Zhang, A. Cholewinski, F. K. Yang, B. Zhao, R. Pinnaratip, P. K. Forooshani and B. Lee, Catechol-functionalized hydrogels: Biomimetic design, adhesion mechanism, and biomedical applications, *Chem. Soc. Rev.*, 2020, **49**, 433–464, DOI: 10.1039/C9CS00285E.
- 224 L. Chen, Y. Duan, M. Cui, R. Huang, R. Su, W. Qi and Z. He, Biomimetic surface coatings for marine antifouling: Natural antifoulants, synthetic polymers and surface microtopography, *Sci. Total Environ.*, 2021, **766**, 144469, DOI: 10.1016/j.scitotenv.2020.144466.
- 225 M. S. Selim, S. A. El-Safty, M. A. Shenashen, S. A. Higazy and A. Elmarakbi, Progress in biomimetic leverages for marine antifouling using nanocomposite coatings, *J. Mater. Chem. B*, 2020, **8**, 3701–3732, DOI: 10.1039/C9TB02119A.
- 226 I. Manolakis and U. Azhar, Recent advances in mussel-inspired synthetic polymers as marine antifouling coatings, *Coatings*, 2020, **10**, 653, DOI: 10.3390/coatings10070653.
- 227 Z. Wang, H.-C. Yang, F. He, S. Peng, Y. Li, L. Shao and S. B. Darling, Mussel-inspired surface engineering for water-remediation materials, *Matter*, 2019, **1**, 115–155, DOI: 10.1016/j.matt.2019.05.002.
- 228 D. K. Yeon, S. Ko, S. Jeong, S.-P. Hong, S. M. Kang and W. K. Cho, Oxidation-mediated, zwitterionic polydopamine coatings for marine antifouling applications, *Langmuir*, 2019, **35**, 1227–1234, DOI: 10.1021/acs.langmuir.8b03454.
- 229 J. Wang and C. He, Photopolymerized biomimetic self-adhesive Polydimethylsiloxane-based amphiphilic cross-linked coating for anti-biofouling, *Appl. Surf. Sci.*, 2019, **463**, 1097–1106, DOI: 10.1016/j.apsusc.2018.08.214.
- 230 P. Cao, C. Dub, X. He, C. Zhang and C. Yuan, Modification of a derived antimicrobial peptide on steel surface for marine bacterial resistance, *Appl. Surf. Sci.*, 2020, **510**, 145512, DOI: 10.1016/j.apsusc.2020.145512.
- 231 Y. Zhao, J. Wen, Y. Ge, X. Zhang, H. Shi, K. Yang, X. Gao, S. Shi and Y. Gong, Fabrication of stable biomimetic coating on PDMS surface: Cooperativity of multivalent interactions, *Appl. Surf. Sci.*, 2019, **469**, 720–730, DOI: 10.1016/j.apsusc.2018.11.056.
- 232 Y. Ouyang, J. Zhao, R. Qiu, S. Hu, M. Chen and P. Wang, Liquid-infused superhydrophobic dendritic silver matrix: A bio-inspired strategy to prohibit biofouling on titanium, *Surf. Coat. Technol.*, 2019, **367**, 148–155, DOI: 10.1016/j.surfcoat.2019.03.067.
- 233 H. Zhang, Y. Liang, P. Wang and D. Zhang, Design of slippery organogel layer with room-temperature self-healing property for marine anti-fouling application, *Prog. Org. Coat.*, 2019, **132**, 132–138, DOI: 10.1016/j.porgcoat.2019.03.020.
- 234 D. Jiang, X. Xia, J. Hou, G. Cai, X. Zhang and Z. Dong, A novel coating system with self-reparable slippery surface and active corrosion inhibition for reliable protection of Mg alloy, *Chem. Eng. J.*, 2019, **373**, 285–297, DOI: 10.1016/j.cej.2019.05.046.
- 235 Y. Ouyang, J. Zhao, R. Qiu, S. Hu, H. Niu, M. Chen and P. Wang, Biomimetics leading to liquid-infused surface based on vertical dendritic Co matrix: A barrier to inhibit bioadhesion and microbiologically induced corrosion, *Colloids Surf., A*, 2019, **583**, 124006, DOI: 10.1016/j.colsurfa.2019.124006.
- 236 Z. Qiu, R. Qiu, Y. Xiao, J. Zheng and C. Lin, Slippery liquid-infused porous surface fabricated on CuZn: A barrier to abiotic seawater corrosion and microbiologically induced corrosion, *Appl. Surf. Sci.*, 2018, **457**, 468–476, DOI: 10.1016/j.apsusc.2018.06.139.
- 237 R. Jiang, L. Hao, L. Song, L. Tian, Y. Fan, J. Zhao, C. Liu, W. Ming and L. Ren, Lotus-leaf-inspired hierarchical structured surface with non-fouling and mechanical bactericidal performances, *Chem. Eng. J.*, 2020, **398**, 125609, DOI: 10.1016/j.cej.2020.125609.
- 238 Z. Sun, L. Yang, D. Zhang, F. Bian and W. Song, High-performance biocompatible nano-biocomposite artificial muscles based on a renewable ionic electrolyte made of cellulose dissolved in ionic liquid, *Nanotechnology*, 2019, **30**, 285503, DOI: 10.1088/1361-6528/ab0e33.
- 239 A. Elzaabalawy and A. Meguid, Development of novel superhydrophobic coatings using siloxane-modified epoxy nanocomposites, *Chem. Eng. J.*, 2020, **398**, 125403, DOI: 10.1016/j.cej.2020.125403.
- 240 M. Liu, Y. Luo and D. Jia, Fabrication of a versatile composite material with three-dimensional superhydrophobic for aquatic show, *Chem. Eng. J.*, 2020, **398**, 125362, DOI: 10.1016/j.cej.2020.125362.
- 241 S. Li, Y. Liu, Z. Tian, X. Liu, Z. Han and L. Ren, Biomimetic superhydrophobic and antibacterial stainless-steel mesh via double-potentiostatic electrodeposition and modification, *Surf. Coat. Technol.*, 2020, **403**, 126355, DOI: 10.1016/j.surfcoat.2020.126355.
- 242 R. Wang, X. Song, T. Xiang, Q. Liu, B. Su, W. Zhao and C. Zhao, Mussel-inspired chitosan-polyurethane coatings for improving the antifouling and antibacterial properties

- of polyethersulfone membranes, *Carbohydr. Polym.*, 2017, **168**, 310–319, DOI: 10.1016/j.carbpol.2017.03.092.
- 243 J. S. Park and J. H. Lee, Sea-trial verification of ultrasonic antifouling control, *Biofouling*, 2018, **34**, 98–110, DOI: 10.1080/08927014.2017.1409347.
- 244 M. N. Haque and S. Kwon, Effect of ultra-sonication and its use with sodium hypochlorite as antifouling method against *Mytilus edulis* larvae and mussel, *Environ. Geochem. Health*, 2018, **40**, 209–215, DOI: 10.1007/s10653-016-9894-1.
- 245 Y. Shi, D.-Y. Ma and S.-W. Zhai, Revealing the difference of intestinal microbiota composition of cultured European eels (*Anguilla anguilla*) with different growth rates, *Isr. J. Aquac.*, 2020, **72**, 1–12. <http://hdl.handle.net/10524/63212>.
- 246 W. Huang, Z. Cheng, S. Lei, L. Liu, X. Lv, L. Chen, M. Wu, C. Wang, B. Tian and Y. Song, Community composition, diversity, and metabolism of intestinal microbiota in cultivated European eel (*Anguilla anguilla*), *Appl. Microbiol. Biotechnol.*, 2018, **102**, 4143–4157.
- 247 S. Knobloch, J. Philip, S. Ferrari, D. Benhaïm, M. Bertrand and I. Poirier, The effect of ultrasonic antifouling control on the growth and microbiota of farmed European sea bass (*Dicentrarchus labrax*), *Mar. Pollut. Bull.*, 2021, **164**, 112072, DOI: 10.1016/j.marpolbul.2021.112072.
- 248 Z. Tian, Z. Lei, X. Chen, Y. Chen, L.-C. Zhang, J. Bi and J. Liang, Nanosecond pulsed fiber laser cleaning of natural marine micro-biofoulings from the surface of aluminum alloy, *J. Clean. Prod.*, 2020, **244**, 118724, DOI: 10.1016/j.jclepro.2019.118724.
- 249 G. Liu, W. Jiang, Z. Yuan, Y. Xie, X. Tian, D. Leng, A. Incecik and Z. Li, Design and optimization of a water jet-based biomimetic antifouling model for marine structures, *Phys. Fluids*, 2020, **32**, 097101, DOI: 10.1063/5.0020098.
- 250 G. Liu, Z. Yuan, A. Incecik, D. Leng, S. Wang and Z. Li, A new biomimetic antifouling method based on water jet for marine structures, *Proc. IMechE, Part M: J. Eng. Maritime Environment*, 2019, **234**, 573–584, DOI: 10.1177/1475090219892420.
- 251 R. Zhou, R. Zhou, P. Wang, B. Luan, X. Zhang, Z. Fang, Y. Xian, X. Lu, K. Ostrikov and K. Bazaka, Microplasma bubbles: Reactive vehicles for biofilm dispersal, *ACS Appl. Mater. Interfaces*, 2019, **11**(23), 20660–20669, DOI: 10.1021/acsami.9b03961.
- 252 X. Zhang, R. Zhou, K. Bazaka, Y. Liu, R. Zhou, G. Chen, Z. Chen, Q. Liu, S. Yang and K. Ostrikov, Quantification of plasma produced OH radical density for water sterilization, *Plasma Proc. Polym.*, 2018, **15**, 1700241, DOI: 10.1002/ppap.201700241.